

An 18-year-old man presented to the emergency department with chest pain. What is the most likely childhood diagnosis associated with the findings of this coronary angiogram?

Kawasaki's disease

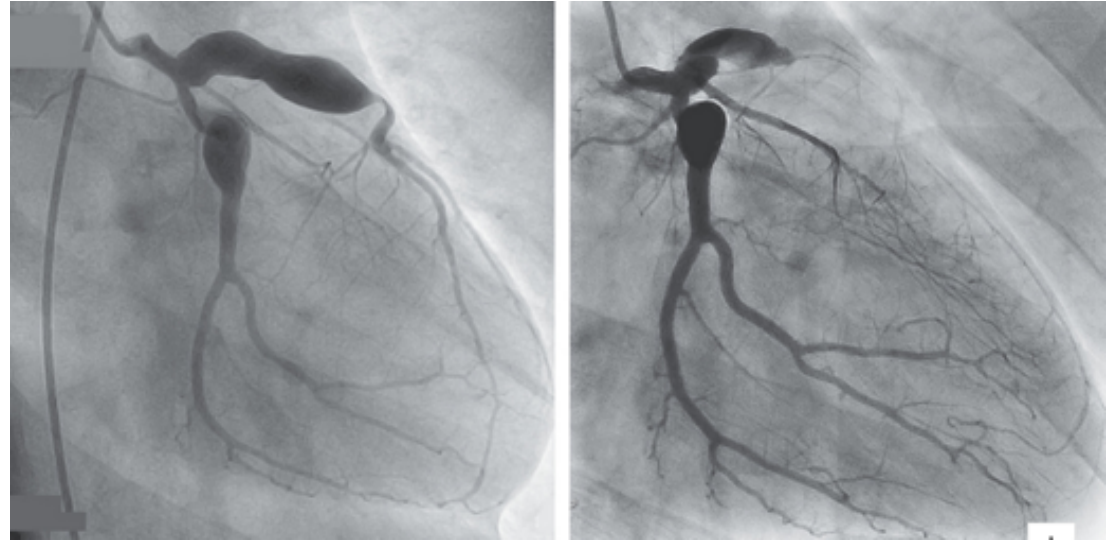


Rheumatic Heart Disease

Marfan's syndrome

Familial hypercholesterolemia

Hodgkin's Lymphoma



Kawasaki's disease is an acute, idiopathic, self-limiting vasculitis that primarily affects children. Clinical features include fever, nonexudative conjunctivitis in both eyes, mucositis, cervical lymphadenopathy, polymorphous rash, and changes in the hands and feet. Because not all these features are necessarily present and there is no specific diagnostic test for Kawasaki's disease, the diagnosis may be missed in childhood or occur at such an early age that the adult patient has no recollection of illness. Affected children are at risk for cardiovascular complications. This patient had a history of Kawasaki's disease, which had been diagnosed when he was 11 years of age. Despite treatment with intravenous immune globulin, coronary artery aneurysms were detected on imaging (the left panel shows a coronary angiogram obtained 3 years before the current presentation). Emergency coronary angiography revealed occlusion of the left anterior descending artery.

Das Kawasaki-Syndrom oder mukokutanen Lymphknotensyndrom (MCLS) ist eine akute, fieberhafte, systemische Erkrankung, die durch eine Gefäßentzündung (nekrotisierende Vaskulitis) der kleinen und mittleren Arterien gekennzeichnet ist. Zusätzlich ist eine systemische Entzündung in vielen Organen vorhanden.

Die Ursache ist unbekannt, man vermutet eine infektiöse Entstehung, die durch eine erbliche Grundlage begünstigt wird. Das Kawasaki-Syndrom betrifft vor allem Kleinkinder und imitiert im anfänglichen Erscheinungsbild Infektionskrankheiten wie Masern oder Scharlach. In Deutschland erkranken pro Jahr etwa neun von 100.000 Kindern unter fünf Jahren, während die Inzidenz für ein Kawasaki-Syndrom in Japan in derselben Altersstufe bei etwa 185 von 100.000 liegt. 75 % aller Patienten sind jünger als fünf Jahre, sehr häufig erkranken Kinder zwischen dem ersten und zweiten Lebensjahr. Jungen sind von der Krankheit etwa eineinhalb mal so oft betroffen wie Mädchen. Auf der nördlichen Hemisphäre gibt es einen saisonalen Gipfel der Neuerkrankungen im Winter und Frühjahr, während in tropischen Regionen keine Saisonalität beobachtet wird.

Es folgen aufeinander drei Phasen:

1. Die *akute fieberhafte Periode*: Sie dauert bis zu zehn Tage. Das Fieber beginnt meist abrupt, und es entwickeln sich im Verlauf von drei bis vier Tagen die typischen Symptome, die dann zur Diagnose des Kawasaki-Syndroms führen können (siehe unten bei diagnostische Kriterien).

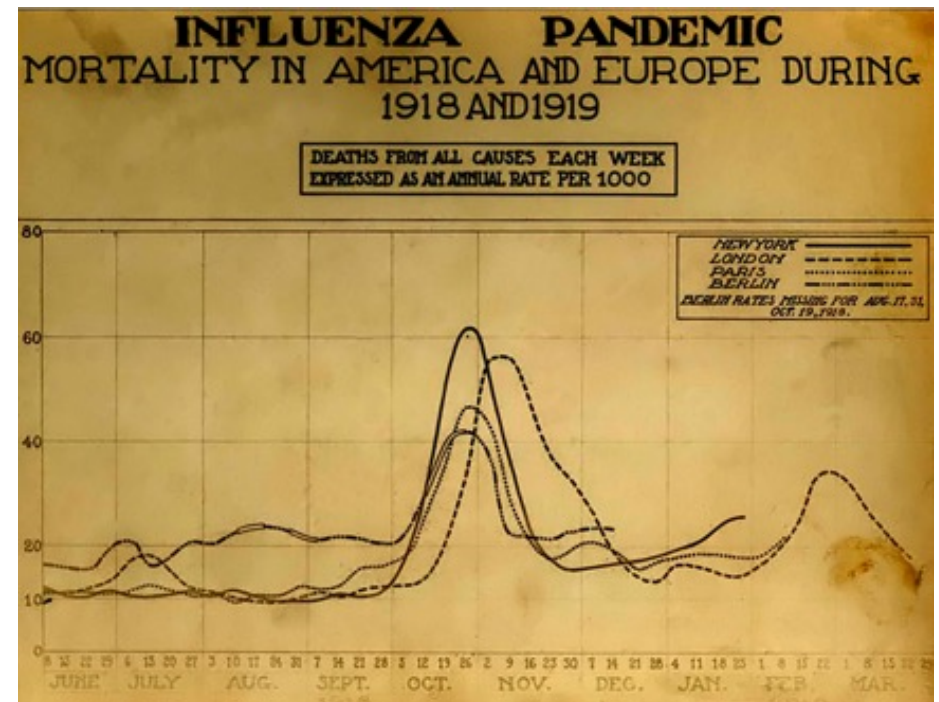
2. Die *subakute Phase*: Sie hat eine Dauer von zwei bis vier Wochen. Typisch ist eine Schuppung von Händen und Füßen.

3. Die Phase der *Rekonvaleszenz*: Sie kann Monate dauern mit gelegentlich bestehender Müdigkeit und Leistungsschwäche.



Die Spanische Grippe war eine Pandemie, die durch einen ungewöhnlich virulenten Abkömmling des Influenzavirus (Subtyp A/H1N1) verursacht wurde und zwischen 1918 und 1920 mindestens 25 Millionen, nach einer Bilanz der Fachzeitschrift Bulletin of the History of Medicine vom Frühjahr 2002 sogar knapp 50 Millionen Todesopfer forderte. Die Auswirkung der Pandemie ist damit in absoluten Zahlen mit dem Ausbruch der Pest von 1348 vergleichbar, der damals mehr als ein Drittel der europäischen Bevölkerung zum Opfer fiel. Eine Besonderheit der Spanischen Grippe war, dass ihr vor allem 20- bis 40-jährige Menschen erlagen, während Influenzaviren sonst besonders Kleinkinder und alte Menschen gefährden.

Varianten des Subtyps A H1N1 verursachten 1977/1978 den Ausbruch der Russischen Grippe und 2009 der „Schweinegrippe“-Pandemie. Der Name Spanische Grippe entstand, nachdem die ersten Nachrichten über die Seuche aus Spanien kamen; als neutrales Land hatte Spanien im Ersten Weltkrieg eine relativ liberale Zensur, sodass dort im Unterschied zu anderen betroffenen Ländern Berichte über das Ausmaß der Seuche nicht unterdrückt wurden. Die These, dass es zu den ersten virulenten Grippeausbrüchen in den USA kam und sie von dort aus durch Truppenbewegungen weltweit verbreitet wurde, ist schon in den 1970er Jahren durch den australischen Medizin-Nobelpreisträger Frank Macfarlane Burnet aufgestellt worden. Heute vermutet eine Reihe von Wissenschaftlern, dass die Grippewelle in Haskell County im US-Bundesstaat Kansas ihren Ausgang nahm.



# Influenza Cataclysm, 1918

This year marks the centennial of a true pandemic cataclysm: an influenza pandemic that killed 50 million to 100 million people globally — arguably the single deadliest event in recorded human history. It is an event worth contemplating, since evidence suggests that another pandemic at least as severe may occur one day. What happened? Biomedical scientists have spent a full century piecing together some answers. The epidemiologic patterns of the pandemic were well characterized during and after 1918. The causal influenza A virus was discovered in 1933, allowing seroepidemiologic studies that shed additional light on its origin. Between 1995 and 2005, viral RNA sequences from preserved autopsy tissues and from a frozen corpse were fully sequenced, and the virus was reconstructed by means of reverse genetics techniques. Autopsy studies and pathogenesis studies in experimental animals revealed that the 1918 virus differed significantly from other human and animal influenza viruses. It induced an aberrant immune response in part because of the inherent virulence of its H1 hemagglutinin (HA) protein, and it was highly copathogenic, producing virus-induced bacterial bronchopneumonias in association with commensal bacteria colonizing the nasopharynx (predominantly *Streptococcus pneumoniae*, *S. pyogenes*, and *Staphylococcus aureus*).



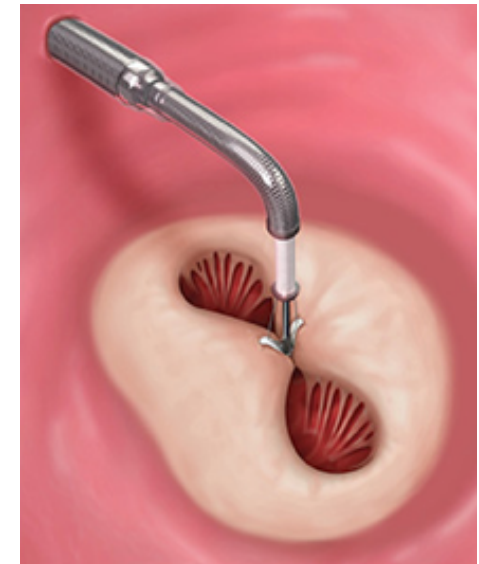
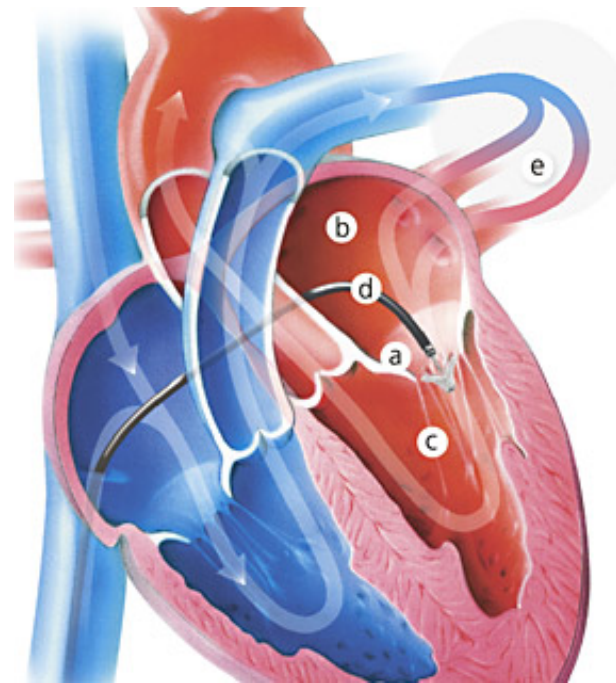
“Death Bed” Photograph of Renowned Viennese Painter Egon Schiele (1890–1918). The 28-year-old Schiele and his wife, Edith Harms, who was 6 months pregnant, developed influenza in late October 1918; they died together.

How could we identify the few patients who would have rapid progression among the many who would do well without special care? Epidemiologic information is helpful: in all influenza pandemics, including that in 1918, the groups at highest risk for severe or fatal outcomes have prominently included infants and toddlers, the elderly, pregnant women, and people of any age with chronic conditions such as respiratory or cardiac diseases, kidney diseases, or diabetes. But everyone else was at risk, too. In 1918, healthy 20-to-40-year-old adults had very high mortality, a still-unexplained phenomenon not seen before or since, which underlines influenza’s capacity to surprise.

## **Kathetergestützte Mitralklappen- Rekonstruktion der Mitralklappeninsuffizienz: MitraClip**

Die Undichtigkeit der Mitralklappe (Mitralklappeninsuffizienz) ist der zweithäufigste erworbene Klappenfehler, der sowohl mit einer erheblichen Abnahme der alltäglichen Belastbarkeit meist aufgrund von Luftnot als auch mit einer Einschränkung der Lebenserwartung einhergeht.

Obwohl die Operation der Mitralklappe das Standardverfahren darstellt, zeigen neuere Erhebungen, dass knapp die Hälfte aller Patienten mit Mitralklappeninsuffizienz einer solchen Operation nicht mehr unterzogen werden können. Ursächlich hierfür ist ein erhöhtes Operationsrisiko aufgrund schwerer Begleiterkrankungen, hohen Alters oder einer hochgradigen Einschränkung der Pumpfunktion des Herzens. Für diese Patienten kann die kathetergestützte Mitralklappenrekonstruktion mit MitraClip eine mögliche Therapiealternative darstellen.



# Percutaneous Repair or Medical Treatment for Secondary Mitral Regurgitation MITRA-FR

In patients who have chronic heart failure with reduced left ventricular ejection fraction, severe secondary mitral-valve regurgitation is associated with a poor prognosis. Whether percutaneous mitral-valve repair improves clinical outcomes in this patient population is unknown. We randomly assigned patients who had severe secondary mitral regurgitation (defined as an effective regurgitant orifice area of >20 mm<sup>2</sup> or a regurgitant volume of >30 ml per beat), a left ventricular ejection fraction between 15 and 40%, and symptomatic heart failure, in a 1:1 ratio, to undergo percutaneous mitral-valve repair in addition to receiving medical therapy (intervention group; 152 patients) or to receive medical therapy alone (control group; 152 patients). **The primary efficacy outcome was a composite of death from any cause or unplanned hospitalization for heart failure at 12 months.**

## Periprocedural Complications and Prespecified Serious Adverse Events (Intention-to-Treat Population).

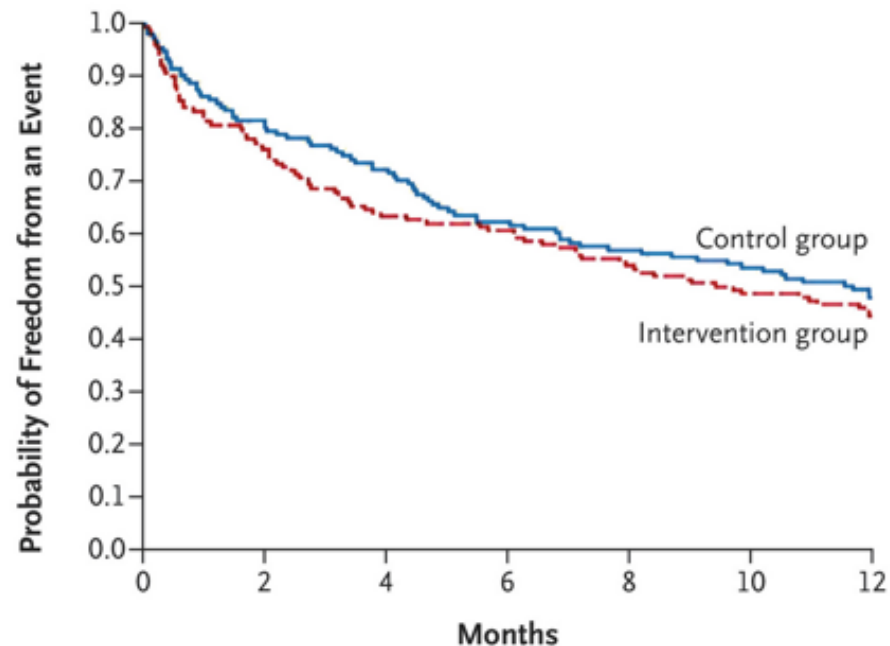
Variable	Intervention Group (N=152)	Control Group (N=152)
<b>Periprocedural complications during device implantation — no./total no. (%)<sup>†</sup></b>		
Device-implantation failure	6/144 (4.2) <sup>‡</sup>	NA
Hemorrhage resulting in transfusion or vascular complication resulting in surgical intervention	5/144 (3.5)	NA
Atrial septum lesion or atrial septal defect	4/144 (2.8)	NA
Cardiogenic shock resulting in intravenous inotropic support	4/144 (2.8)	NA
Cardiac embolism, including gas embolism and stroke	2/144 (1.4)	NA
Tamponade	2/144 (1.4)	NA
Urgent conversion to heart surgery	0	NA
<b>Prespecified serious adverse events at 1 year — no. (%)</b>		
All serious adverse events	125 (82.2)	121 (79.6)
Heart transplantation or mechanical cardiac assistance	6 (3.9)	9 (5.9)
Ischemic or hemorrhagic stroke <sup>§</sup>	7 (4.6)	1 (0.7)
Myocardial infarction	0	2 (1.3)
Need for renal-replacement therapy	5 (3.3)	1 (0.7)
Severe hemorrhage <sup>¶</sup>	11 (7.2)	6 (3.9)
Infections	28 (18.4)	27 (17.8)

Primary funding was provided by the French Ministry of Health and Research National Program. Abbott Vascular, the manufacturer of the trial device, provided the devices as well as support for investigators' meetings; they also proctored the procedures for implantation of the device.

Primary Outcome and Secondary Efficacy Outcomes at 12 Months (Intention-to-Treat Population).

Outcome	Intervention Group (N=152)	Control Group (N=152)	Hazard Ratio or Odds Ratio (95% CI)*	P Value†
Composite primary outcome: death from any cause or unplanned hospitalization for heart failure at 12 months — no. (%)	83 (54.6)	78 (51.3)	1.16 (0.73–1.84)	0.53
Secondary outcomes‡				
Death from any cause	37 (24.3)	34 (22.4)	1.11 (0.69–1.77)	
Cardiovascular death	33 (21.7)	31 (20.4)	1.09 (0.67–1.78)	
Unplanned hospitalization for heart failure	74 (48.7)	72 (47.4)	1.13 (0.81–1.56)	
Major adverse cardiovascular events§	86 (56.6)	78 (51.3)	1.22 (0.89–1.66)	

Shown are estimates of the probability of survival without a primary outcome event (death from any cause or unplanned hospitalization for heart failure) in the two trial groups



Our trial has several limitations. First, in 14 patients (9.2%) in the intervention group, either the procedure was not performed or the device implantation failed. However, in the per-protocol analysis in which the data from these patients were excluded, no significant difference in outcomes was seen between the two groups at 12 months. Second, the considerable amount of missing follow-up data for the assessments of echocardiography, functional status, natriuretic peptide, and quality of life is a limitation of the trial. However, a very low number of patients was lost to follow-up for the primary outcome, with 99% of the patients having complete data at 12 months. Third, the trial was powered to detect a substantial effect on the primary outcome (an event rate of 50% in the control group vs. 33% in the intervention group). Therefore, we did not have power to detect a smaller difference between the groups, although the point estimate for the primary outcome does not suggest a trend in favor of percutaneous mitral-valve repair.

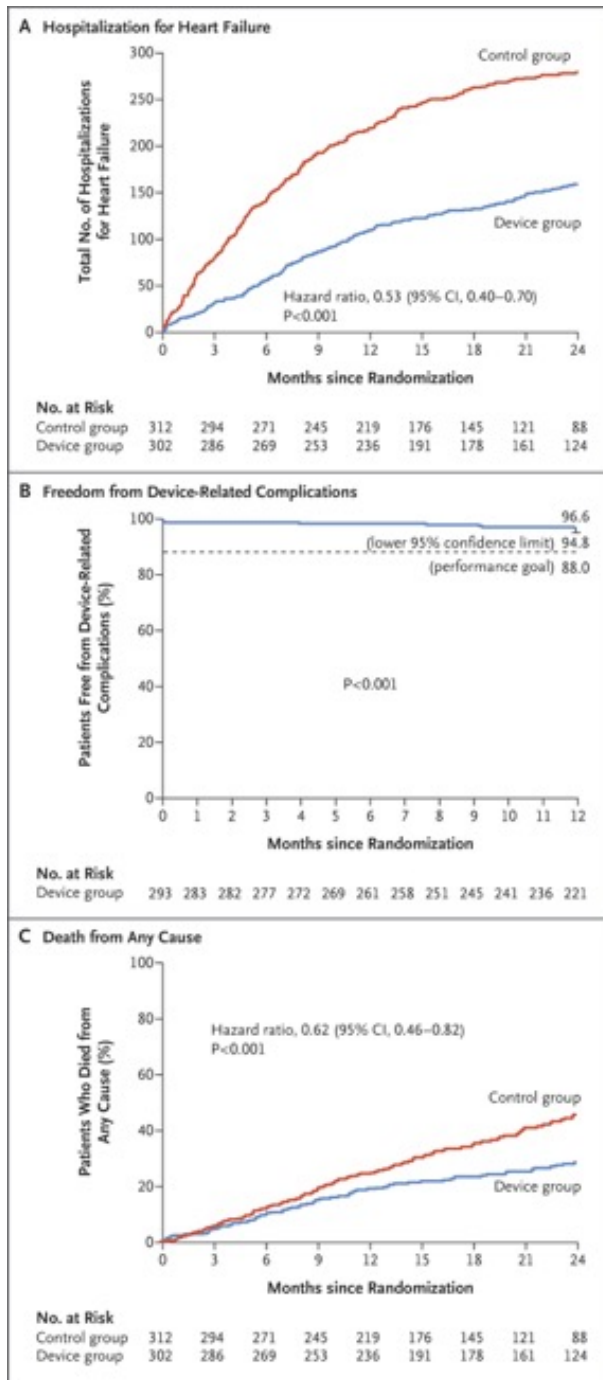
In conclusion, in this multicenter, randomized, open-label, controlled trial involving patients with severe secondary mitral regurgitation, the rate of the composite primary outcome of death or unplanned hospitalization for heart failure at 12 months did not differ significantly between the intervention group and the control group.



# Transcatheter Mitral-Valve Repair in Patients with Heart Failure (COAPT)

Among patients with heart failure who have mitral regurgitation due to left ventricular dysfunction, the prognosis is poor. Transcatheter mitral-valve repair may improve their clinical outcomes. At 78 sites in the United States and Canada, we enrolled patients with heart failure and moderate-to-severe or severe secondary mitral regurgitation who remained symptomatic despite the use of maximal doses of guideline-directed medical therapy. Patients were randomly assigned to transcatheter mitral-valve repair plus medical therapy (device group) or medical therapy alone (control group). The primary effectiveness end point was all hospitalizations for heart failure within 24 months of follow-up. The primary safety end point was freedom from device-related complications at 12 months; the rate for this end point was compared with a prespecified objective performance goal of 88.0%. The trial was sponsored by Abbott.

End Point	Device Group (N=302)	Control Group (N=312)	Hazard Ratio (95% CI)	P Value†
<b>Primary</b>				
Effectiveness: all hospitalizations for heart failure within 24 mo — no. of events/total no. of patient-yr (annualized rate)	160/446.5 (35.8)	283/416.8 (67.9)	0.53 (0.40 to 0.70)‡	<0.001§
Safety: freedom from device-related complications at 12 mo — Kaplan–Meier estimate of event-free rate (lower 95% confidence limit)	96.6 (94.8)	—	—	<0.001 for comparison with goal of 88.0%¶
<b>Secondary, listed in hierarchical order</b>				
Mitral regurgitation grade of 2+ or lower at 12 mo — no./total no. (%)	199/210 (94.8)	82/175 (46.9)	—	<0.001**
Death from any cause at 12 mo — no. of events (Kaplan–Meier estimate of event rate)	57 (19.1)	70 (23.2)	0.81 (0.57 to 1.15)††	<0.001 for noninferiority‡‡
Death or hospitalization for heart failure within 24 mo	—	—	—	<0.001§§
Change in KCCQ score from baseline to 12 mo — points¶¶	12.5±1.8	-3.6±1.9	16.1 (11.0 to 21.2)	<0.001***
Change in distance on 6-min walk test from baseline to 12 mo — m†††	-2.2±9.1	-60.2±9.0	57.9 (32.7 to 83.1)	<0.001***
All hospitalizations for any cause within 24 mo — no. of events/total no. of patient-yr (annualized rate)	474/446.5 (106.2)	610/416.8 (146.4)	0.76 (0.60 to 0.96)	0.02§
NYHA functional class of I or II at 12 mo — no./total no. (%)	171/237 (72.2)	115/232 (49.6)	—	<0.001**
Change in left ventricular end-diastolic volume from baseline to 12 mo — ml	-3.7±5.1	17.1±5.1	-20.8 (-34.9 to -6.6)	0.004***
Death from any cause within 24 mo — no. of events (Kaplan–Meier estimate of event rate)	80 (29.1)	121 (46.1)	0.62 (0.46 to 0.82)	<0.001‡‡‡
Freedom from death from any cause, stroke, myocardial infarction, and nonelective cardiovascular surgery for a device-related complication at 30 days — % (lower 95% confidence limit)	96.9 (94.7)	—	—	<0.001 for comparison with goal of 80.0%***

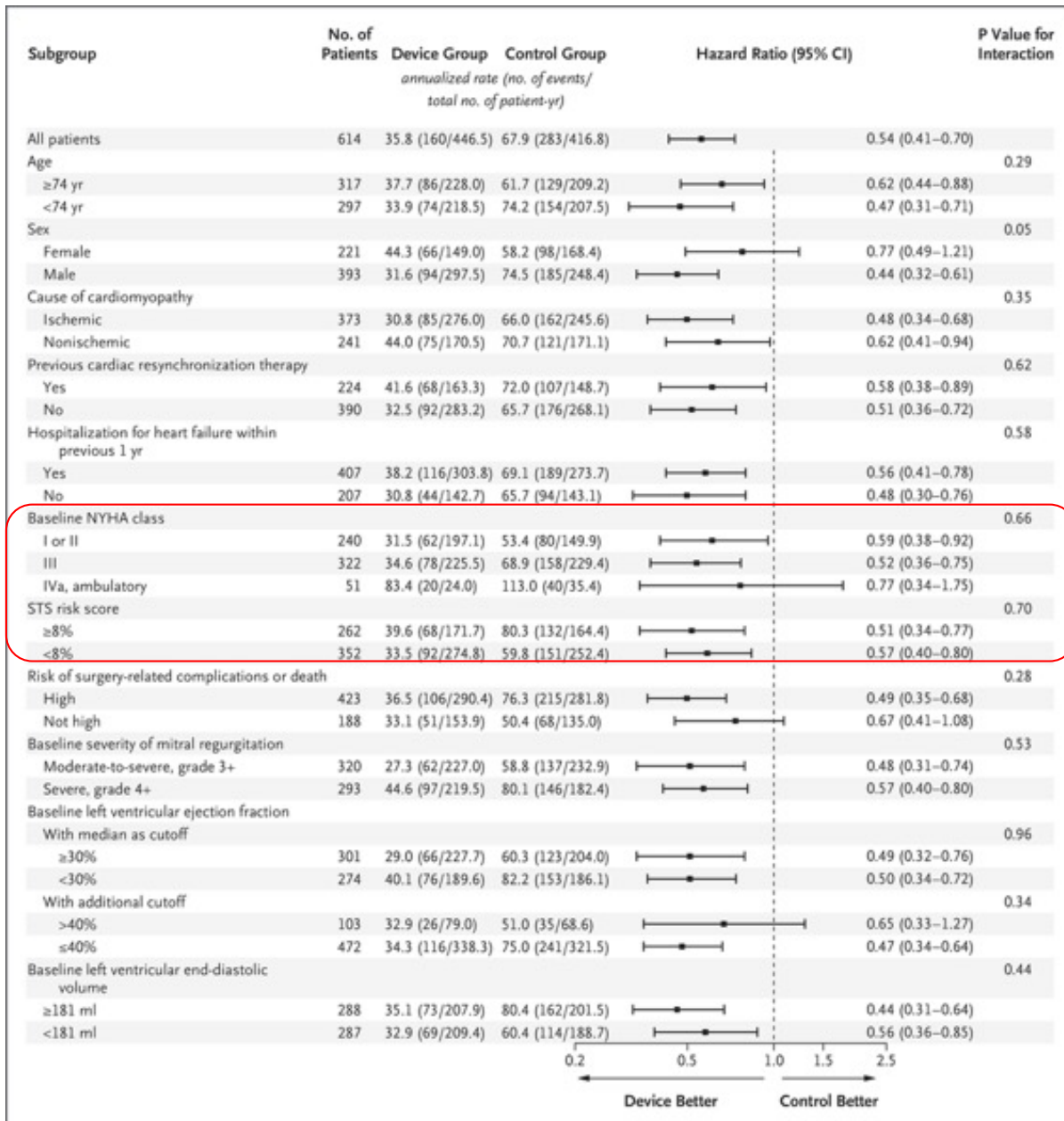


Primary Effectiveness and Safety End Points and Death. Panel A shows the cumulative incidence of the primary effectiveness end point of all hospitalizations for heart failure within 24 months of follow-up among patients who underwent transcatheter mitral-valve repair and received guideline-directed medical therapy (device group) and among those who received guideline-directed medical therapy alone (control group). The data shown here do not account for the competing risk of death, which was considered in the joint frailty model. A total of 160 hospitalizations for heart failure occurred in 92 patients in the device group, and a total of 283 hospitalizations for heart failure occurred in 151 patients in the control group. Panel B shows the rate of the primary safety end point of freedom from device-related complications at 12 months among the 293 patients in whom device implantation was attempted, as compared with an objective performance goal. Panel C shows time-to-event curves for all-cause mortality in the device group and the control group.

**Table 3. Adverse Events within 24 Months in the Intention-to-Treat Population.\***

Event	Device Group (N = 302)	Control Group (N = 312)	Hazard Ratio (95% CI)	P Value
	<i>no. of patients with event (Kaplan–Meier estimate of event rate)</i>			
Death from any cause	80 (29.1)	121 (46.1)	0.62 (0.46–0.82)	<0.001
Cardiovascular cause	61 (23.5)	97 (38.2)	0.59 (0.43–0.81)	0.001
Related to heart failure	28 (12.0)	61 (25.9)	0.43 (0.27–0.67)	<0.001
Not related to heart failure	33 (13.1)	36 (16.6)	0.86 (0.54–1.38)	0.53
Noncardiovascular cause	19 (7.3)	24 (12.7)	0.73 (0.40–1.34)	0.31
Hospitalization for any cause	194 (69.6)	228 (81.8)	0.77 (0.64–0.93)	0.01
Cardiovascular cause	138 (51.9)	180 (66.5)	0.68 (0.54–0.85)	<0.001
Related to heart failure	92 (35.7)	151 (56.7)	0.52 (0.40–0.67)	<0.001
Not related to heart failure	72 (29.4)	72 (31.0)	0.98 (0.71–1.36)	0.92
Noncardiovascular cause	124 (48.2)	128 (52.9)	0.91 (0.71–1.17)	0.47
Death or hospitalization for heart failure	129 (45.7)	191 (67.9)	0.57 (0.45–0.71)	<0.001
Death from cardiovascular cause or hospitalization for heart failure	117 (42.7)	177 (63.6)	0.56 (0.44–0.70)	<0.001
Unplanned mitral-valve intervention	10 (4.0)	15 (9.0)	0.61 (0.27–1.36)	0.23
MitraClip implantation	9 (3.7)	8 (6.6)	0.99 (0.38–2.58)	0.99
Mitral-valve surgery	1 (0.4)	7 (2.5)	0.14 (0.02–1.17)	0.07
PCI or CABG	7 (2.8)	13 (4.3)	0.62 (0.24–1.60)	0.32
PCI	7 (2.8)	11 (3.6)	0.75 (0.28–2.02)	0.57
CABG	0	2 (0.7)	—	—
Stroke	11 (4.4)	11 (5.1)	0.96 (0.42–2.22)	0.93
Myocardial infarction	12 (4.7)	14 (6.5)	0.82 (0.38–1.78)	0.62
New cardiac resynchronization therapy	7 (2.9)	8 (3.3)	0.85 (0.31–2.34)	0.75
LVAD implantation or heart transplantation	9 (4.4)	22 (9.5)	0.37 (0.17–0.81)	0.01
LVAD implantation	6 (3.0)	16 (7.1)	0.34 (0.13–0.87)	0.02
Heart transplantation	3 (1.4)	8 (3.6)	0.35 (0.09–1.32)	0.12

\* CABG denotes coronary-artery bypass grafting, LVAD left ventricular assist device, and PCI percutaneous coronary intervention.



Subgroup Analyses of Hospitalization for Heart Failure within 24 Months. Shown are annualized estimates of all hospitalizations for heart failure within 24 months of follow-up across subgroups. The median value was used as a cutoff for age (median, 74 years), left ventricular ejection fraction (median, 30%), and left ventricular end-diastolic volume (median, 181 ml). For the additional cutoff for left ventricular ejection fraction, a value of 40% or less indicates the presence of heart failure with reduced ejection fraction and a value of more than 40% the presence of heart failure with preserved ejection fraction, two different diseases associated with different prognoses and treatments. Society of Thoracic Surgeons (STS) scores for the risk of death within 30 days after mitral-valve replacement range from 0.4 to 98.1%, with higher percentages indicating greater risk. The risk of surgery-related complications or death was determined by the central eligibility committee, with high risk defined as an STS score for the risk of death within 30 days after mitral-valve replacement of 8% or higher or the presence of features that portend an extremely high risk of operative stroke or death. NYHA denotes New York Heart Association.

# COAPT

# MITRA-FR

Characteristic	Device Group (N=302)	Control Group (N=312)
<b>Clinical</b>		
Age — yr	71.7±11.8	72.8±10.5
Male sex — no. (%)	201 (66.6)	192 (61.5)
Diabetes — no. (%)	106 (35.1)	123 (39.4)
Hypertension — no. (%)	243 (80.5)	251 (80.4)
Hypercholesterolemia — no. (%)	166 (55.0)	163 (52.2)
Previous myocardial infarction — no. (%)	156 (51.7)	160 (51.3)
Previous percutaneous coronary intervention — no. (%)	130 (43.0)	153 (49.0)
Previous coronary-artery bypass grafting — no. (%)	121 (40.1)	126 (40.4)
Previous stroke or transient ischemic attack — no. (%)	56 (18.5)	49 (15.7)
Peripheral vascular disease — no. (%)	52 (17.2)	57 (18.3)
Chronic obstructive pulmonary disease — no. (%)	71 (23.5)	72 (23.1)
History of atrial fibrillation or flutter — no. (%)	173 (57.3)	166 (53.2)
Body-mass index†	27.0±5.8	27.1±5.9
<b>Creatinine clearance</b>		
Mean — ml/min‡	50.9±28.5	47.8±25.0
≤60 ml/min — no./total no. (%)	214/299 (71.6)	227/302 (75.2)
Anemia — no./total no. (%)§	180/301 (59.8)	192/306 (62.7)
<b>STS risk score¶</b>		
Mean — %	7.8±5.5	8.5±6.2
≥8% — no. (%)	126 (41.7)	136 (43.6)
<b>Risk of surgery-related complications or death — no./total no. (%)  </b>		
High	205/299 (68.6)	218/312 (69.9)
Not high	94/299 (31.4)	94/312 (30.1)
<b>Related to heart failure</b>		
Cause of cardiomyopathy — no. (%)		
Ischemic	184 (60.9)	189 (60.6)
Nonischemic	118 (39.1)	123 (39.4)
NYHA class — no./total no. (%)		
I	1/302 (0.3)	0/311 (0)
II	129/302 (42.7)	110/311 (35.4)
III	154/302 (51.0)	168/311 (54.0)
IVa, ambulatory	18/302 (6.0)	33/311 (10.6)

Characteristic	Intervention Group (N=152)	Control Group (N=152)
Age — yr	70.1±10.1	70.6±9.9
Age >75 yr — no. (%)	51 (33.6)	59 (38.8)
Male sex — no. (%)	120 (78.9)	107 (70.4)
<b>Medical and surgical history — no./total no. (%)</b>		
Ischemic cardiomyopathy	95/152 (62.5)	85/151 (56.3)
Nonischemic cardiomyopathy	57/152 (37.5)	66/151 (43.7)
Previous myocardial infarction	75/152 (49.3)	52/152 (34.2)
Previous coronary revascularization	71/152 (46.7)	64/151 (42.4)
Atrial fibrillation	49/142 (34.5)	48/147 (32.7)
Diabetes	50/152 (32.9)	39/152 (25.7)
Renal insufficiency	22/152 (14.5)	19/152 (12.5)
<b>NYHA class — no. (%)</b>		
II	56 (36.8)	44 (28.9)
III	82 (53.9)	96 (63.2)
IV	14 (9.2)	12 (7.9)
Systolic blood pressure — mm Hg	109±16	108±18
Heart rate — beats/min	73±13	72±13
Median EuroSCORE II (IQR)†	6.6 (3.5–11.9)	5.9 (3.4–10.4)
Left ventricular ejection fraction — %	33.3±6.5	32.9±6.7
Left ventricular end-diastolic volume — ml/m <sup>2</sup>	136.2±37.4	134.5±33.1
Effective regurgitant orifice area — mm <sup>2</sup>	31±10	31±11
Regurgitant volume — ml	45±13	45±14
Median NT-proBNP (IQR) — ng/liter‡	3407 (1948–6790)	3292 (1937–6343)
Median brain natriuretic peptide (IQR) — ng/liter‡	765 (417–1281)	835 (496–1258)
Glomerular filtration rate — ml/min	48.8±19.7	50.2±20.1

## COAPT

Hospitalization for heart failure within previous 1 yr — no. (%)	176 (58.3)	175 (56.1)
Previous cardiac resynchronization therapy — no. (%)	115 (38.1)	109 (34.9)
Previous implantation of defibrillator — no. (%)	91 (30.1)	101 (32.4)
B-type natriuretic peptide level — pg/ml	1014.8±1086.0	1017.1±1212.8
N-terminal pro-B-type natriuretic peptide level — pg/ml	5174.3±6566.6	5943.9±8437.6
<b>Assessed at the echocardiographic core laboratory</b>		
Severity of mitral regurgitation — no./total no. (%)		
Moderate-to-severe, grade 3+	148/302 (49.0)	172/311 (55.3)
Severe, grade 4+	154/302 (51.0)	139/311 (44.7)
Effective regurgitant orifice area — cm <sup>2</sup>	0.41±0.15	0.40±0.15
Left ventricular end-systolic dimension — cm	5.3±0.9	5.3±0.9
Left ventricular end-diastolic dimension — cm	6.2±0.7	6.2±0.8
Left ventricular end-systolic volume — ml	135.5±56.1	134.3±60.3
Left ventricular end-diastolic volume — ml	194.4±69.2	191.0±72.9
Left ventricular ejection fraction		
Mean — %	31.3±9.1	31.3±9.6
≤40% — no./total no. (%)	231/281 (82.2)	241/294 (82.0)
Right ventricular systolic pressure — mm Hg	44.0±13.4 (253)	44.6±14.0 (275)

MITRA-FR trial showed no significant difference between the trial groups with respect to the rate of death from any cause or unplanned hospitalization for heart failure at 1 year (the composite primary outcome), whereas the COAPT trial showed a significantly lower rate of hospitalization for heart failure at 2 years (the primary outcome) and significantly lower all-cause mortality at 2 years (a secondary outcome) in the device group.

**First, medical management before and after enrollment may have differed between the two trials.** In the COAPT trial, the heart team at each site, which included a heart-failure specialist, stipulated that current heart-failure treatments be implemented at the maximum tolerated dose before randomization, and patients were subsequently excluded if their symptoms abated or if the degree of mitral regurgitation decreased during the intensified run-in phase. This approach may have led to enrollment of more patients with heart failure that was truly refractory to medical therapy in the COAPT trial than in the MITRA-FR trial. This assessment is supported by a comparison of the medical-treatment groups in the two trials: patients in the COAPT trial had a higher baseline level of N-terminal pro-B-type natriuretic peptide, as well as a higher annualized rate of hospitalization for heart failure, than patients in the MITRA-FR trial (68% vs. 47%); a lower percentage of patients in the COAPT trial than in the MITRA-FR trial had a New York Heart Association functional class of I or II at 1 year; and patients in the COAPT trial had a greater increase in left ventricular end-diastolic volume at follow-up than patients in the MITRA-FR trial. Further details regarding changes in medical therapy that occurred in both trials after enrollment are needed; there was a small but significant increase from baseline in beta-blocker therapy in the device group of the COAPT trial.

The **second** possible explanation for the differences in outcomes between the two trials was that there were differences in **baseline valvular and ventricular characteristics between the patient populations of the two trials**. As assessed on the basis of the effective regurgitant orifice area, mitral regurgitation was more **severe in the COAPT trial than in the MITRA-FR trial (41 mm<sup>2</sup> vs. 31 mm<sup>2</sup>)**. Conversely, the left ventricular end-diastolic volume (reflecting the status of the left ventricle) was smaller in the COAPT trial. Symptoms and outcomes in these patients are related to a complex interplay between the mitral regurgitation and the left ventricular dysfunction, with only the former targeted by the device therapy. Whether eligibility differed between the two trials on the basis of suitable mitral-valve leaflet anatomy, which could also influence procedural success, is unclear.

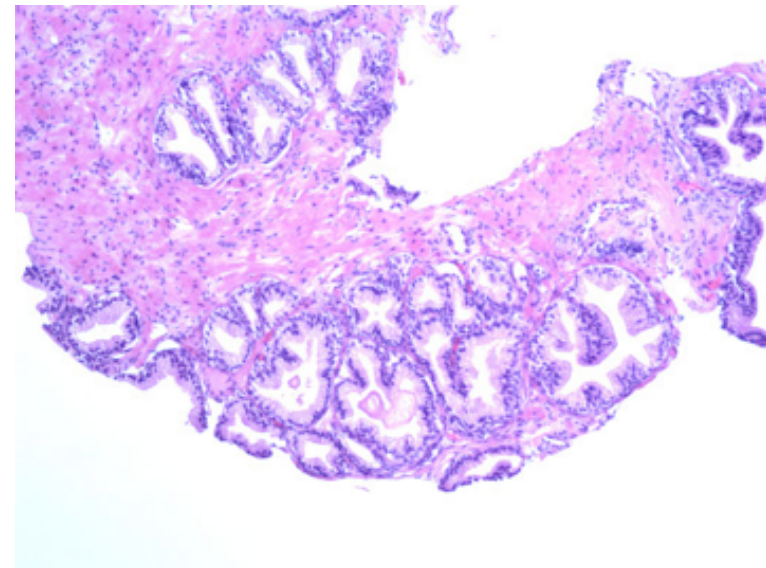
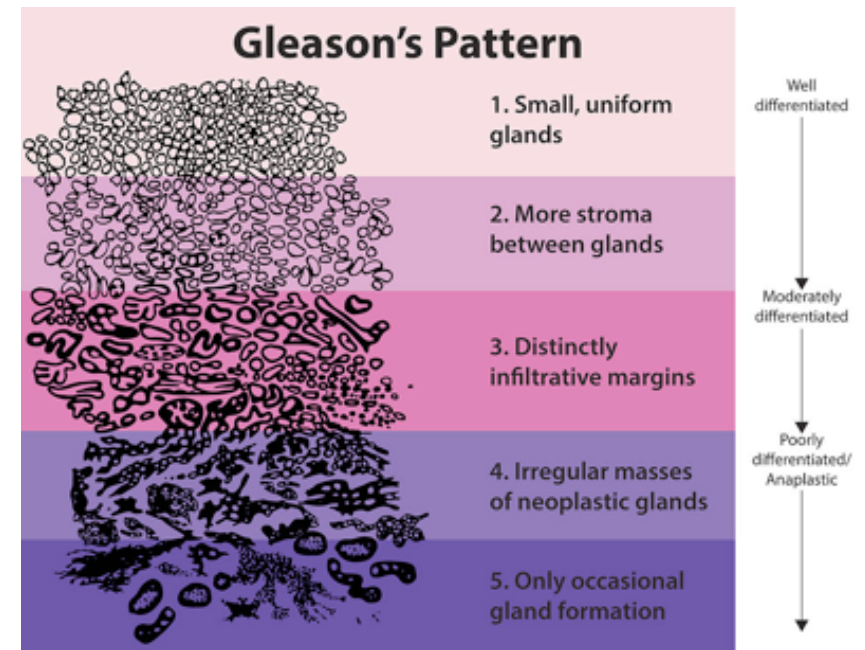
**Third, procedural performance** may have differed between the two trials, since **a greater proportion of patients in the COAPT trial than in the MITRA-FR trial received more than a single clip**. A larger percentage of patients in the MITRA-FR trial than in the COAPT trial had moderate-to-severe or severe mitral regurgitation at 1 year, although the limitations of echocardiographic follow-up must be acknowledged (assessment of the severity of mitral regurgitation is difficult after clip implantation). It is also worth noting that the Kaplan–Meier survival curves in the two trials appeared roughly similar at 1 year, after which point the trial groups in the COAPT trial diverged. One wonders what the results of the MITRA-FR trial might have shown with longer follow-up.

**It is difficult to fully reconcile the differences** in patient outcomes between these two trials. However, there are several important take-home messages. Secondary mitral regurgitation is a disease of the left ventricle. Management of left ventricular dysfunction with guideline-directed medical therapy and, when indicated, biventricular pacing, should be pursued before any intervention involving the mitral valve is considered. Edge-to-edge transcatheter mitral-valve repair can be performed in experienced centers with a high degree of success and can result in a sustained reduction in the severity of mitral regurgitation. Whether this translates into lower rates of death and hospitalization appears to depend, at least in part, on patient characteristics. **We hypothesize that the patients enrolled in the COAPT trial had heart failure symptoms that were truly refractory to medical therapy, with a greater degree of mitral regurgitation and less left ventricular dilatation than the patients enrolled in the MITRA-FR trial.**

Der Gleason-Score dient der histologischen (feingeweblichen) Beurteilung der Drüsenmorphologie der Prostata (vergleiche: Grading). Dabei werden verschiedene Drüsenformationen bewertet und einem Gleason-Grad zwischen 1 und 5 zugeordnet. Je höher der Wert, desto höher ist der Grad der Entdifferenzierung. Zur mikroskopischen Einschätzung dient Material einer Prostata-Stanzbiopsie oder einer bereits operativ entfernten Prostata. Der Gleason-Score errechnet sich aus der Addition zweier Gleason-Grade (s. Beurteilung des Gleason-Score). **Das Scoring-System wurde 1966 von dem amerikanischen Pathologen Donald F. Gleason entwickelt und später nach ihm benannt.** Die Einteilung umfasst fünf Grade, wobei Grad 1 die am besten differenzierten Tumoren beschreibt und Grad 5 die am schlechtesten differenzierten Tumoren, deren Wachstumsmuster fast jede Ähnlichkeit mit normalem Prostatagewebe verloren haben. Die Grade 2 bis 4 liegen dazwischen.

Der Gleason-Score wird stets durch Addition aus zwei solcher Grad-Einteilungen gebildet, wobei in der Stanzbiopsie der häufigste und der am schlechtesten differenzierte Gleason-Grad addiert wird. Ist bereits die gesamte Prostata entfernt, so wird der Gleason-Score hier mit Hilfe der beiden häufigsten Gleason-Grade ermittelt. Liegt nur ein Wachstumsmuster vor, so wird der Grad verdoppelt. In diesem Schema beschreibt also der Score  $1 + 1 = 2$  die am besten differenzierten Tumoren, der Score  $5 + 5 = 10$  stellt die schlechteste Kombination dar.

Der häufigere und für diagnostische Zwecke wichtigere Fall einer Bestimmung des Gleason-Score ist die Untersuchung von Gewebematerial durch einen Pathologen, das der Urologe mittels Stanzbiopsie aus der Prostata entnommen hat. Da bei einer Biopsie stets nur ein kleiner Teil des Tumors entnommen wird, ist die Diagnose eines Gleason-Grades 1 oder 2 in der Stanze jedoch in der Regel nicht möglich. Daher ist der niedrigste Score in der Stanzbiopsie  $3+2$ , in der Regel aber  $3+3$ .





# Radical Prostatectomy or Watchful Waiting in Prostate Cancer — 29-Year Follow-up

Radical prostatectomy reduces mortality among men with clinically detected localized prostate cancer, but evidence from randomized trials with long-term follow-up is sparse. We randomly assigned 695 men with localized prostate cancer to watchful waiting or radical prostatectomy from October 1989 through February 1999 and collected follow-up data through 2017. Cumulative incidence and relative risks with 95% confidence intervals for death from any cause, death from prostate cancer, and metastasis were estimated in intention-to-treat and per-protocol analyses, and numbers of years of life gained were estimated. We evaluated the prognostic value of histopathological measures with a Cox proportional-hazards model.

Characteristic	All Patients		Patients <65 Yr of Age		Patients ≥65 Yr of Age	
	Radical Prostatectomy (N=347)	Watchful Waiting (N=348)	Radical Prostatectomy (N=157)	Watchful Waiting (N=166)	Radical Prostatectomy (N=190)	Watchful Waiting (N=182)
Age — yr	64.6±64.6	64.5±64.5	60.0±60.0	60.2±60.2	68.4±68.4	68.4±68.4
Mean PSA level — ng/ml	13.5	12.3	12.7	12.4	14.2	12.2
Tumor stage — no. (%)†						
T1b	33 (9.5)	50 (14.4)	14 (8.9)	22 (13.3)	19 (10.0)	28 (15.4)
T1c	43 (12.4)	38 (10.9)	24 (15.3)	21 (12.7)	19 (10.0)	17 (9.3)
T2	270 (77.8)	259 (74.4)	119 (75.8)	123 (74.1)	151 (79.5)	136 (74.7)
Missing data	1 (0.3)	1 (0.3)	0	0	1 (0.5)	1 (0.5)
WHO grade — no. (%)‡						
1	168 (48.4)	166 (47.7)	76 (48.4)	83 (50.0)	92 (48.4)	83 (45.6)
2	178 (51.3)	182 (52.3)	81 (51.6)	83 (50.0)	97 (51.1)	99 (54.4)
Missing data	1 (0.3)	0	0	0	1 (0.5)	0
Gleason score of biopsy specimen — no. (%)§						
2–4	45 (13.0)	46 (13.2)	25 (15.9)	27 (16.3)	20 (10.5)	19 (10.4)
5 or 6	165 (47.6)	166 (47.7)	69 (43.9)	81 (48.8)	96 (50.5)	85 (46.7)
7	77 (22.2)	82 (23.6)	33 (21.0)	32 (19.3)	44 (23.2)	50 (27.5)
8 or 9	14 (4.0)	21 (6.0)	5 (3.2)	10 (6.0)	9 (4.7)	11 (6.0)
Missing data¶	46 (13.3)	33 (9.5)	25 (15.9)	16 (9.6)	21 (11.1)	17 (9.3)
Method of detection — no. (%)						
Screening‡	18 (5.2)	18 (5.2)	9 (5.7)	7 (4.2)	9 (4.7)	11 (6.0)
Coincidental**	87 (25.1)	91 (26.1)	41 (26.1)	46 (27.7)	46 (24.2)	45 (24.7)
TURP	40 (11.5)	56 (16.1)	19 (12.1)	29 (17.5)	21 (11.1)	27 (14.8)
Symptoms	152 (43.8)	138 (39.7)	68 (43.3)	66 (39.8)	84 (44.2)	72 (39.6)
Other	49 (14.1)	44 (12.6)	20 (12.7)	17 (10.2)	29 (15.3)	27 (14.8)
Missing data	1 (0.3)	1 (0.3)	0	1 (0.6)	1 (0.5)	0
PSA level — no. (%)						
<4 ng/ml	43 (12.4)	63 (18.1)	27 (17.2)	32 (19.3)	16 (8.4)	31 (17.0)
4–6.9 ng/ml	60 (17.3)	60 (17.2)	33 (21.0)	24 (14.5)	27 (14.2)	36 (19.8)
7–10 ng/ml	68 (19.6)	67 (19.3)	23 (14.6)	28 (16.9)	45 (23.7)	39 (21.4)
10.1–20 ng/ml	100 (28.8)	95 (27.3)	43 (27.4)	51 (30.7)	57 (30.0)	44 (24.2)
>20 ng/ml	69 (19.9)	60 (17.2)	30 (19.1)	28 (16.9)	39 (20.5)	32 (17.6)
Missing data	7 (2.0)	3 (0.9)	1 (0.6)	3 (1.8)	6 (3.2)	0
Surgery — no. (%)						
Radical prostatectomy††	289 (83.3)	17 (4.9)	140 (89.2)	9 (5.4)	149 (78.4)	8 (4.4)
Lymph node dissection only	23 (6.6)	4 (1.1)	7 (4.5)	2 (1.2)	16 (8.4)	2 (1.1)
No surgery†††	35 (10.1)	327 (94.0)	10 (6.4)	155 (93.4)	25 (13.2)	172 (94.5)

# Stacked Cumulative Incidence of Causes of Death According to Treatment and Age Group.

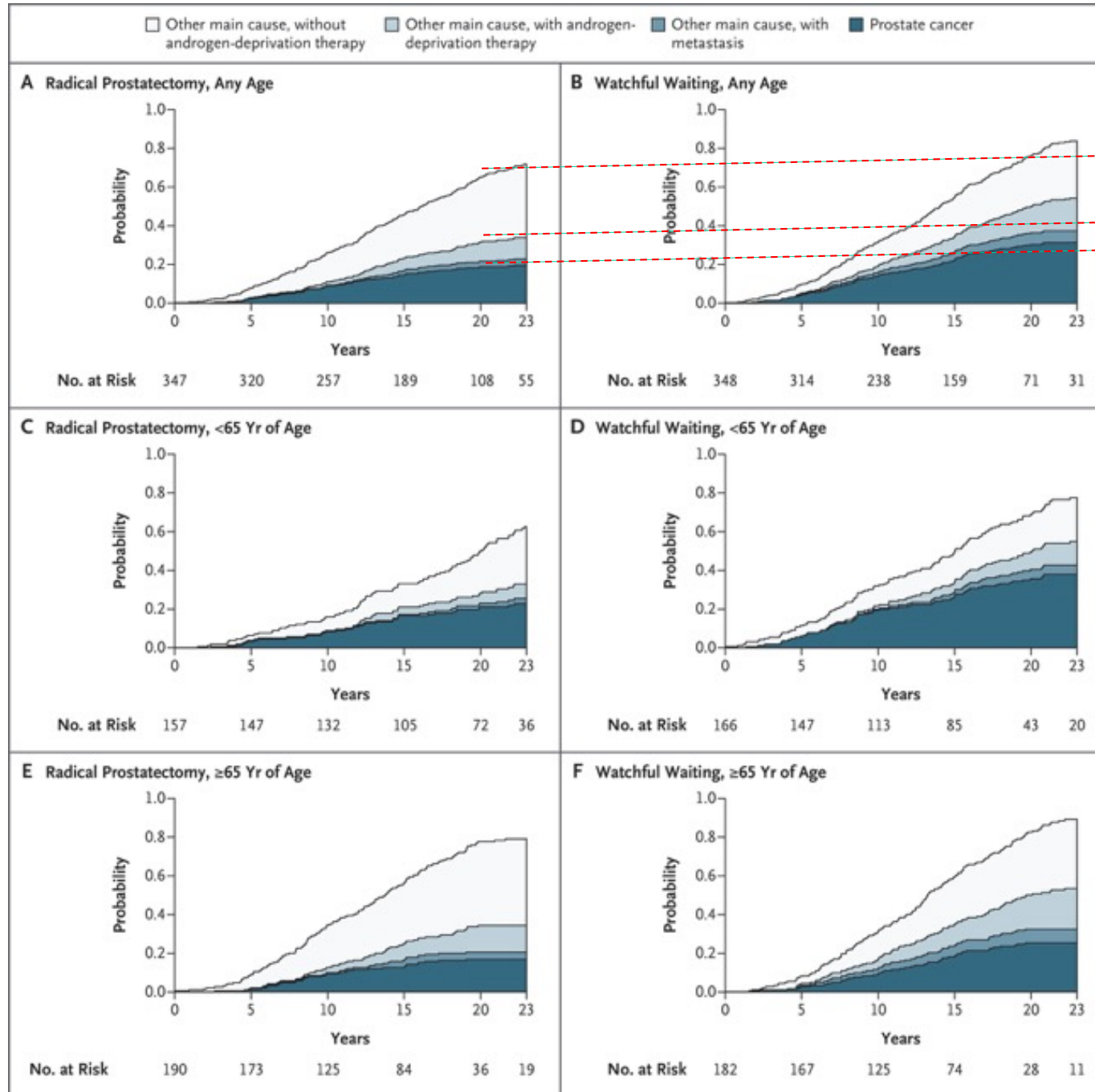


**Table 2. End-Point Estimates at 23 Years and Relative Risk Over the 29-Year Trial Period.\***

End Point	Radical Prostatectomy		Watchful Waiting		Absolute Difference in Risk at 23 Yr (95% CI)	No. Needed to Treat to Prevent End Point at 23 Yr (95% CI)	Relative Risk, Radical Prostatectomy vs. Watchful Waiting (95% CI)†	P Value‡
	No. of Events/ Total No.§	Cumulative Incidence at 23 Yr¶ %	No. of Events/ Total No.§	Cumulative Incidence at 23 Yr¶ %				
Death from any cause								
All patients	261/347	71.9 (67.0–77.0)	292/348	83.8 (79.8–88.1)	12.0 (5.5–18.4)	8.4 (5.4–18.2)	0.74 (0.62–0.87)	<0.001
Patients <65 yr of age	105/157	62.6 (55.1–71.2)	129/166	77.6 (71.1–84.7)	15.0 (4.4–25.5)	6.7 (3.9–22.6)	0.62 (0.48–0.80)	—
Patients ≥65 yr of age	156/190	79.2 (73.4–85.4)	163/182	89.3 (84.6–94.3)	10.1 (2.4–17.8)	9.9 (5.6–41.4)	0.86 (0.69–1.07)	—
Death from prostate cancer‖								
All patients	71/347	19.6 (15.8–24.4)	110/348	31.3 (26.8–36.6)	11.7 (5.2–18.2)	8.6 (5.5–19.3)	0.55 (0.41–0.74)	<0.001
Patients <65 yr of age	39/157	22.8 (17.0–30.6)	63/166	37.9 (31.1–46.3)	15.1 (5.0–25.2)	6.6 (4.0–20.0)	0.50 (0.34–0.75)	—
Patients ≥65 yr of age	32/190	16.9 (12.3–23.1)	47/182	25.3 (19.7–32.6)	8.5 (0.2–16.8)	11.8 (6.0–601.0)	0.63 (0.40–0.99)	—
Distant metastasis**								
All patients	92/347	26.6 (22.3–31.7)	150/348	43.3 (38.3–48.9)	16.7 (9.6–23.7)	6.0 (4.2–10.4)	0.54 (0.42–0.70)	<0.001
Patients <65 yr of age	48/157	30.8 (24.3–39.0)	81/166	49.4 (42.2–57.8)	18.6 (7.9–29.2)	5.4 (3.4–12.7)	0.49 (0.34–0.70)	—
Patients ≥65 yr of age	44/190	23.2 (17.9–30.0)	69/182	37.7 (31.2–45.6)	14.6 (5.2–23.9)	6.9 (4.2–19.2)	0.59 (0.41–0.86)	—

\* The widths of the confidence intervals have not been adjusted for multiplicity.

† Relative risk values are based on a Cox regression of data from the entire 29-year follow-up period.

‡ Since no adjustments were planned for multiplicity, P values are not shown for comparisons within age groups.

§ Data are the numbers of events at 29 years (through December 31, 2017).

¶ Values are estimates of cumulative incidence at 23 years.

‖ Death from other causes was considered as a competing risk in the analysis.

\*\* Death from other causes without previous metastasis was considered as a competing risk in the analysis.

# Stacked Cumulative Incidence of Sites of Metastasis According to Treatment and Age Group.

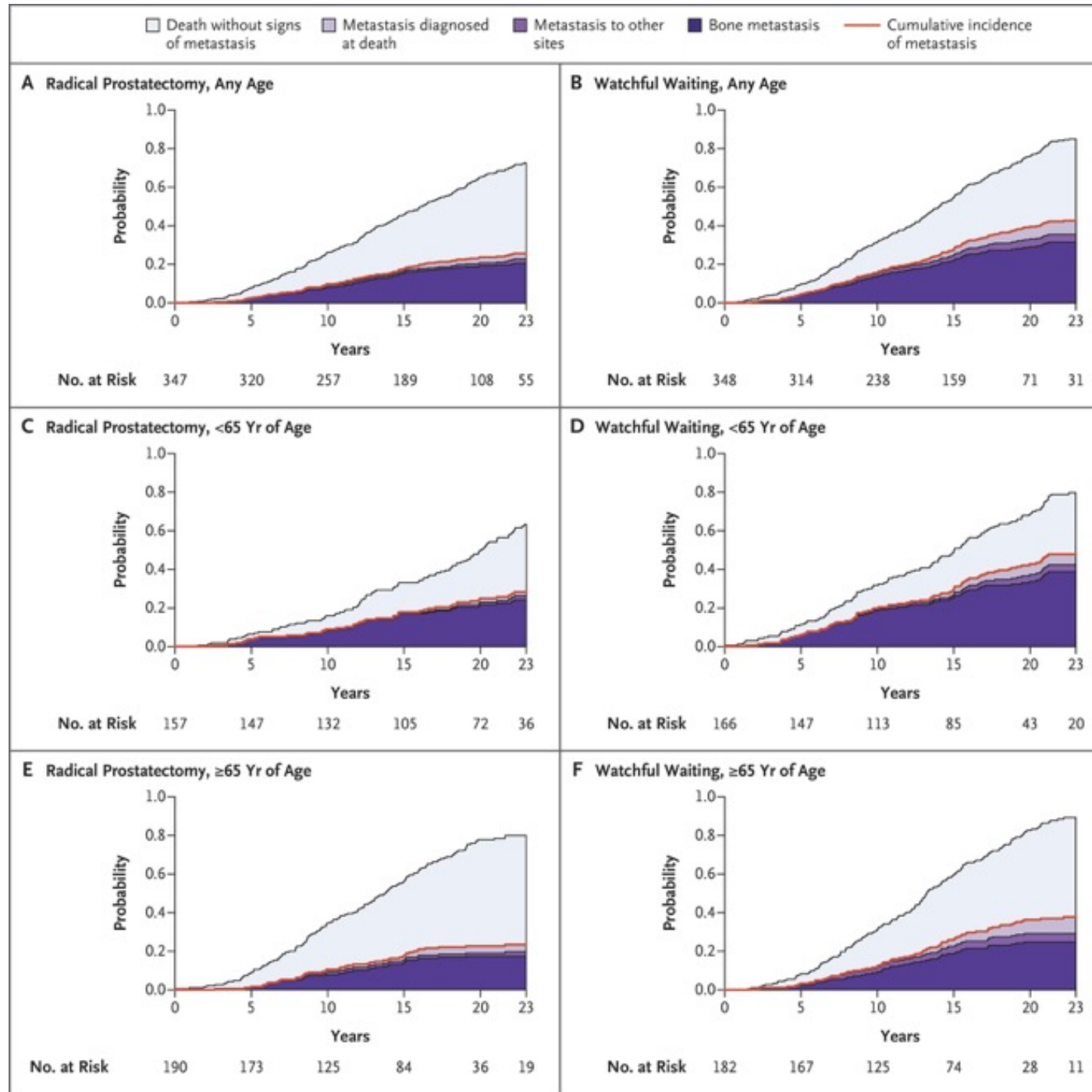


**Table 3.** Univariate and Multivariate Cox Regression Analyses of Histopathological Risk Factors Based on Tumor Specimens from Radical Prostatectomy.

End Point and Risk Factor	No. of Men	No. of Events	Relative Risk with Adjustment for Age Group (95% CI)*	Relative Risk with Adjustment for Age Group and Additional Factors (95% CI)†
<b>Distant metastasis</b>				
Margins				
Negative	184	29	Reference	Reference
Positive	99	32	2.73 (1.63–4.57)	1.26 (0.73–2.20)
Extracapsular extension				
Absent	151	13	Reference	Reference
Present	132	47	6.59 (3.54–12.27)	4.50 (2.34–8.64)
Gleason score of prostatectomy specimen				
3–6	88	4	Reference	Reference
7	157	37	6.27 (2.23–17.59)	3.10 (1.05–9.11)
8 or 9	38	20	17.82 (6.08–52.28)	9.44 (3.09–28.84)
<b>Death from prostate cancer</b>				
Margins				
Negative	184	24	Reference	Reference
Positive	99	24	2.55 (1.42–4.56)	1.16 (0.62–2.15)
Extracapsular extension				
Absent	151	9	Reference	Reference
Present	132	38	7.61 (3.66–15.84)	5.21 (2.42–11.22)
Gleason score of prostatectomy specimen				
3–6	88	3	Reference	Reference
3+4	87	5	1.91 (0.46–7.99)	0.99 (0.23–4.33)
4+3	70	21	11.78 (3.51–39.55)	5.73 (1.59–20.67)
8 or 9	38	19	20.06 (5.93–67.91)	10.63 (3.03–37.30)

\* The model was adjusted for age group (<65 vs. ≥65 years).

† The model was adjusted for age group (<65 vs. ≥65 years), PSA level, margins, capsular extension, and Gleason score.

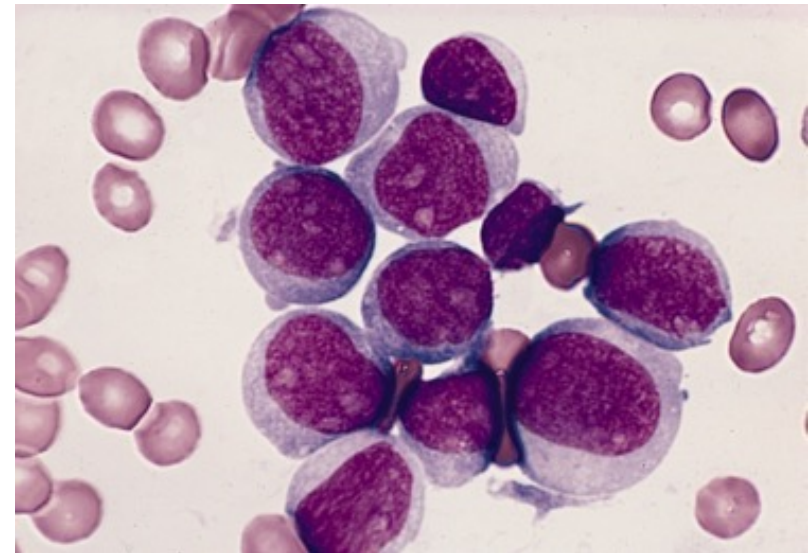
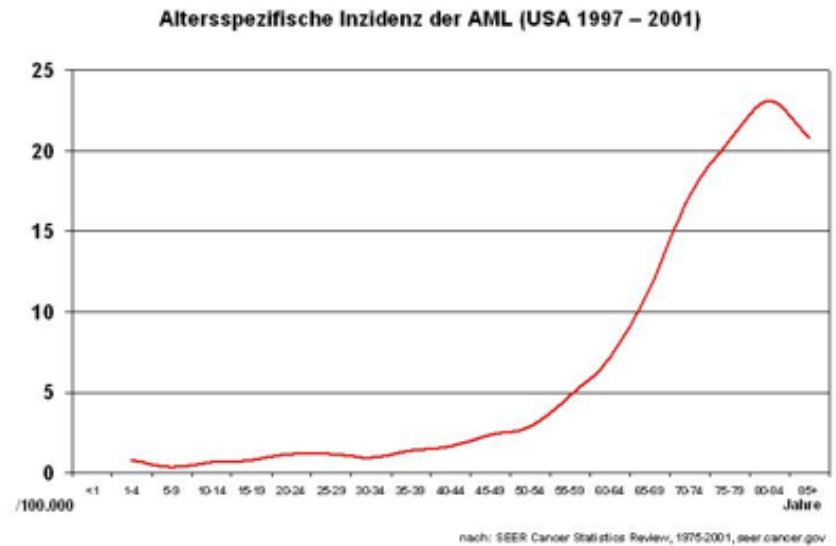
After 29 years of follow-up, at a time when 80% of all the participants had died, lower overall mortality, lower mortality due to prostate cancer, and a lower risk of metastasis prevailed in the radical-prostatectomy group. The findings from a per-protocol analysis with adjustment for nonadherence to the assigned treatment did not differ from the main findings from the intention-to-treat analysis. At 23 years of follow-up, radical prostatectomy resulted in a mean of 2.9 years of life gained. Extracapsular extension and a Gleason score of 8 or 9 in the radical-prostatectomy group were strong predictors of death from prostate cancer.

In our trial, the absolute benefit associated with radical prostatectomy increased by a factor of more than 2 between 10 and 23 years of follow-up for both overall mortality (from 5.0 to 12.0 percentage points) and disease-specific mortality (from 5.5 to 11.7 percentage points), whereas the relative risks remained stable during this period for both overall mortality (0.75 to 0.74) and disease-specific mortality (0.56 to 0.54). In the Prostate Cancer Intervention versus Observation Trial (PIVOT), at 19 years of follow-up, the relative risk of death from prostate cancer was 0.65 and thus similar to our results, but the absolute difference in risk was only 4 percentage points, reflecting the low baseline risk. The difference in risk in PIVOT is similar to that in the SPCG-4 10-year follow-up analysis. Only long-term follow-up can reveal whether the PIVOT results will catch up with the SPCG-4 results after passing of the lead time associated with PSA testing or whether they will remain unchanged as a result of a substantial overdiagnosis of nonlethal prostate cancer.

**In clinically detected prostate cancer, the benefit of radical prostatectomy in otherwise healthy men can be substantial, with a mean gain of almost 3 years of life after 23 years of follow-up.**

The remaining expected lifetime is important in decision making, with the reservation that it is hard to predict. When our results are applied to inform current practice, several issues have to be considered: the lead time induced by screening, the addition to modern cohorts of overdiagnosed nonlethal cancers, and the influence of modern diagnostics on the definition of risk groups. Furthermore, even if the relative risks in our trial were fully applicable to modern studies, the amount of absolute benefit is highly dependent on baseline risk.

Die akute myeloische Leukämie (AML) ist eine maligne (bösartige) Erkrankung des blutbildenden Systems, und zwar der Myelopoese, also des Teils des blutbildenden Systems, der für die Bildung von Granulozyten, Monozyten, Erythrozyten und Megakaryozyten verantwortlich ist. Sie führt zu einer zum Teil massiven Vermehrung unreifer Vorstufen der Myelopoese im Knochenmark und in der Mehrzahl der Fälle auch im Blut (Leukozytose). Die AML ist eine seltene Erkrankung mit einer Inzidenz von etwa drei Neuerkrankungen/100.000 im Jahr. In Deutschland treten etwa 3.600 Neuerkrankungen pro Jahr auf. Sie ist überwiegend eine Erkrankung des höheren Lebensalters, das mediane Alter bei Diagnosestellung liegt bei 63 Jahren. Die AML macht etwa 80 % aller akuten Leukämien bei Erwachsenen aus. Männer sind etwas häufiger betroffen als Frauen (Verhältnis 1,4:1). Im Kindesalter haben nur 15 bis 20 % der Patienten mit einer akuten Leukämie eine AML. Allerdings handelt es sich bei der seltenen akuten Leukämie im Neugeborenenalter meist um eine AML. Grundlage der Diagnostik ist die mikroskopische Untersuchung von Knochenmarkausstrichen. Charakteristische Merkmale wie z. B. der Nachweis von Auerstäbchen ermöglichen die Zuordnung der Blasten zur myeloischen Reihe. Bei Auerstäbchen handelt es sich um feine, stäbchenförmige Granula oder große, ovale bis elliptiforme Einschlüsse (Auer-Körper) im Zytoplasma unreifer Leukämiezellen. Gegebenenfalls mit Hilfe zusätzlicher zytochemischer Untersuchungen (Peroxidase, Esterase, PAS-Reaktion) gelingt in der Mehrzahl der Fälle die Abgrenzung einer AML von einer ALL und die Einordnung entsprechend der FAB-Klassifikation.



# Immune Escape of Relapsed AML Cells after Allogeneic Transplantation

As consolidation therapy for acute myeloid leukemia (AML), allogeneic hematopoietic stem-cell transplantation provides a benefit in part by means of an immune-mediated graft-versus-leukemia effect. We hypothesized that the immune-mediated selective pressure imposed by allogeneic transplantation may cause distinct patterns of tumor evolution in relapsed disease. We performed enhanced exome sequencing on paired samples obtained at initial presentation with AML and at relapse from 15 patients who had a relapse after hematopoietic stem-cell transplantation (with transplants from an HLA-matched sibling, HLA-matched unrelated donor, or HLA-mismatched unrelated donor) and from 20 patients who had a relapse after chemotherapy. We performed RNA sequencing and flow cytometry on a subgroup of these samples and on additional samples for validation.

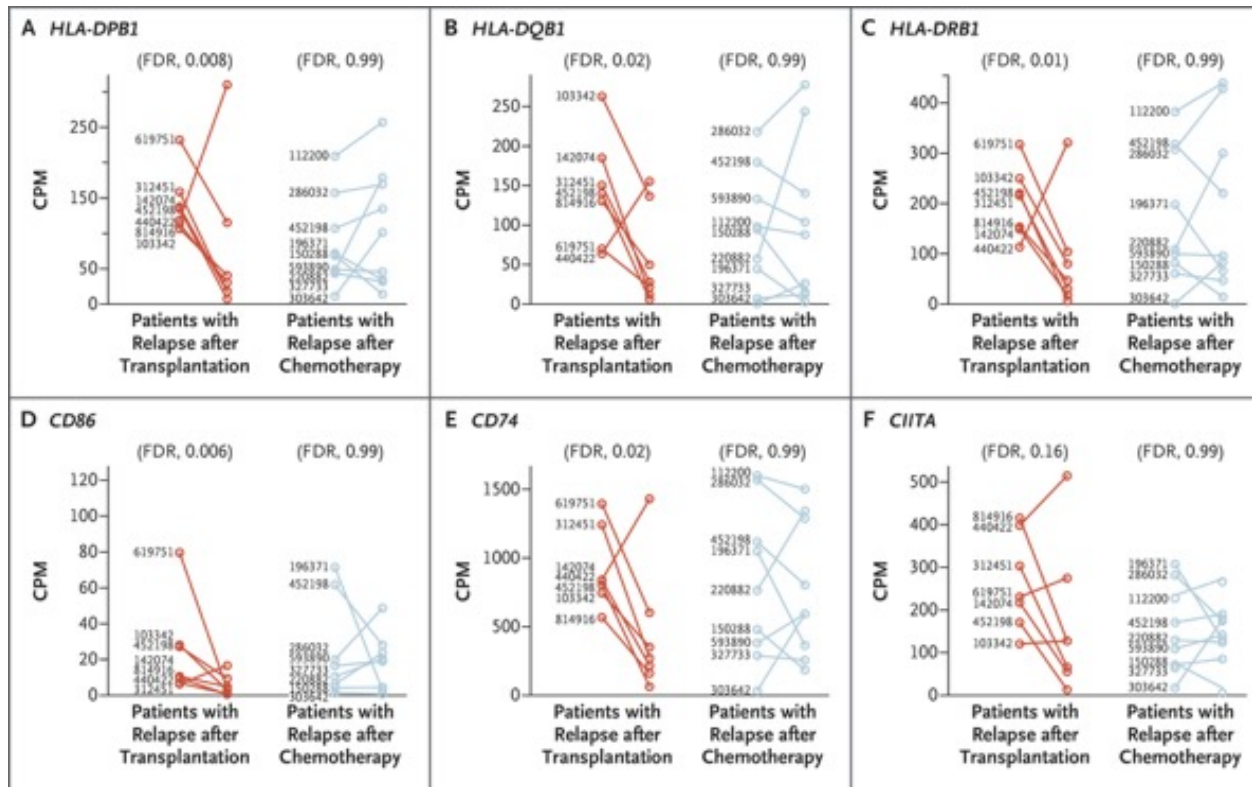
Most patients with acute myeloid leukemia (AML) ultimately have a relapse and die from progressive disease, despite initial sensitivity to chemotherapy. For this reason, patients who are in complete remission generally receive consolidation treatment with either additional chemotherapy or allogeneic hematopoietic stem-cell transplantation, a therapy that is thought to provide a benefit in part by means of an immune-mediated graft-versus-leukemia effect. Although allogeneic transplantation is an effective therapy for patients with AML, relapse after transplantation is common and is associated with particularly poor outcomes.

In this study, we performed a comprehensive analysis of samples from patients who had a relapse of AML after transplantation to define the genetic and epigenetic alterations that allow leukemic cells to escape the graft-versus-leukemia effect and to determine whether the dysregulation of known immune-related genes is a common feature of relapse after transplantation.

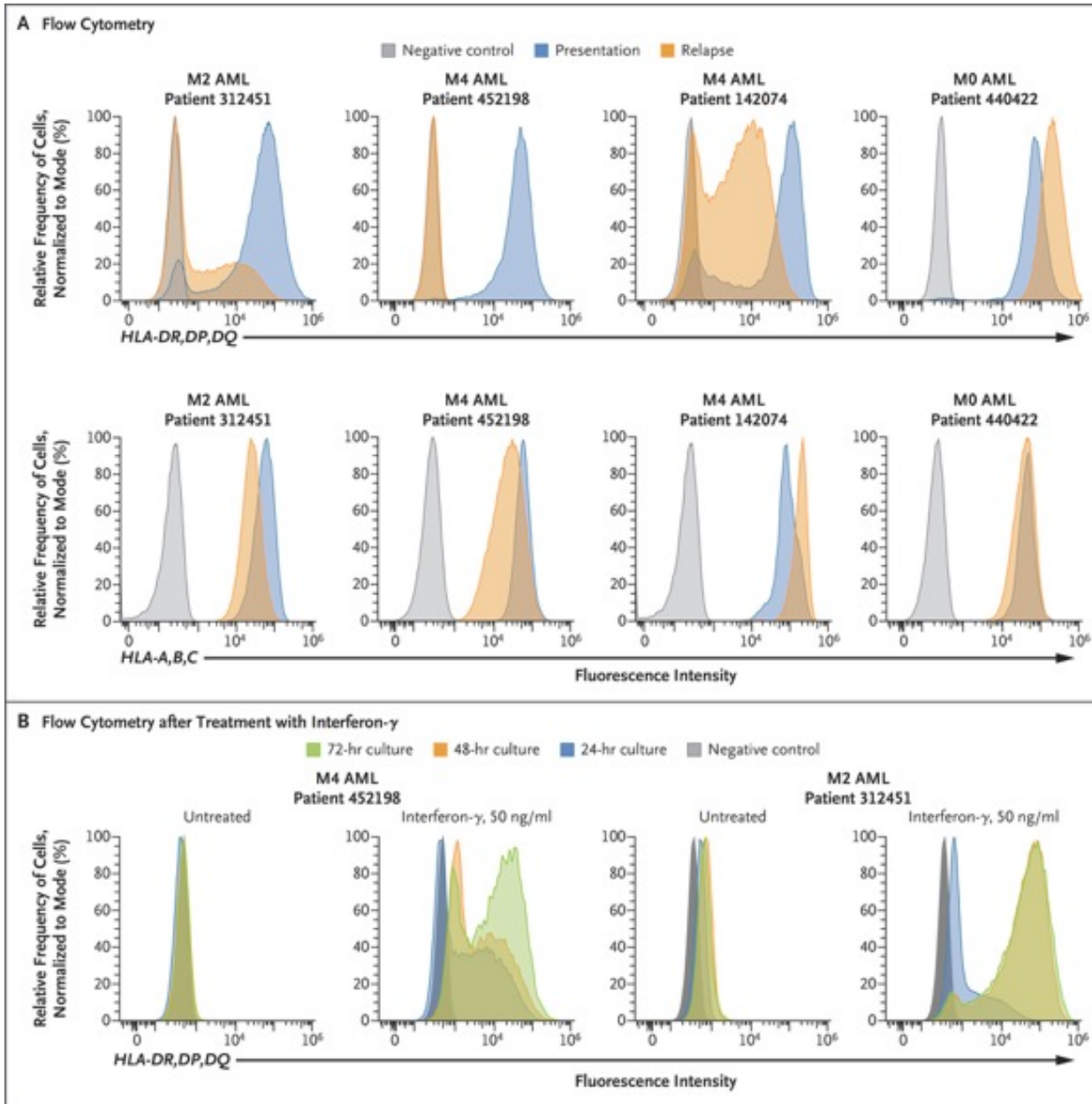
Previous studies showed down-regulation or inactivation of major histocompatibility complex (MHC) genes in AML cells at the time of relapse. MHC genes have a critical role in antigen presentation and stimulation of antitumor immune responses, and their loss in post-transplantation relapse is one clear-cut mechanism by which relapsing tumors can escape immune surveillance.

AML relapse after transplantation was not associated with the acquisition of relapse-specific mutations in immune-related genes. However, it was associated with dysregulation of pathways that may influence immune function, including down-regulation of MHC class II genes, which are involved in antigen presentation. These epigenetic changes may be reversible with appropriate therapy.



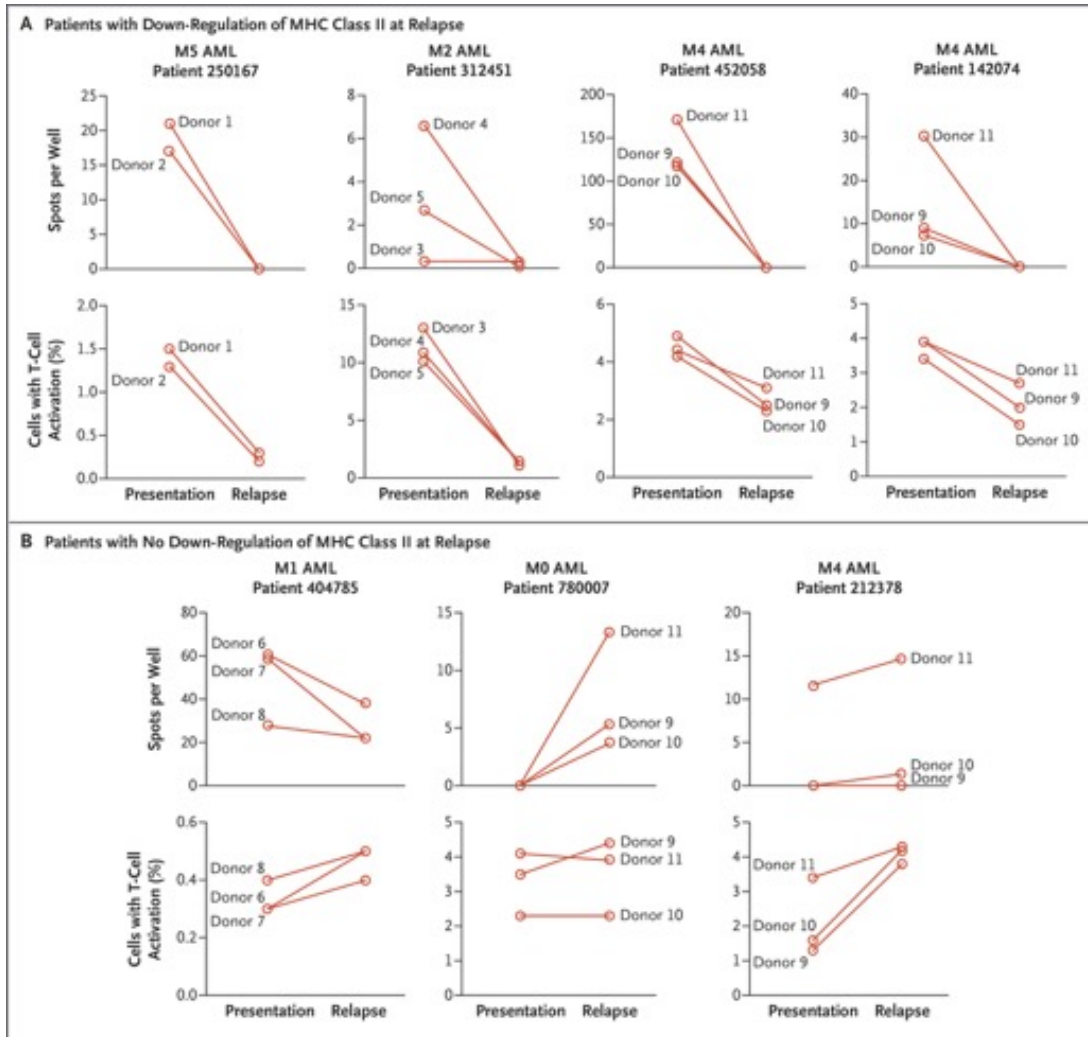


**Expression of Immune-Related Genes among Patients with a Relapse of AML.** RNA sequencing was performed on enriched acute myeloid leukemia (AML) blasts from paired samples obtained at initial presentation and at relapse from patients who had a relapse after transplantation and from patients who had a relapse after chemotherapy. Each panel shows the gene expression in individual patients; the numbers are patient identifiers. The lines show the change in gene expression between the presentation sample (left data point) and the relapse sample (right data point). Among the patients with a post-transplantation relapse, 221 genes showed significant (false discovery rate [FDR], <0.05) differential expression between the presentation and relapse samples. These included genes involved in immune function, such as the major histocompatibility complex (MHC) class II genes *HLA-DPB1*, *HLA-DQB1*, and *HLA-DRB1* (Panels A, B, and C, respectively), as well as the gene encoding the T-cell costimulatory protein CD86 and the gene encoding the MHC class II invariant chain CD74 (Panels D and E, respectively). In four of seven post-transplantation relapse samples, there was also decreased expression of *CIITA*, a master transcriptional regulator of MHC class II genes (Panel F); this change was not significant. CPM denotes count per million mapped sequence reads.



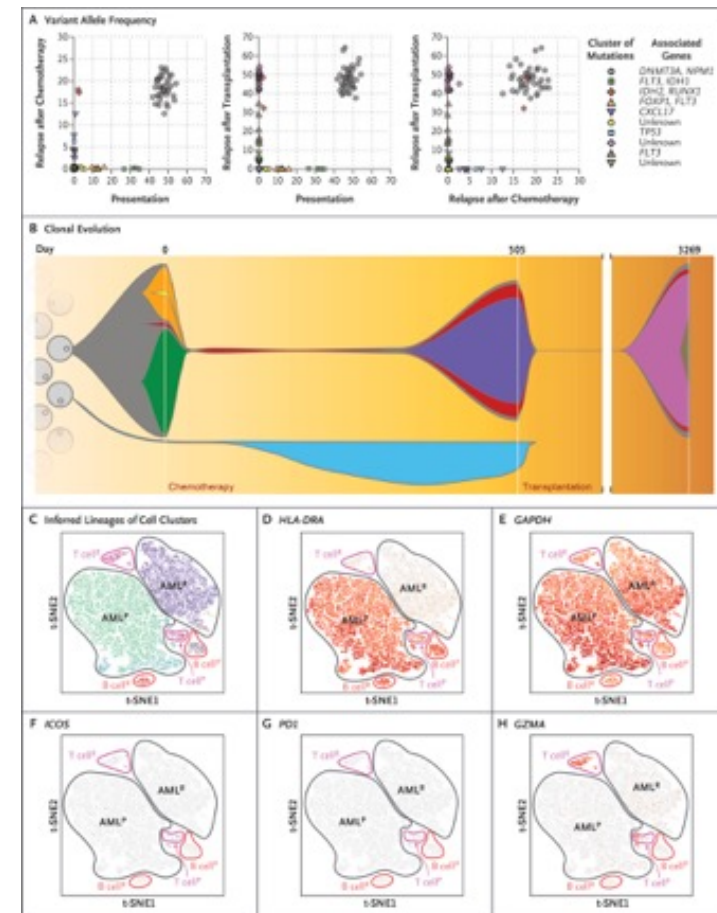
**Expression of MHC Proteins on the Surface of AML Cells from Patients with a Relapse after Transplantation.** To validate the results of RNA sequencing, which showed down-regulation of MHC class II genes in some patients with a relapse of AML after transplantation, flow cytometry was performed (Panel A). Shown is the expression of MHC proteins on AML cells (CD45 dim, side scatter low) in presentation and relapse samples from patients with a post-transplantation relapse, as compared with negative controls. The samples were stained with a fluorescently tagged antibody that recognized MHC class II proteins (HLA-DR, HLA-DP, and HLA-DQ; top row) or an antibody that recognized MHC class I proteins (HLA-A, HLA-B, and HLA-C; bottom row). The sample from Patient 440422 is an example of a case that did not show down-regulation of MHC class II at relapse; this finding is consistent with the data from RNA sequencing for this patient. To determine whether the down-regulation of MHC class II at relapse was reversible, flow cytometry was performed on samples that were treated with interferon- $\gamma$  (Panel B). Shown is the expression of MHC class II proteins on AML cells in relapse samples from patients with a post-transplantation relapse associated with down-regulation of MHC class II, as compared with negative controls. The cells were cultured for up to 72 hours in the presence or absence of interferon- $\gamma$ , and the expression of MHC class II proteins was assessed at different time points.

## In Vitro CD4+ T-Cell Activation Induced by AML Cells from Patients with a Relapse after Transplantation.



Cryopreserved presentation and relapse samples from patients with a post-transplantation relapse who had down-regulation of MHC class II at relapse (Panel A) or did not have down-regulation of MHC class II at relapse (Panel B) were incubated with HLA-mismatched third-party donor CD4+ T cells for 4 days. CD4+ T cells from two or three separate donors were used for each assay. Activation of CD4+ T cells was measured with an interferon- $\gamma$  enzyme-linked immunospot assay (top row in each panel) or with flow cytometry for activation markers CD137 and CD279 (bottom row in each panel). Relapse samples from patients who had down-regulation of MHC class II (Panel A) caused minimal stimulation of third-party CD4+ T cells, whereas paired presentation samples stimulated third-party CD4+ T cells effectively. In contrast, paired presentation and relapse samples from patients who did not have down-regulation of MHC class II (Panel B) stimulated CD4+ T cells equivalently. For each patient, the French–American–British classification of AML is shown; a classification of M0 AML indicates AML with minimal differentiation, M1 AML indicates AML with minimal maturation, M2 AML indicates AML with maturation, M4 AML indicates acute myelomonocytic leukemia, and M5 AML indicates acute monoblastic leukemia.

Clonal Evolution of AML in a Patient with a Relapse after Chemotherapy and after Transplantation. Clonal evolution with post-chemotherapy and post-transplantation relapse was analyzed in one patient in the study (Patient 452198). Panel A shows scatter plots of somatic mutations that were found in AML cells obtained at presentation, at relapse after chemotherapy, and at relapse after transplantation according to variant allele frequency. Each data point represents the variant allele frequency of a single somatic mutation in the two indicated samples. At each time point, clusters of mutations are designated with a distinct color and shape to indicate that they represent distinct clonal populations. The mutated genes associated with each cluster are indicated in the key. Panel B shows a “fish plot” that represents the clonal evolution that can be inferred from the variant allele frequencies of somatic mutations that are shown on the scatter plots. Chemotherapy began on day 0, the first relapse was detected at day 505, and the second relapse was detected at day 3269. The dominant subclone at both post-chemotherapy relapse and post-transplantation relapse was derived from a small subclone that was detected at presentation (in red), which evolved with new mutations of unknown significance after each therapy. Panels C through H show the results of single-cell RNA sequencing that was performed on cryopreserved presentation and post-transplantation relapse samples. Cells obtained at both presentation and relapse were superimposed onto a single two-dimensional plot and clustered according to their unique expression profiles with the use of t-distributed stochastic neighbor embedding (t-SNE). The axes (t-SNE1 and t-SNE2) show dimensionless values that were assigned to individual cells by the t-SNE algorithm, which places cells that have similar expression profiles close to one another. At presentation (P) and relapse (R), AML cells (AML<sup>P</sup> and AML<sup>R</sup>) represent the dominant cell type, and small populations of T cells (T cell<sup>P</sup> and T cell<sup>R</sup>) and B cells (B cell<sup>P</sup> and B cell<sup>R</sup>) can also be discerned. Panel C shows a t-SNE plot in which the cells are colored and labeled according to their inferred identity (AML<sup>P</sup>, AML<sup>R</sup>, B cell, or T cell); AML cells from presentation and relapse have unique expression patterns that identify them as distinct entities. In Panels D through H, the intensity of the coloring is relative to the expression of each indicated gene.



In Panel D, expression of *HLA-DRA* is detected in the vast majority of AML cells at presentation but in virtually none at relapse; however, expression of *HLA-DRA* is detected in B cells at both presentation and relapse. In Panel E, expression of the housekeeping gene *GAPDH* is similar in all cell types at both presentation and relapse. In Panels F and G, expression of genes associated with T-cell exhaustion (*ICOS* and *PD1*, respectively) is detected in scattered T cells at presentation and is not increased at relapse. In Panel H, expression of the gene encoding the T-cell activation marker granzyme A (*GZMA*) is strongly detected in a subset of T cells at both presentation and relapse.

Since the graft-versus-leukemia effect contributes to the therapeutic benefit of allogeneic hematopoietic stem-cell transplantation in patients with AML, we speculated that relapse of AML after transplantation might be driven by genetic changes that influence immune function. In this small sample, mutations in known immune-regulatory genes were uncommon in post-transplantation relapses, a finding consistent with the idea that such changes are not a common cause of relapse.

The reversibility of down-regulation of MHC class II by interferon- $\gamma$  suggests that this event is epigenetic in nature. Single-cell RNA sequencing in one patient (Patient 452198) revealed high expression of MHC class II genes in the vast majority of AML cells at presentation. This finding suggests that immunologically resistant AML cells were rare or absent at presentation; furthermore, there was no evidence of a subclone with low MHC class II gene expression. Selection of these cells presumably occurred after the transplanted immune cells exerted selective pressure against AML cells that could be recognized immunologically. This process has been described as immunoediting in solid tumors, in which tumor clones evolve in response to immune-mediated selective pressure and ultimately escape, leading to relapse. Although the use of immunosuppression after transplantation could potentially contribute to down-regulation of MHC class II, we did not detect a significant correlation between loss of MHC class II expression and use of graft-versus-host disease prophylaxis at the time of relapse.

In conclusion, this study showed that AML cells that escaped the immune surveillance provided by allogeneic T cells after allogeneic hematopoietic stem-cell transplantation frequently had dysregulation of a number of pathways that regulate immune function. These changes appeared to be epigenetic in nature in at least some cases, which suggests that therapeutic strategies to resensitize AML cells to the graft-versus-leukemia effect may be feasible.

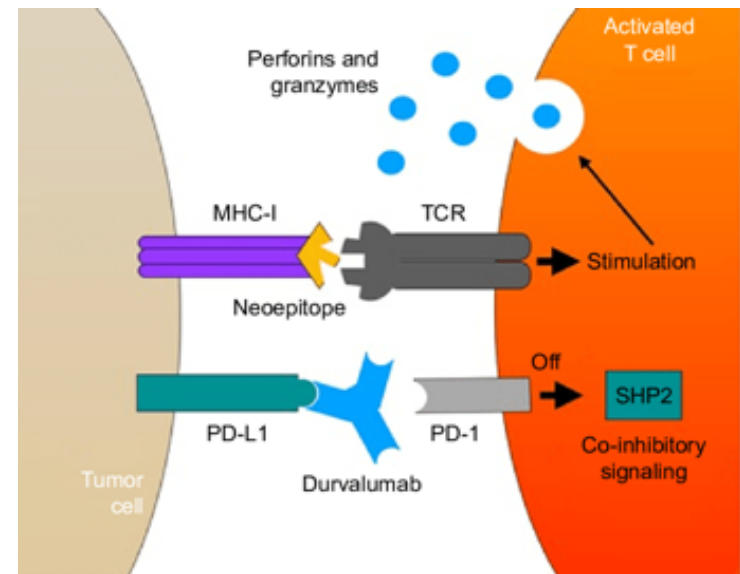
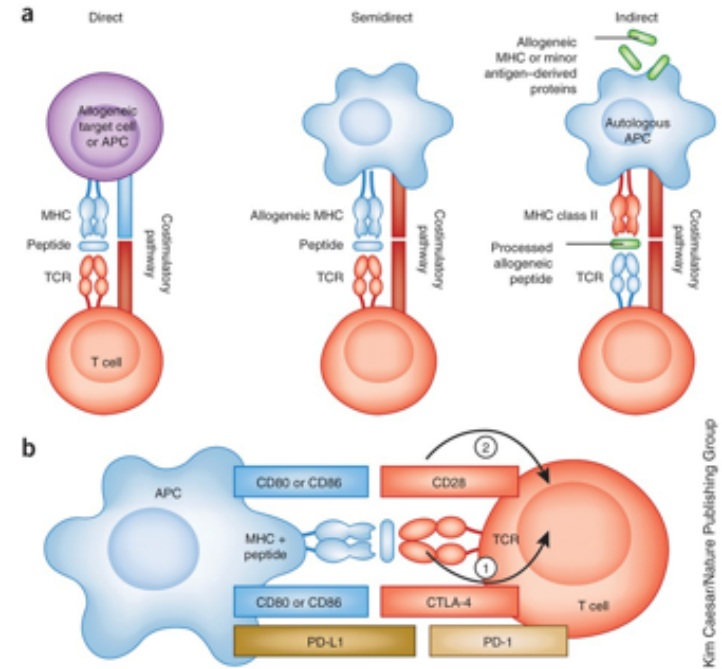


A 73-year-old man presented to the dermatology clinic with a persistent, generalized rash that had been present for 3 months and was associated with occasional itching. He had no history of any previous dermatoses or drug allergies; he was an active smoker, with a smoking history of 40 pack-years. Physical examination revealed a symmetric, generalized erythematous rash (Panel A), with overlying scaling and desquamation involving the hands and feet. He was initially treated with topical glucocorticoid therapy, then with oral prednisone and antihistamines, and then with intravenous glucocorticoids, but had no relief. Skin biopsy revealed a slight acanthosis and parakeratosis with a granulocytic infiltrate — findings that were consistent with an erythrodermic dermatitis. Given the patient's smoking history and concern that there was an underlying neoplasm associated with the dermatitis, a radiograph of the chest was obtained, which showed an opacity in the left lung. Paraneoplastic erythroderma was suspected, and computed tomography of the chest confirmed the presence of a pulmonary nodule in the left upper lobe (Panel B). The patient underwent upper lobectomy of the left lung and lymph node dissection. Histologic examination revealed a moderately differentiated squamous-cell carcinoma. Paraneoplastic erythroderma is an uncommon initial manifestation of lung cancer. It can also be associated with hematologic cancers and other solid-organ cancers. One month after resection, the patient had complete resolution of the rash (Panel C). One year later, he had no further rash or tumor recurrence.

CD80 bzw. B7-1 ist ein Oberflächenmerkmal antigenpräsentierender Zellen (B-Lymphozyten, dendritische Zellen und Makrophagen), das die Aktivierung und das Überleben von T-Zellen kostimuliert. CD80 ist ein Typ-I-Membranprotein, das Mitglied der Immunglobulin-Superfamilie (IgSF) ist. Es dient als Ligand für 2 verschiedene Oberflächenproteine der T-Zelle, CD28 und CTLA-4, und wirkt im Tandem mit CD86. B7-1 wird von aktivierten antigenpräsentierenden Zellen wie Makrophagen und dendritischen Zellen gebildet. Es bildet Homodimere. Die Aktivierung über einen Kostimulator liefert das notwendige zweite Aktivierungssignal für T-Zellen. B7-1 bindet – wie auch B7-2 – an CD28 (T-Zell-aktivierend), CTLA-4 (T-Zell-inaktivierend) oder PD-L1. B7-1 ist glykosyliert und phosphoryliert.

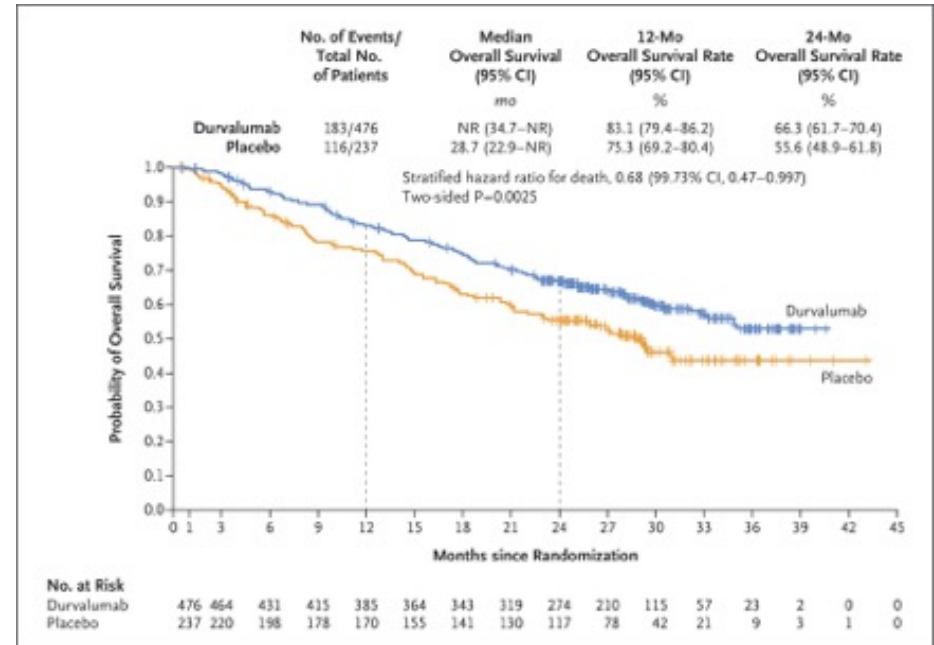
Durvalumab ist ein Checkpointinhibitor und wird zur Immuntherapie eingesetzt. Der Antikörper bindet spezifisch an PD-L1 (programmed cell death ligand 1). Durvalumab ist ein Checkpointinhibitor und wird zur Immuntherapie eingesetzt. Der Antikörper bindet spezifisch an PD-L1 (programmed cell death ligand 1).

PD-L1 interagiert mit PD-1 (programmed cell death protein 1) und CD80 (Lymphozyten-Aktivierungsantigen) und hemmt dadurch die Aktivität von T-Zellen (zytotoxische Aktivität, Proliferation, Produktion von Zytokinen). Dies ist ein Mechanismus der Tumorzellen, um sich gegen das körpereigene Immunsystem zu schützen (Immunevasion). Durch Durvalumab werden die Wechselwirkung von PD-L1/PD-1 und PD-L1/CD80 unterdrückt sowie Proliferation und Aktivität von T-Zellen gegenüber Tumorzellen (antitumorale Antwort) verstärkt. Die Plasmahalbwertszeit beträgt circa 18 Tage.



# Overall Survival with Durvalumab after Chemoradiotherapy in Stage III NSCLC

An earlier analysis in this phase 3 trial showed that durvalumab significantly prolonged progression-free survival, as compared with placebo, among patients with stage III, unresectable non–small-cell lung cancer (NSCLC) who did not have disease progression after concurrent chemoradiotherapy. Here we report the results for the second primary end point of overall survival. We randomly assigned patients, in a 2:1 ratio, to receive durvalumab intravenously, at a dose of 10 mg per kilogram of body weight, or matching placebo every 2 weeks for up to 12 months. Randomization occurred 1 to 42 days after the patients had received chemoradiotherapy and was stratified according to age, sex, and smoking history. The primary end points were progression-free survival (as assessed by blinded independent central review) and overall survival. Secondary end points included the time to death or distant metastasis, the time to second progression, and safety. Durvalumab is a selective, high-affinity, engineered, human IgG1 monoclonal antibody that blocks PD-L1 binding to PD-1 and CD80, allowing T cells to recognize and kill tumor cells.



Overall Survival in the Intention-to-Treat Population. Shown are Kaplan–Meier curves for overall survival. Tick marks indicate censored data, and the dashed vertical lines indicate the times of landmark analyses of overall survival. The intention-to-treat population included all the patients who underwent randomization. In this analysis of overall survival, the hazard ratio and its corresponding confidence interval of 100[1– $\alpha$ ], with adjustment for the interim analysis, are presented. NR denotes not reached.



Updated Analysis of Time to Death or Distant Metastasis in the Intention-to-Treat Population. Shown are Kaplan–Meier curves for the time to death or distant metastasis, defined according to the Response Evaluation Criteria in Solid Tumors, version 1.1, and assessed by means of blinded independent central review. Tick marks indicate censored data.

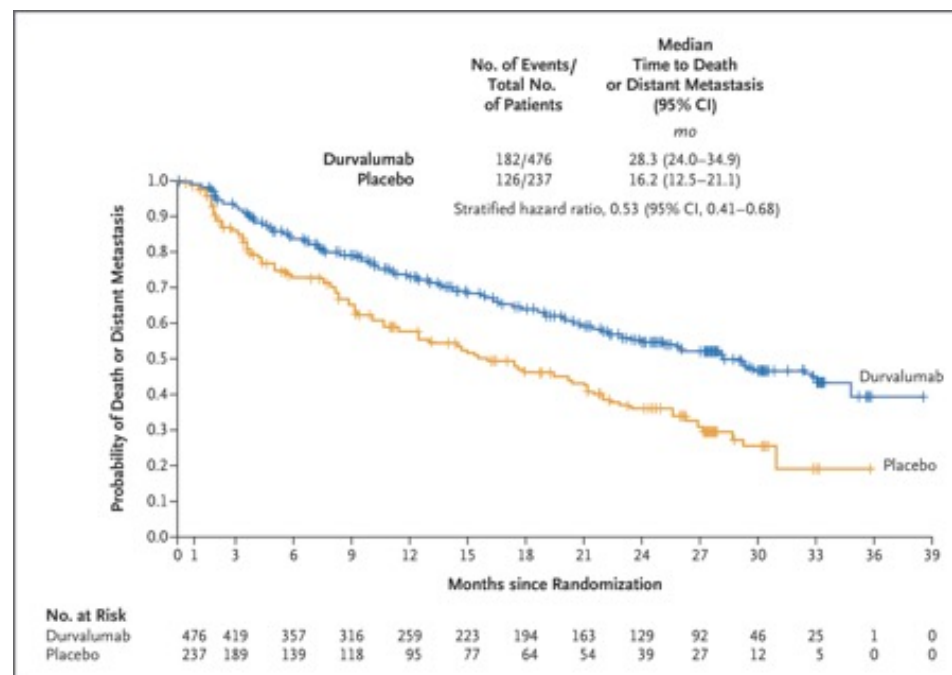


**Table 1.** Updated Incidence of New Lesions, as Assessed by Blinded Independent Central Review, in the Intention-to-treat Population.\*

New Lesion Site	Durvalumab Group (N=476)	Placebo Group (N=237)
	<i>no. of patients (%)</i>	
Any site	107 (22.5)	80 (33.8)
Lung	60 (12.6)	44 (18.6)
Lymph nodes	31 (6.5)	27 (11.4)
Brain	30 (6.3)	28 (11.8)
Liver	9 (1.9)	8 (3.4)
Bone	8 (1.7)	7 (3.0)
Adrenal gland	3 (0.6)	5 (2.1)
Other	10 (2.1)	5 (2.1)

\* Lesions were assessed according to the Response Evaluation Criteria in Solid Tumors, version 1.1. A patient may have had more than one new lesion site.

As of the data-cutoff date, a second progression event or death occurred in 361 patients (217 in the durvalumab group and 144 in the placebo group). The time to second progression or death as assessed by the investigators according to local standard practice was longer in the durvalumab group than in the placebo group (median, 28.3 months [95% CI, 25.1 to 34.7] vs. 17.1 months [95% CI, 14.5 to 20.7]; stratified hazard ratio, 0.58; 95% CI, 0.46 to 0.73)

The updated results for secondary end points, including the time to death or distant metastasis, the incidence of new lesions, and the objective response rate, remain consistent with those that were previously reported and continue to show the substantial anticancer activity of durvalumab treatment in patients after induction therapy and its favorable effect on preventing metastatic spread, which may help to explain the observed survival benefit. In addition, durvalumab therapy resulted in a longer time to second progression or death than placebo, as well as longer times to the first subsequent therapy or death and to the second subsequent therapy or death — results that show the long-term benefit of durvalumab treatment.

No new safety signals were identified after further follow-up. These findings help to define the safety profile of durvalumab use after chemoradiotherapy, despite the trial being limited in its ability to distinguish or assign causality for some adverse events or to identify risk factors for their occurrence, owing to incomplete data regarding previous treatment.

In conclusion, this trial showed a survival advantage with durvalumab therapy after concurrent chemoradiation therapy in patients with stage III, unresectable NSCLC.

# Substance-Use Disorders in Later Life

**Table 1. Use of DSM-5 Criteria for the Diagnosis of Substance-Use Disorder in Older Adults.\***

DSM-5 Criterion	Application of Criterion for Older Adult
Substance taken in greater amount than intended	Older adult may be impaired using the same amount taken when younger
There is persistent desire or unsuccessful effort to cut down or control use	Older adult may not realize use is problematic, especially with long-term use
There is excessive time spent to obtain, use, or recover from the substance	Same
There is craving for the substance	Same
Repeated use leads to inability to perform role in the workplace or at school or home	Role impairment is less pertinent; older adult may be retired and may be living alone
Use continues despite negative consequences in social and interpersonal situations	Same
Valued social or work-related roles are stopped because of use	Effect of substance use on social roles is less obvious if older adult is no longer working
Repeated substance use occurs in potentially dangerous situations	Same; older adult may be at increased risk for impaired driving
Substance use not deterred by medical or psychiatric complication	Same; medical consequences can be serious, including confusion, falls with injury, and psychiatric symptoms
Tolerance develops: increasing amount is needed to obtain effects	Symptomatic impairment may occur without an obvious need for increasing the amount
Withdrawal syndrome occurs or patient takes substance to prevent withdrawal	Withdrawal syndrome can occur with more subtle symptoms such as confusion

\* DSM-5 denotes *Diagnostic and Statistical Manual of Mental Disorders*, fifth edition.

Because of changes in physiology and metabolism with aging, older adults may have increased sensitivity to illicit substances without evidence of tolerance. Relying on an older patient's report of the frequency and quantity of substance use as indicators of problematic use can lead to an underestimate of negative consequences, especially for persons with lower levels of alcohol consumption or use of other substances. Older adults and their family members may not realize that long-term patterns of drinking or drug use can have deleterious effects with aging. Coexisting medical conditions and prescription medications heighten the risk of adverse consequences, including new or exacerbated cognitive impairment, difficulty sleeping, and increased susceptibility to falls.

**Table 2. Signs of Possible Problematic Substance Use in Older Adults.**

Psychiatric symptoms: sleep disturbances, frequent mood swings, persistent irritability, anxiety, depression

Physical symptoms: nausea, vomiting, poor coordination, tremors

Physical signs: unexplained injuries, falls, or bruises; malnutrition; evidence of self-neglect, such as poor hygiene

Cognitive changes: confusion and disorientation, memory impairment, daytime drowsiness, impaired reaction time

Social and behavioral changes: withdrawal from usual social activities, family discord, premature requests for refills of prescription medications

A validated approach specifically designed to screen older adults for substance-use disorders is currently lacking. However, use of a two-question prescreening tool, such as the one described above, combined with further investigative questions from the clinician to identify possible areas of concomitant impairment in functioning, may be useful in general practice for detecting problems involving substance use. Since older patients may lack awareness that their substance use is problematic or harmful, it is important that the assessment includes input from family members and acquaintances who know the patient well. A number of changes in an older adult's functional status may indicate problematic substance use. **The 2013 National Survey on Drug Use and Health showed heavy drinking (defined as drinking five or more drinks on the same occasion on each of 5 or more days in the past 30 days) among 4.7% of persons 60 to 64 years of age and among 2.1% of those 65 years of age or older, as well as binge drinking (defined as drinking five or more drinks on the same occasion on at least 1 day in the past 30 days) among 14.1% of persons 60 to 64 years of age and 9.1% among those 65 years of age or older.**

**Table 3. Treatment of Alcohol-Use Disorder in Older Patients.**

Indication and Medication	Onset of Action	Rate of Metabolism	Metabolized by Liver	Dose* <i>mg</i>
<b>Treatment of alcohol withdrawal</b>				
Chlordiazepoxide	Intermediate	Long	Yes	25–50
Diazepam	Fast	Long	Yes	5–10
Lorazepam	Intermediate	Intermediate	No	1–2
Oxazepam	Slow	Short	No	15–30
<b>Long-term management†</b>				
Naltrexone			Yes	25–50, daily
Acamprosate			No	666, three times a day
Disulfiram			Yes	500, daily

\* Dosing frequency for the treatment of alcohol withdrawal should be based on assessment of alcohol withdrawal symptoms.

† Naltrexone is an opioid-receptor antagonist, acamprosate is a possible partial *N*-methyl-D-aspartate (NMDA) receptor agonist, and disulfiram is an acetaldehyde dehydrogenase inhibitor.

Alcohol withdrawal should be considered as a cause of confusion in an older patient and may be manifested as new-onset confusion in a hospitalized older patient. Interviewing family members can be crucial in establishing the diagnosis and may reveal previously undetected alcohol-use disorder. For older adults who are attempting to stop drinking and who do not have a history of severe withdrawal, alcohol withdrawal can be managed at home with supportive care, as long as a family member will be present at all times.

The pharmacologic agents for long-term management of alcohol-use disorder — disulfiram, acamprosate, and naltrexone — have not been studied adequately in older adults, but their use may be considered in older patients. Naltrexone, an opioid antagonist, may limit heavy drinking by curbing the craving for alcohol but has not been shown to prevent relapse. Patients cannot be receiving opioids for pain while taking naltrexone. Acamprosate has shown limited effectiveness, and diarrhea is a common adverse effect. Disulfiram, an acetaldehyde dehydrogenase inhibitor, causes diaphoresis, flushing, and hypotension if the patient consumes alcohol while taking the medication.

**Table 4. FRAMES Approach to Brief Intervention.\***

Feedback is provided from screening assessments

Responsibility for change comes from the patient

Advice for making a change comes from the clinician

Menu of options is given to the patient

Empathy characterizes the clinician's approach

Self-efficacy will enable the patient to pursue ongoing follow-up

\* The information is adapted from Miller and Sanchez.<sup>36</sup>

---

Motivational interviewing, which is a well-regarded approach to addressing behavioral changes geared toward better health, began as a treatment approach for problematic drinking. Although motivational interviewing has been studied in a range of disorders, its effectiveness has not been evaluated specifically in older patients. Essentially, motivational interviewing is a structured, nonjudgmental conversation in which the clinician encourages the patient to examine his or her substance use and adopt a committed attitude toward changing the behavior. The framework is shown.

## **Misuse of Prescription Medication**

Nonmedical use of prescription drugs is defined as intentional or unintentional use of a prescribed medication that does not conform to prescribed directions. It includes taking more of a medication than directed or taking the medication for purposes other than the one for which it was prescribed, such as for mood-altering effects. Prescription rates for benzodiazepines and opioid medications are high among older adults. Approximately 8.7% of adults who are 65 to 80 years of age use benzodiazepines, a rate that is higher than the rates in the younger age groups, and the prevalence of prescription opioid medications is 4 to 9% in adults 65 years of age or older.

The Beers Criteria of the American Geriatrics Society identify benzodiazepines as medications that are potentially inappropriate for the elderly. Because of physiological changes related to aging, older adults are more vulnerable to the adverse effects associated with benzodiazepines, such as delirium, falls, and traffic accidents.

## **Use of Illicit Substances**

Rates of illicit-substance use are substantially lower for older adults than for younger adults.<sup>59</sup> Members of the “baby boomer generation,” born between 1946 and 1964, are a sizable demographic population. By 2030, adults 65 years of age or older will account for 20% of the population. Aging baby boomers constitute a cohort with high rates of illicit-drug use dating back to their early adult years, and they continue to use illicit drugs at higher rates than previous generations of older persons. This has led to concerns that these persons may have higher rates of substance use as they age than did aging people of earlier generations. Indeed, it has been projected that substance-use rates among people 50 years of age or older will rise from 2.8 million in 2006 to 5.7 million in 2020.

## **Summary and Recommendations**

Alcohol-use disorder, prescription-drug misuse, and illicit-drug use are growing health problems in later life yet may be overlooked by health care providers. All clinicians who care for older adults must be alert for possible signs and symptoms of substance-use disorders in their patients. Use of prescription-drug monitoring programs will help identify persons who obtain multiple prescriptions for medications with high misuse potential. Although opioid abuse is growing among older adults, marijuana is currently the most frequently used illicit substance in this age group. However, alcohol-use disorder remains the most prevalent substance-use disorder in later life.

## A 54-Year-Old Man with New Heart Failure

One month before this evaluation, a nonproductive cough developed after the patient took a business trip to Tennessee. During the next week, the cough became productive of intermittent yellowish-brown sputum and was associated with fatigue and dyspnea. The patient thought he had bronchitis and stopped smoking. During the subsequent 3 weeks, he had progressive debilitating fatigue, anorexia, 10 kg of weight gain, difficulty sleeping while lying flat, and swelling in both legs. The patient's dyspnea worsened, was provoked by any amount of exertion, and then started to occur at rest. He presented to the emergency department of another hospital. He could not sleep while lying flat owing to severe dyspnea; he had slept in a recliner for a few nights and had awakened several times with paroxysmal dyspnea. The temperature was 36.6° C, the heart rate 107 beats per minute, the blood pressure 155/73 mm Hg, the respiratory rate 28 breaths per minute, and the oxygen saturation 96% while he was receiving oxygen through a nasal cannula at a rate of 2 liters per minute. Examination was notable for crackles in the lungs and edema in the legs.

**Table 1. Laboratory Data.\***

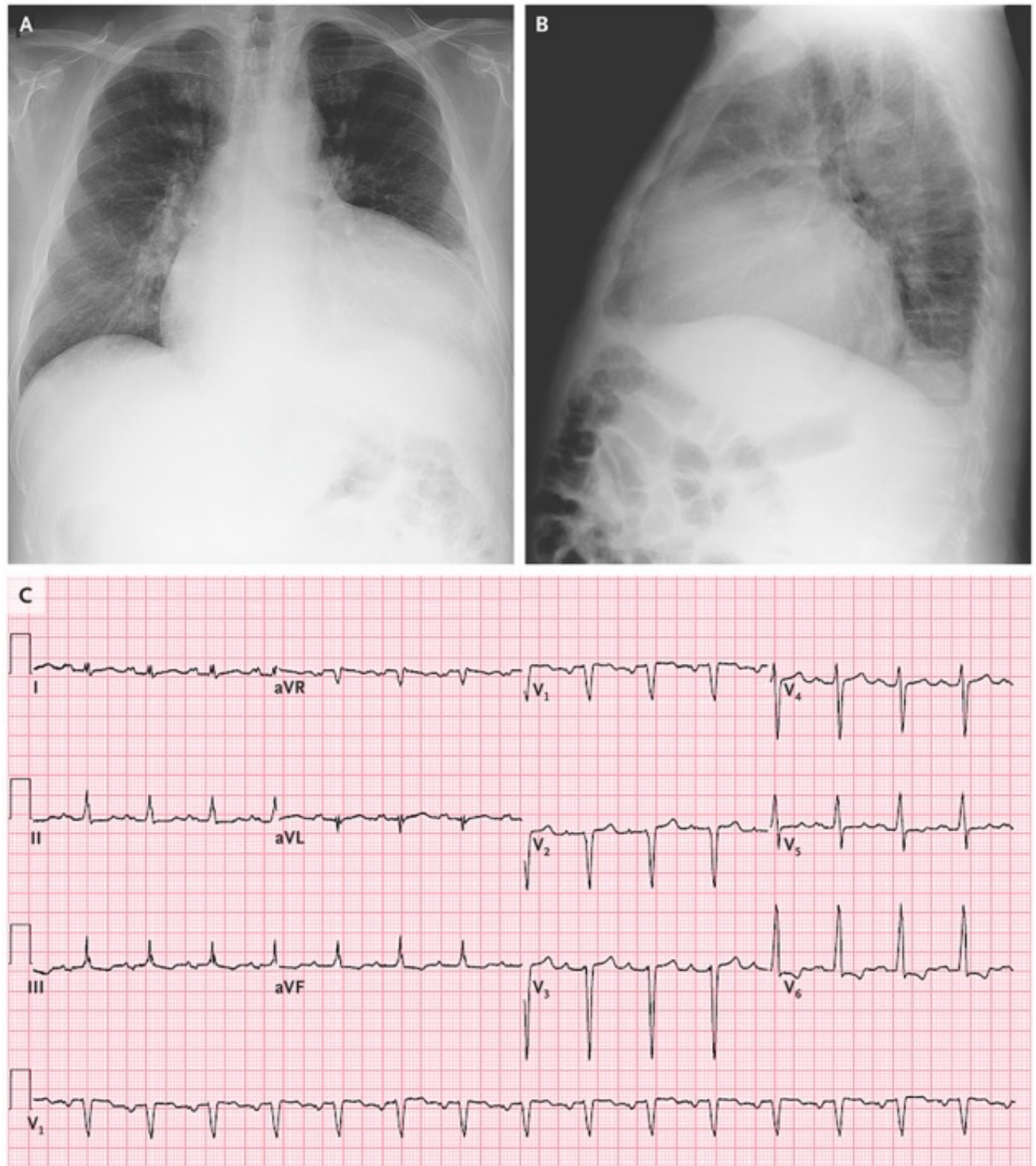
Variable	Reference Range, Other Hospital	On Presentation, Emergency Department, Other Hospital	Reference Range, Adults, This Hospital†	4 Hr Later, This Hospital
Hemoglobin (g/dl)	13.5–17.5	16.3	13.5–17.5	15.7
Hematocrit (%)	38.0–50.0	47.9	41.0–53.0	47.0
White-cell count (per mm <sup>3</sup> )	4000–11,000	8600	4500–11,000	8040
Platelet count (per mm <sup>3</sup> )	135,000–400,000	244,000	150,000–400,000	220,000
Sodium (mmol/liter)	136–145	134	135–145	135
Potassium (mmol/liter)	3.5–5.2	4.9	3.4–5.0	4.1
Chloride (mmol/liter)	99–109	96	98–108	98
Carbon dioxide (mmol/liter)	20–31	21	23–32	23
Urea nitrogen (mg/dl)	9–23	16	8–25	16
Creatinine (mg/dl)	0.5–1.3	0.86	0.60–1.50	0.89
Glucose (mg/dl)	74–106	103	70–110	114
Albumin (g/dl)	3.5–4.8	4.1	3.3–5.0	3.4
Troponin T (ng/ml)	<0.03	<0.01	<0.03	<0.01
N-terminal pro-B-type natriuretic peptide (pg/ml)	<900	21,332	<900	23,774
Alanine aminotransferase (U/liter)	10–49	87	10–55	76
Aspartate aminotransferase (U/liter)	6–40	34	10–40	32
Alkaline phosphatase (U/liter)	27–129	66	45–115	66
Total bilirubin (mg/dl)	0.0–1.0	3.9	0.0–1.0	3.5
Direct bilirubin (mg/dl)			0.0–0.4	1.0
Lactate (mmol/liter)			0.5–2.2	1.2
Venous blood pH			7.30–7.40	7.43
Erythrocyte sedimentation rate (mm/hr)			0–13	2
Antinuclear antibody			Negative at 1:80 and 1:160	Positive at 1:40, speckled pattern
Antitreponemal antibody			Negative	Negative

\* To convert the values for urea nitrogen to millimoles per liter, multiply by 0.357. To convert the values for creatinine to micromoles per liter, multiply by 88.4. To convert the values for glucose to millimoles per liter, multiply by 0.05551. To convert the values for bilirubin to micromoles per liter, multiply by 17.1. To convert the values for lactate to milligrams per deciliter, divide by 0.1110.

† Reference values are affected by many variables, including the patient population and the laboratory methods used. The ranges used at Massachusetts General Hospital are for adults who are not pregnant and do not have medical conditions that could affect the results. They may therefore not be appropriate for all patients.

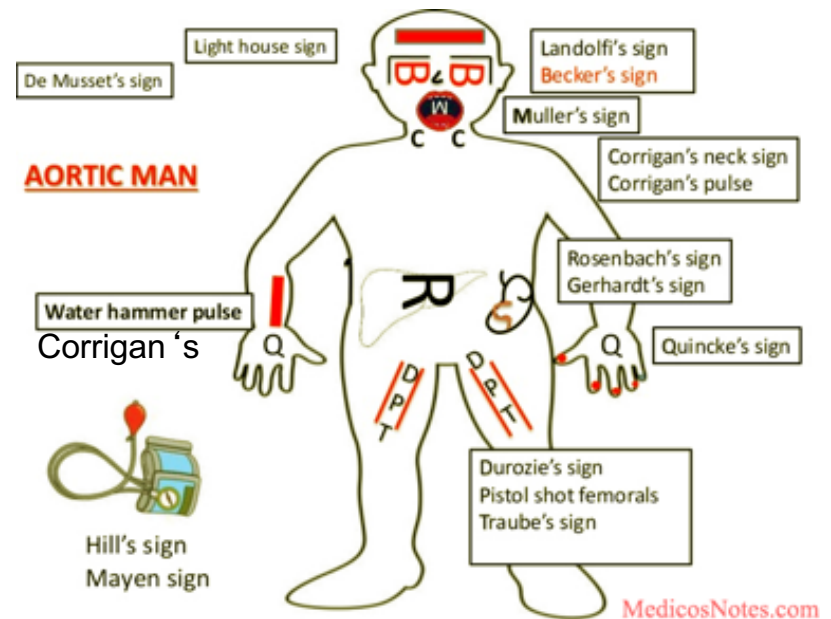


Furosemide was administered intravenously, and the patient was transferred to the emergency department of this hospital. During the initial evaluation at this hospital, he reported a history of untreated systemic hypertension. A review of systems was notable for the presence of occasional streaks of blood in the sputum during the previous weeks and dysgeusia; the patient had no fever, chills, night sweats, chest pain, chest pressure, palpitations, light-headedness, dizziness, leg pain, claudication, rash, or focal neurologic symptoms. On examination, the temperature was 36.4° C, the heart rate 102 beats per minute, the blood pressure 142/75 mm Hg, the respiratory rate 24 breaths per minute, and the oxygen saturation 94% while the patient was receiving oxygen through a nasal cannula at a rate of 4 liters per minute. He was middle-aged and of normal stature, without dysmorphic features, and he appeared to be anxious, fatigued, diaphoretic, and in mild respiratory distress.



The jugular venous pulse was elevated to 12 cm of water, and the carotid pulse was described as “collapsing.” The point of maximum cardiac impulse was shifted laterally to the anterior axillary line. The heart rate was tachycardic; a decrescendo murmur (grade 2 of 4) was heard nearly throughout diastole and was most prominent at the right upper sternal border, and there was no S<sub>3</sub> gallop. There were bibasilar lung crackles. The abdomen was mildly distended. The arms and legs had robust, symmetric pulses and were warm; there was symmetric 3+ leg edema to the mid thighs. Examination of the fingernails revealed alternating reddening and blanching pallor that was synchronized with the heart rate. The stool was guaiac-negative. There was no rash or lymphadenopathy, and the remainder of the examination was normal.

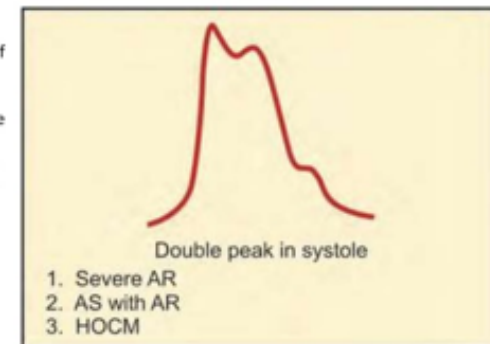
What was the cause of this patient’s heart murmur? The grade 2 decrescendo diastolic murmur, which was loudest at the right upper sternal border, is typical in timing, shape, and location of a murmur associated with aortic regurgitation. Alternative causes of isolated diastolic murmurs include mitral stenosis, tricuspid stenosis, and pulmonary regurgitation. The location at the right upper sternal border is not consistent with mitral or tricuspid stenosis. Murmurs associated with pulmonary regurgitation are typically loudest at the left upper sternal border, but they can be loudest on the right side. Clinically significant severe pulmonary regurgitation can cause heart failure on the right side, but this condition alone would not cause left ventricular dilatation and heart failure on the left side. Therefore, we can conclude that this patient’s diastolic murmur was due to aortic regurgitation.



## Pulsus Bisferiens

Pulsus bisferiens is a single pulse wave with two peaks in systole best felt in brachial and femoral artery

due to ejection of rapid jet of blood through the aortic valve. During the peak of flow, Bernoulli's effect on the walls of ascending aorta causes a sudden decrease in lateral pressure on the inner aspect of the wall.



Dissection of aorta (unilateral bisferiens).

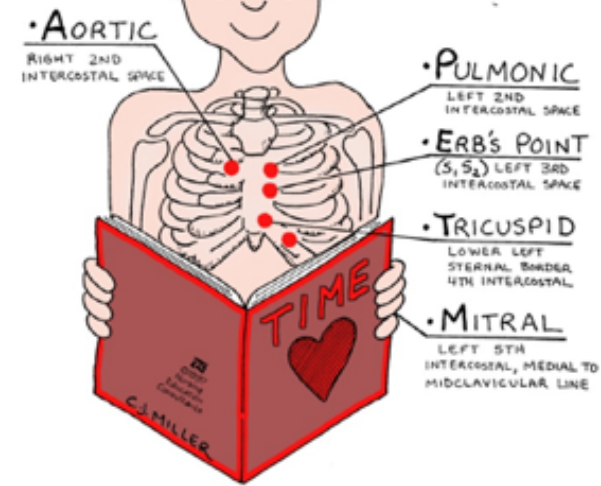
# Physical signs

- **Durosier's sign:**
  - femoral retrograde bruits
- **Traube's sign:**
  - pistol shot femorals



- **Hill's sign:**
  - BP Lower extremity > BP Upper extremity by
    - > 20 mm Hg - mild AR
    - > 40 mm Hg - mod AR
    - > 60 mm Hg - severe AR

## 5 AREAS FOR LISTENING TO THE HEART



ALL PEOPLE ENJOY TIME MAGAZINE

## Aortic regurgitation

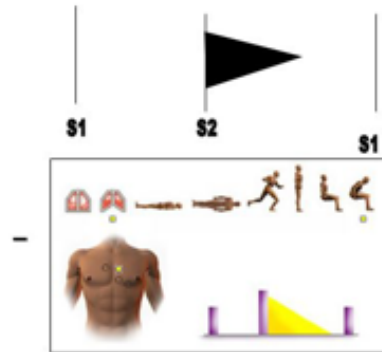
### Physical examination

Widened pulse pressure  
systolic – diastolic = pulse pressure

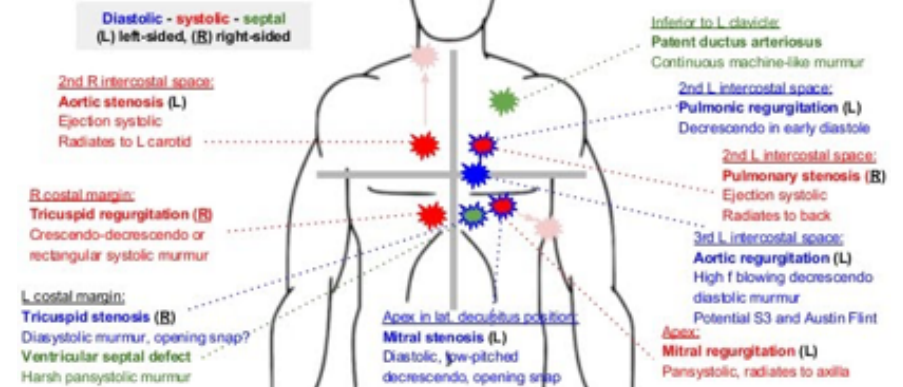
### AUSCULTATION

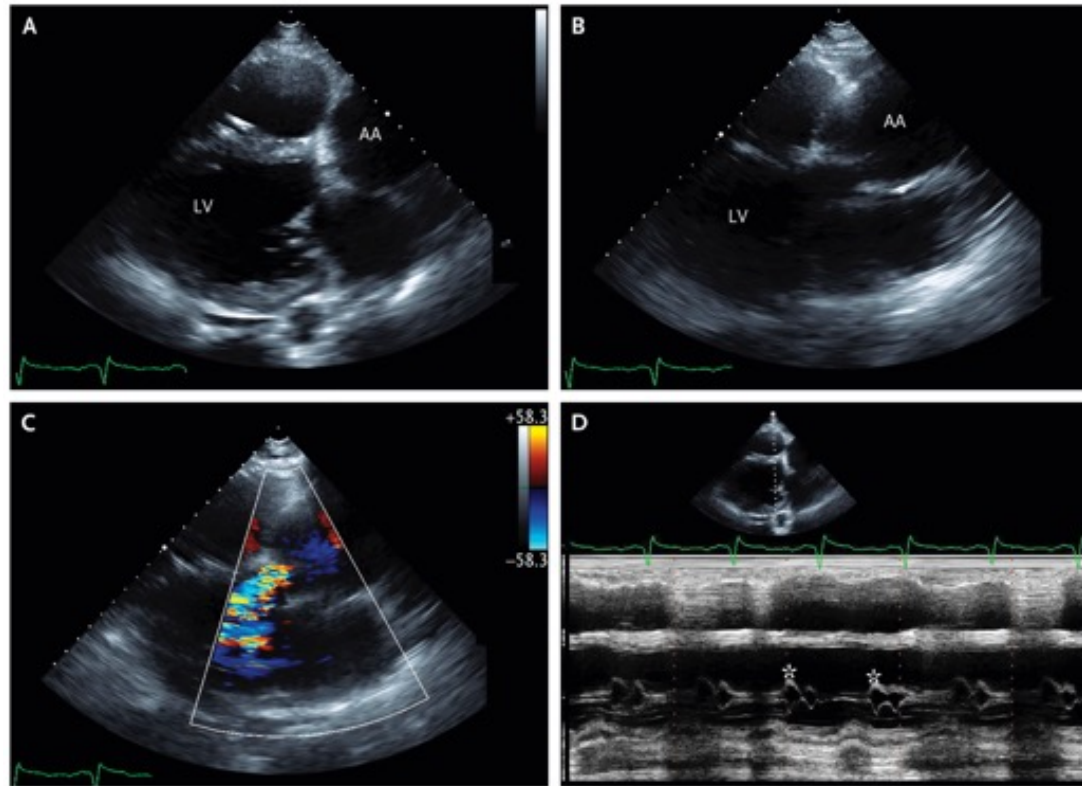
Murmur: high-pitched, blowing, decrescendo diastolic murmur, heard best in the third intercostal space along the left sternal border (holodiastolic in severe AR)

When the murmur is soft, it can be heard best with the diaphragm of the stethoscope and with the patient sitting up, leaning forward, and with the breath held in forced expiration.

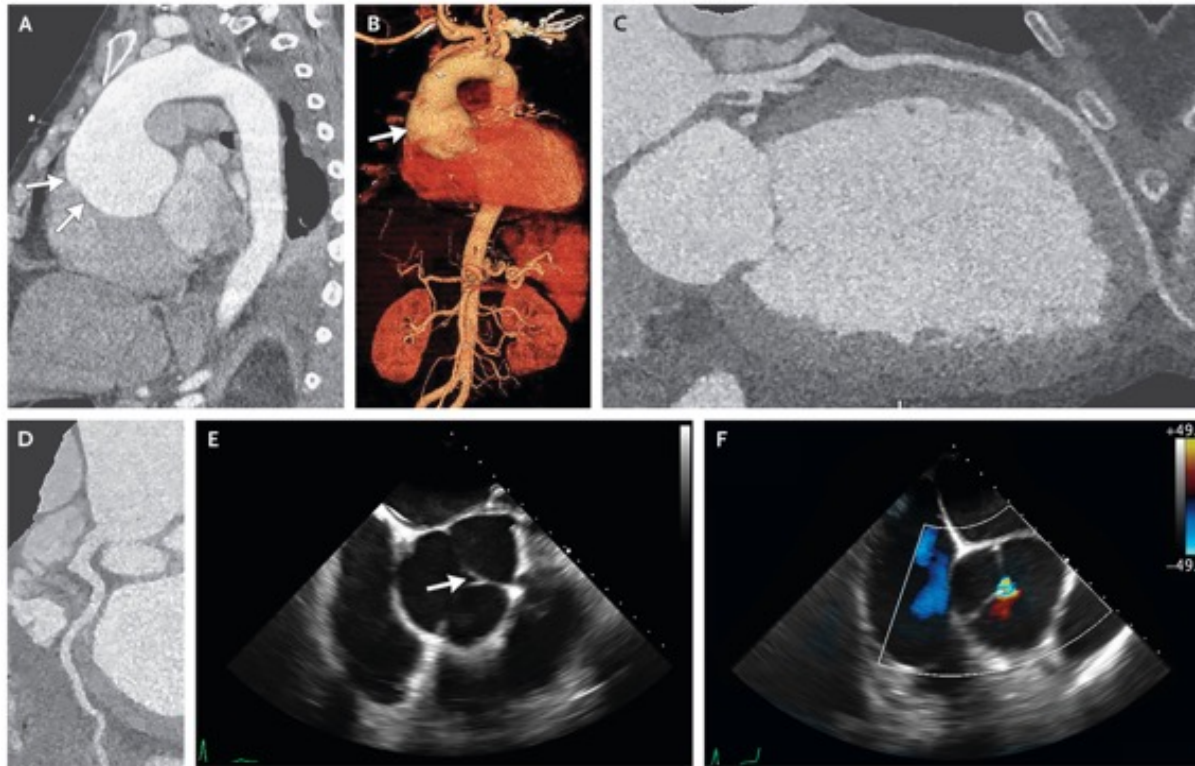


## Where murmurs are heard loudest





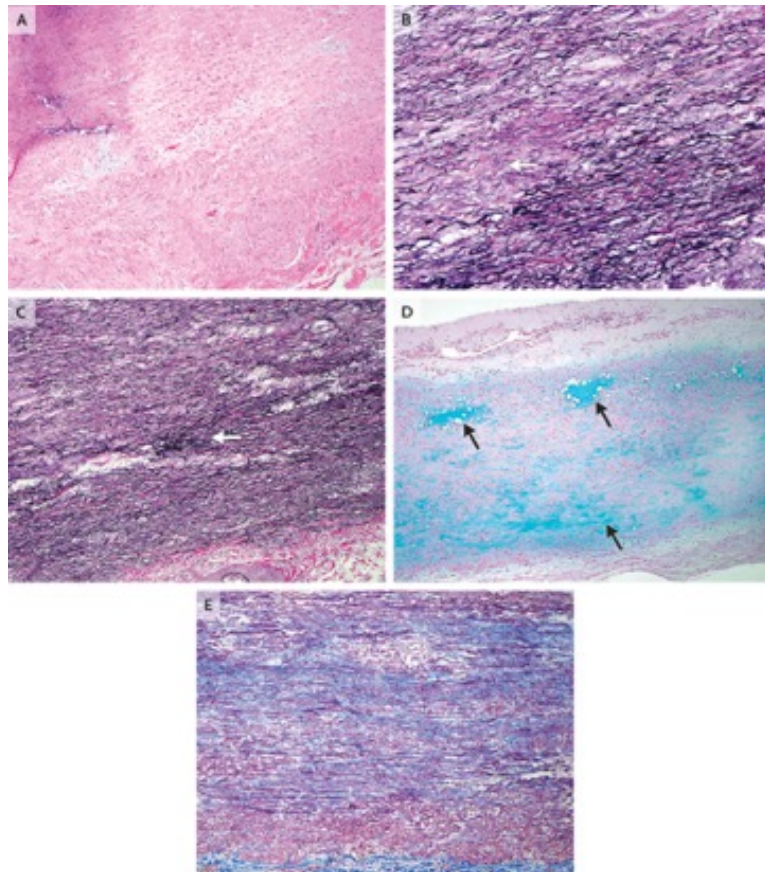
Transthoracic Echocardiogram. An image of the left ventricle (LV) obtained in the parasternal long-axis view (Panel A) shows marked left ventricular dilatation (end-diastolic dimension, 76 mm; end-systolic dimension, 69 mm). An image of the ascending aorta (AA) obtained in a higher parasternal long-axis view (Panel B) shows dilatation of the aortic root and ascending aorta and effacement of the sinotubular junction. An image obtained with color Doppler (Panel C) shows evidence of severe aortic regurgitation, which is most likely a consequence of clinically significant dilatation of the aortic root and incomplete coaptation of the aortic-valve leaflets. An M-mode image obtained through the mitral valve (Panel D) shows fluttering of the anterior leaflet (asterisks), a finding consistent with aortic regurgitant flow into the left ventricle in diastole that impinges on the motion of this leaflet; this is a sign of severe aortic regurgitation.



Cardiac Studies. Contrast-enhanced CT angiography of the chest, abdomen, and pelvis was performed. A sagittal oblique reformatted image (Panel A) and a volume-rendered reformatted image (Panel B) show an aneurysm involving the aortic root and ascending aorta (arrows) that measures up to 7.5 cm in the ascending aorta. Electrocardiographically gated contrast-enhanced CT angiography of the coronary arteries was also performed. Curved planar reformatted images of the left and right coronary arteries (Panels C and D, respectively) show only minimal luminal narrowing. Intraoperative transesophageal echocardiography was performed. An image obtained in a midesophageal short-axis view of the aortic valve (Panel E) confirms the presence of a trileaflet aortic valve with incomplete leaflet coaptation (arrow) but no other leaflet abnormalities. An image obtained with color Doppler (Panel F) shows that the incomplete leaflet coaptation results in aortic regurgitation.

Intraoperative transesophageal echocardiography confirmed the presence of a trileaflet aortic valve with incomplete leaflet coaptation in the context of severe dilatation of the aortic root and ascending aorta, which resulted in severe aortic regurgitation.

The patient underwent excision of the affected portion of the aorta and of the aortic valve. Gross examination of the aortic valve was notable for three tan membranous cusps, each with nodular calcifications; these findings are diagnostic of calcific degeneration. Examination of the excised portion of aorta revealed tan, rubbery soft tissue and evidence of focal calcifications.



Specimens of the Aorta. On hematoxylin and eosin staining (Panel A), linearly arranged, well-organized smooth-muscle cells are shown (top right) in contrast with disorganized smooth-muscle cells (bottom left). On elastic staining (Panel B), elastin fibers are heterogeneously fragmented (upper third) and lost (arrow) in some areas but relatively preserved in other areas (lower third); there is also evidence of focal lamellar medial collapse (Panel C, arrow). On Alcian blue staining (Panel D), there is an accumulation of extracellular-matrix material (arrows). On trichrome staining (Panel E), there is medial fibrosis in the aortic wall (in blue).

The term “aortic degenerative disease” refers to a constellation of pathologic changes that affect the tunica media of the thoracic aorta, but the term does not necessarily imply a cause. The development of aortic degenerative disease may be categorized as syndromic, familial, or sporadic. Syndromic causes include Marfan’s syndrome, the Ehlers–Danlos syndrome, and the Loeys–Dietz syndrome. Familial nonsyndromic causes typically involve a mutation in the *TGFBR2*, *ACTA2*, or *MYH11* gene or at another locus. Sporadic aneurysmal aortic degenerative disease can be idiopathic but has also been linked to a broad range of conditions, including infections (syphilis and tuberculosis), autoimmune disease (rheumatoid arthritis), and vasculitides (giant-cell arteritis and Takayasu’s arteritis). This patient had no known syndromic or familial conditions, but the link between a history of hypertension and the presence of medial degeneration is especially salient: 70 to 85% of patients with thoracic aortic aneurysm have concurrent hypertension,<sup>14</sup> and thus hypertensive disease is the foremost risk factor for the development of aortic degenerative disease.

This patient had a complicated postoperative course, which included the development of inotrope-dependent heart failure, along with polymicrobial empyema on the left side. The empyema was associated with growth of *Streptococcus mitis*, *Actinomyces odontolyticus*, *Escherichia coli*, and mixed anaerobic bacteria. The patient was treated with the placement of a chest tube and the administration of ceftriaxone and metronidazole. He was gradually weaned off inotropes, but his persistently low systolic blood pressure limited the initiation of appropriate neurohormonal blockade to treat persistent left ventricular systolic dysfunction. Fortunately, at the time of discharge, the left ventricular end-diastolic dimension had decreased from 76 mm to 59 mm (reference range, 42 to 58), although the ejection fraction was 26%. Lisinopril and furosemide were prescribed on discharge, with the goal of adding metoprolol succinate and spironolactone in the future.

# Global patterns of mortality in international migrants: a systematic review and meta-analysis

258 million people reside outside their country of birth; however, to date no global systematic reviews or meta-analyses of mortality data for these international migrants have been done. We aimed to review and synthesise available mortality data on international migrants. In this systematic review and meta-analysis, we searched MEDLINE, Embase, the Cochrane Library, and Google Scholar databases for observational studies, systematic reviews, and randomised controlled trials published between Jan 1, 2001, and March 31, 2017, without language restrictions. We included studies reporting mortality outcomes for international migrants of any age residing outside their country of birth. Studies that recruited participants exclusively from intensive care or high dependency hospital units, with an existing health condition or status, or a particular health exposure were excluded. We also excluded studies limited to maternal or perinatal outcomes. We screened studies using systematic review software and extracted data from published reports. The main outcomes were all-cause and International Classification of Diseases, tenth revision (ICD-10) cause-specific standardised mortality ratios (SMRs) and absolute mortality rates. We calculated summary estimates using random-effects models.

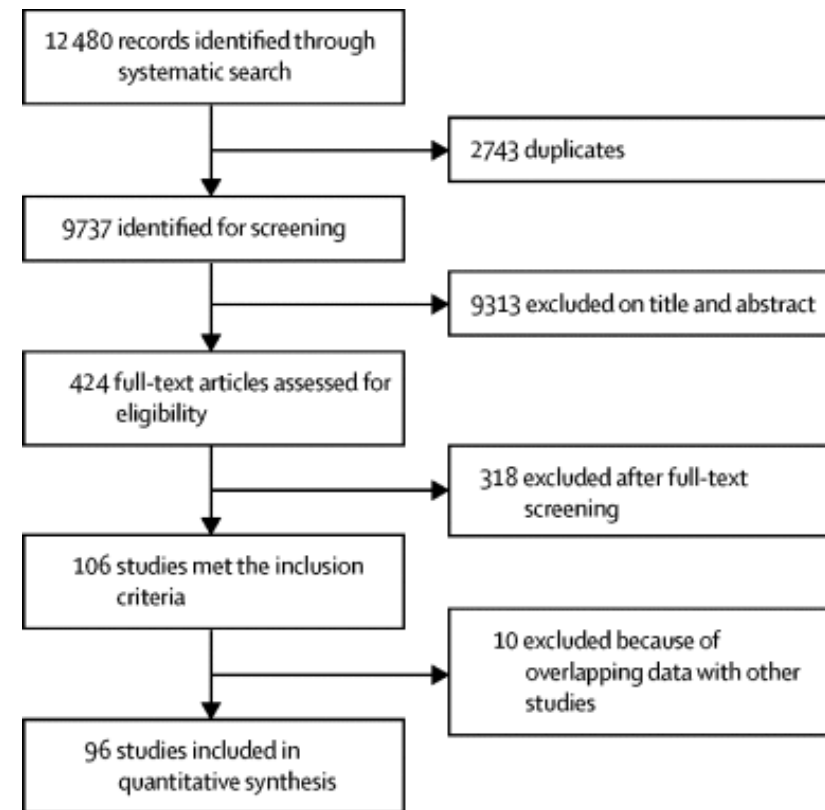


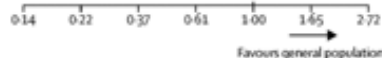
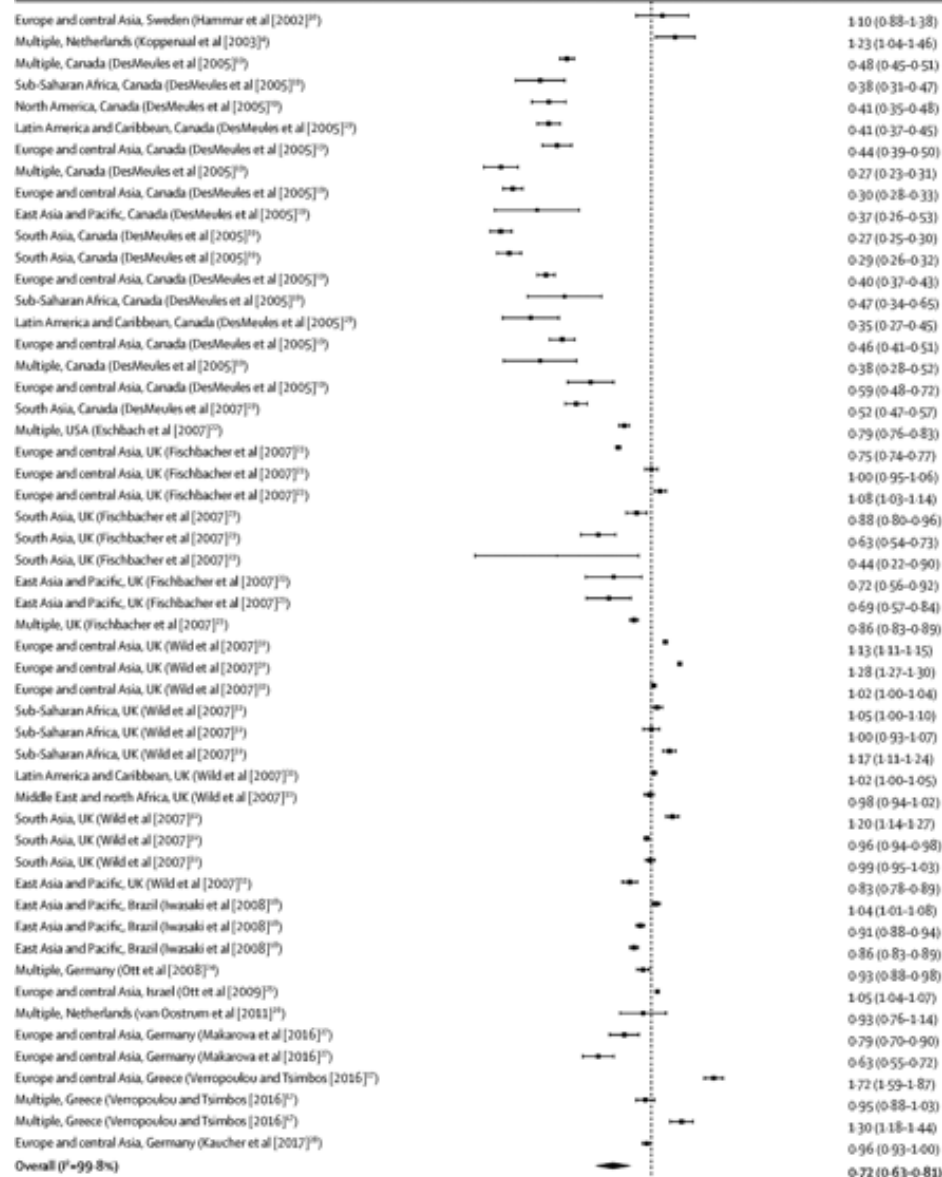


**Table Characteristics of studies included in the meta-analyses of all-cause standardised mortality**

	Country	Study years	Study design	Migrants (n)	Population description	Migrant countries or regions of origin	Quality assessment <sup>†</sup> (%)
Deckert et al <sup>29</sup>	Germany	1990–2010	Cohort	6378	Ethnic German repatriates from the former Soviet Union	Former Soviet Union	100%
DesMeules et al <sup>20</sup>	Canada	1980–98	Cohort	369 972	Canadian immigrants, including both refugees and non-refugees	Northeast Asia, western Europe, eastern Europe and Russia, south Asia, southeast Asia, the Middle East and Africa, north Africa, the Caribbean, North America, South America, Central America, Oceania, and the Pacific	63%
DesMeules et al <sup>19</sup>	Canada	1980–98	Cohort	369 972	Canadian immigrants, including both refugees and non-refugees	Northeast Asia, western Europe, eastern Europe and Russia, south Asia, southeast Asia, the Middle East and Africa, the Caribbean, North America, South America, Central America, Oceania, and the Pacific	100%
Eschbach et al <sup>22</sup>	USA	1999–2001	Cohort	NR	Foreign-born Hispanics in California and Texas	Mexico, Central America, and South America	88%
Fischbacher et al <sup>23</sup>	Scotland	1997–2003	Cohort	NR	Foreign-born residents of Scotland	England and Wales, Northern Ireland, Ireland, India, Pakistan, Bangladesh, China, Hong Kong, rest of the world	100%
Hammar et al <sup>30</sup>	Sweden	1975–95	Cohort	1994	Finnish migrants to Sweden with $\leq 20$ years residency	Finland	88%
Iwasaki et al <sup>18</sup>	Brazil	1999–2001	Cohort	51 445	First-generation Japanese Brazilians	Japan	100%
Kaucher et al <sup>28</sup>	Germany	1990–2009	Cohort	59 390	Resettlers (ethnic German immigrants) in Germany	Former Soviet Union	88%
Koppelaar et al <sup>4</sup>	Netherlands	1998–99	Cohort	45 889	Asylum seekers to the Netherlands	Multiple	88%
Makarova et al <sup>27</sup>	Germany	2004–10	Cohort	NR	Migrants from the former Soviet Union and Turkey	Former Soviet Union	100%
Ott et al <sup>24</sup>	Germany and Israel	1990–2005	Cohort	34 393 (Germany), 589 388 (Israel)	Regular migrants from the former Soviet Union to Israel and Germany who arrived between 1990 and 2001	Former Soviet Union	88%
Ott et al <sup>25</sup>	Israel	1990–2003	Cohort	926 870	Migrants from the former Soviet Union	Former Soviet Union	88%
Ronellenfisch et al <sup>21</sup>	Germany	1990–2002	Cohort	34 393	Ethnic German immigrants from the former Soviet Union	Former Soviet Union	100%
van Oostrum et al <sup>26</sup>	Netherlands	2002–05	Cohort	NR	Asylum seekers residing in asylum seeker centres in the Netherlands	West Africa, central Africa, southern Africa, north Africa, east Africa, horn of Africa, central Europe, eastern Europe, southern Europe, the Middle East, southwest Asia, central Asia, east Asia, and south Asia	88%
Verropoly and Tsimbos <sup>17</sup>	Greece	2010–12	Cohort	911 929	International migrants	International migrants from all geographical regions	88%

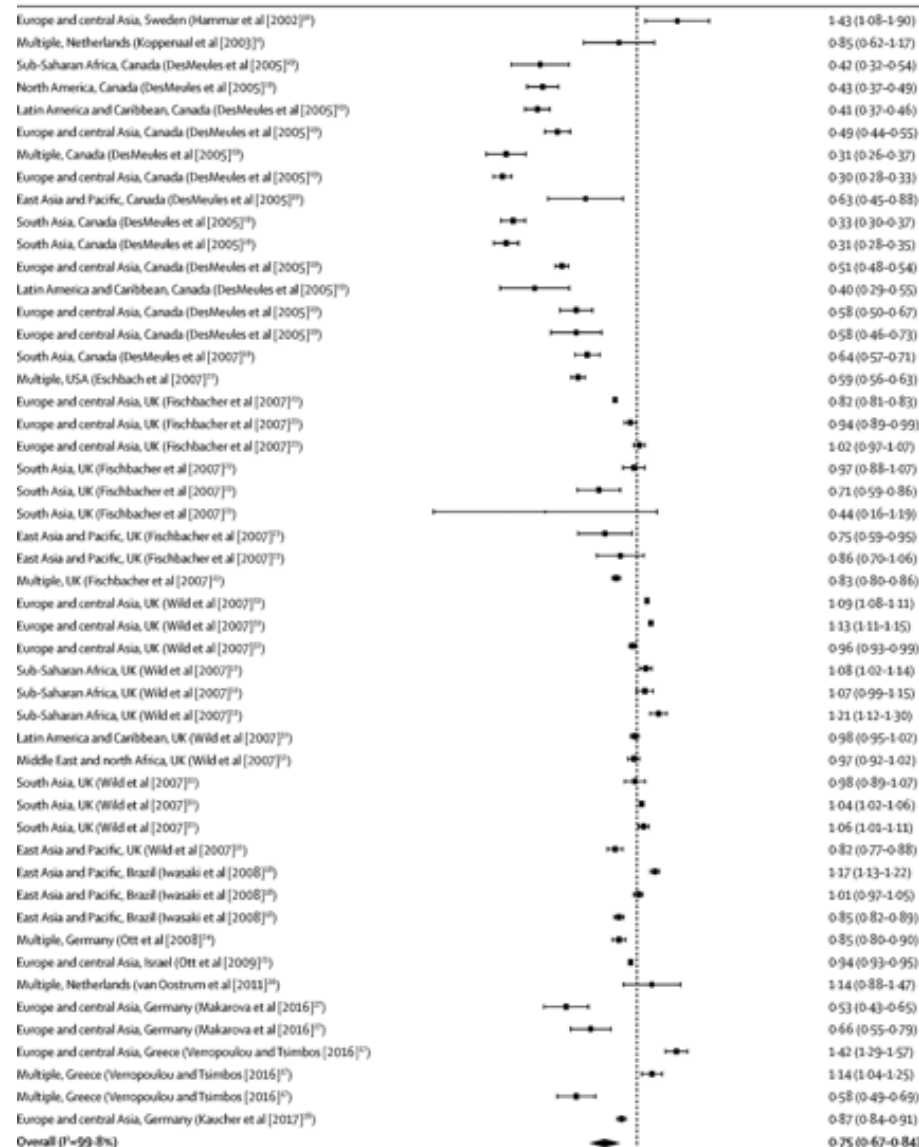
**A Male individuals**

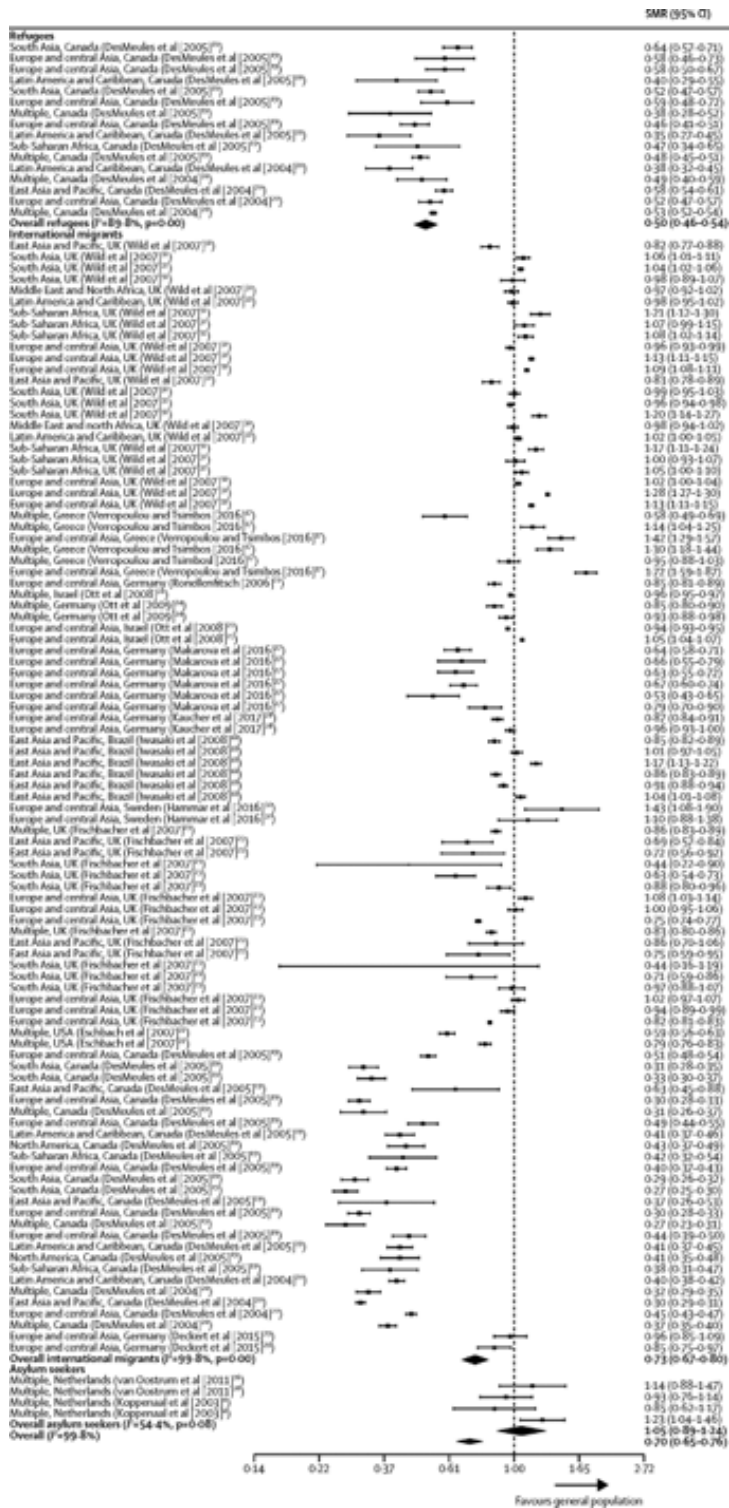
SMR (95% CI)



**B Female individuals**

SMR (95% CI)





## Discussion

We found substantial evidence of a mortality advantage in international migrants relative to the general population, with most studies done in high-income countries. This mortality advantage was observed across geographical region of origin and the majority of ICD-10 categories, with the exception of infectious diseases and external causes, in which migrants had increased mortality compared with the general population in destination countries. Infectious disease mortality was increased for viral hepatitis, tuberculosis, and HIV. Assaults and deaths of undetermined intent were increased among migrants for external causes of mortality.

Our results were obtained for international migrants (often reported as foreign-born) in high-income settings and populations reported as foreign born. Data on international migration suggest that of the 258 million international migrants worldwide, 150 million are migrant workers and 5 million are students. Our results are therefore more likely to better reflect outcomes in these groups than other migrant groups. Since the mortality estimates used for our meta-analyses were rarely reported according to migrant subgroup, caution must be taken when generalising these estimates to refugees, asylum seekers, and undocumented migrants, particularly those living in low-income and middle-income countries. These individuals might be at increased risk of mortality, and were underrepresented in research and routine mortality data and thus in our meta-analysis of SMRs. In contrast to many other subgroups of international migrants, a large proportion of refugees move between low-income and middle-income countries, representing an important gap in the existing published literature.

### **Added value of this study**

Our systematic review of the published literature provides a robust analysis of the available evidence base, suggesting that overall, mortality among international migrants was lower than the general population in high-income destination countries. Our results might not be generalisable to more marginalised migrants, and in particular forced migrants and those living in low-income and middle-income countries, as a result of the scarcity of data on their mortality outcomes. Therefore, caution is urged when generalising estimates to these populations and locations. International migrants had increased mortality due to infectious diseases (viral hepatitis, tuberculosis, and HIV) and external causes of deaths (assault and events of undetermined intent), and no mortality advantage was identified for asylum seekers, for whom limited data were available. Our systematic review and meta-analysis supports the healthy migrant hypothesis, and provides the most comprehensive synthesis of evidence to date on mortality outcomes in international migrants. Our results also indicate infectious disease and external causes of mortality as two key areas in which opportunities exist for prevention and ability to improve the health of migrants and the wider public. Our results also highlight the need to improve data collection in migrant groups such as refugees, asylum seekers, and undocumented migrants, and migrants living in low-income and middle-income countries, who might be at increased risk of morbidity and mortality and were more likely to be underrepresented. Heterogeneity was high in our study and this could not be explained by subgroup analyses. This heterogeneity indicates that some groups of migrants will continue to have unmet health needs and the summary mortality advantage presented must not be used as a justification for any restrictions in access to health care for migrant groups, which is a growing issue across many countries.

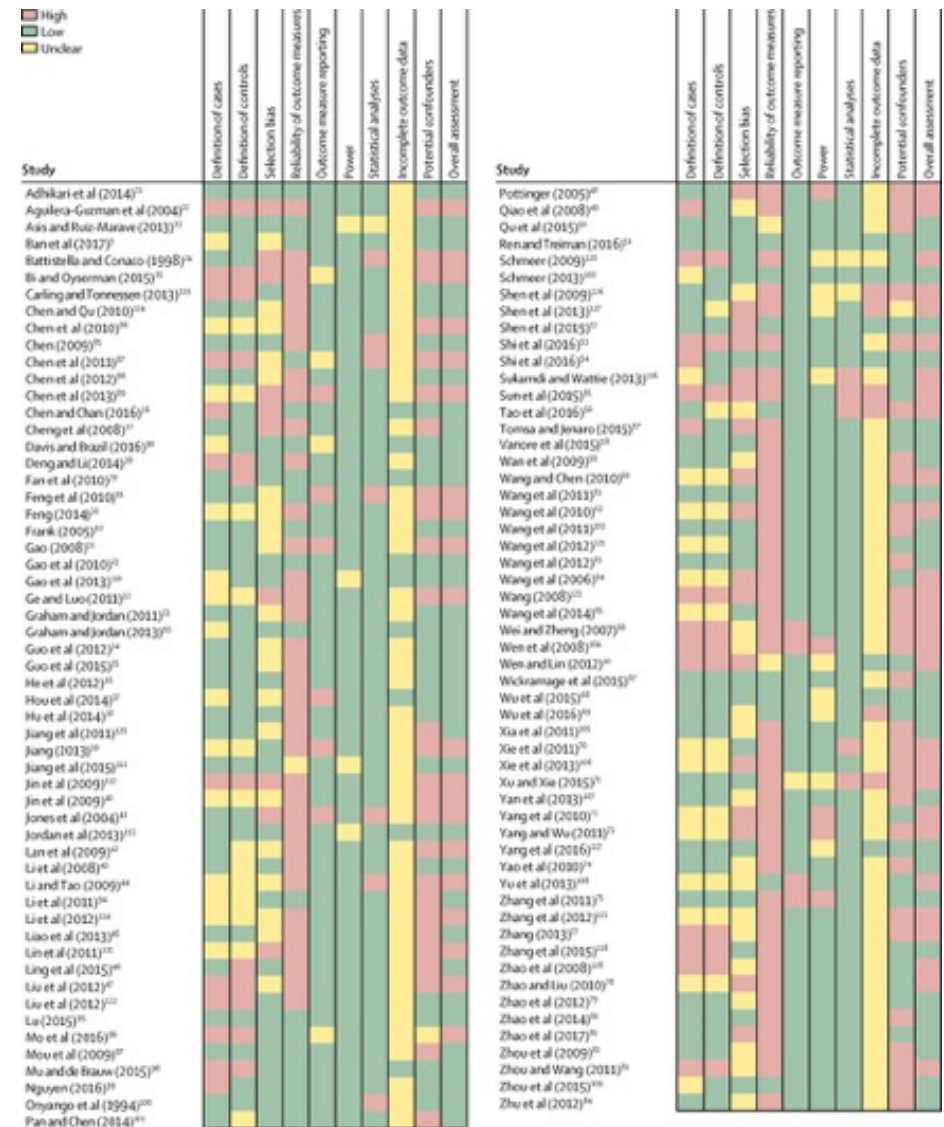
### **Implications of all the available evidence**

Public perception that migrants place an undue burden on societies is guiding governments across the globe to tighten access to health care and generate so-called hostile environments for these groups. Our findings contradict claims that migrants are a health burden in high-income countries and suggest that these policies do not align with the available evidence. Our results show that current perceptions underestimate the positive contributions of migrants to host societies in these settings. Migrants have a mortality advantage compared with general populations across the majority of disease categories, with the exception of infectious diseases and external causes. Improving access to health services and treating infectious diseases in specific migrant subpopulations is likely to have multiple benefits: lowering mortality rates, strengthening global health security and effective infection prevention and control, and reducing the burden of diseases such as hepatitis, tuberculosis, and HIV in destination countries. This will require host health services to better adapt to increase their accessibility and responsiveness to the needs of some migrant groups. Risk of mortality from infectious disease varies greatly among migrants and therefore screening should be context and epidemiology specific, codeveloped with migrants, and only done in areas where a health benefit to migrants can be demonstrated. Future research should seek to address the scarcity of data specific to migrant subgroups who are marginalised, in particular forced migrants and those originating from and living in low-income and middle-income countries. These groups might have a higher mortality burden and further research into these populations should be prioritised.

# Health impacts of parental migration on left-behind children and adolescents:

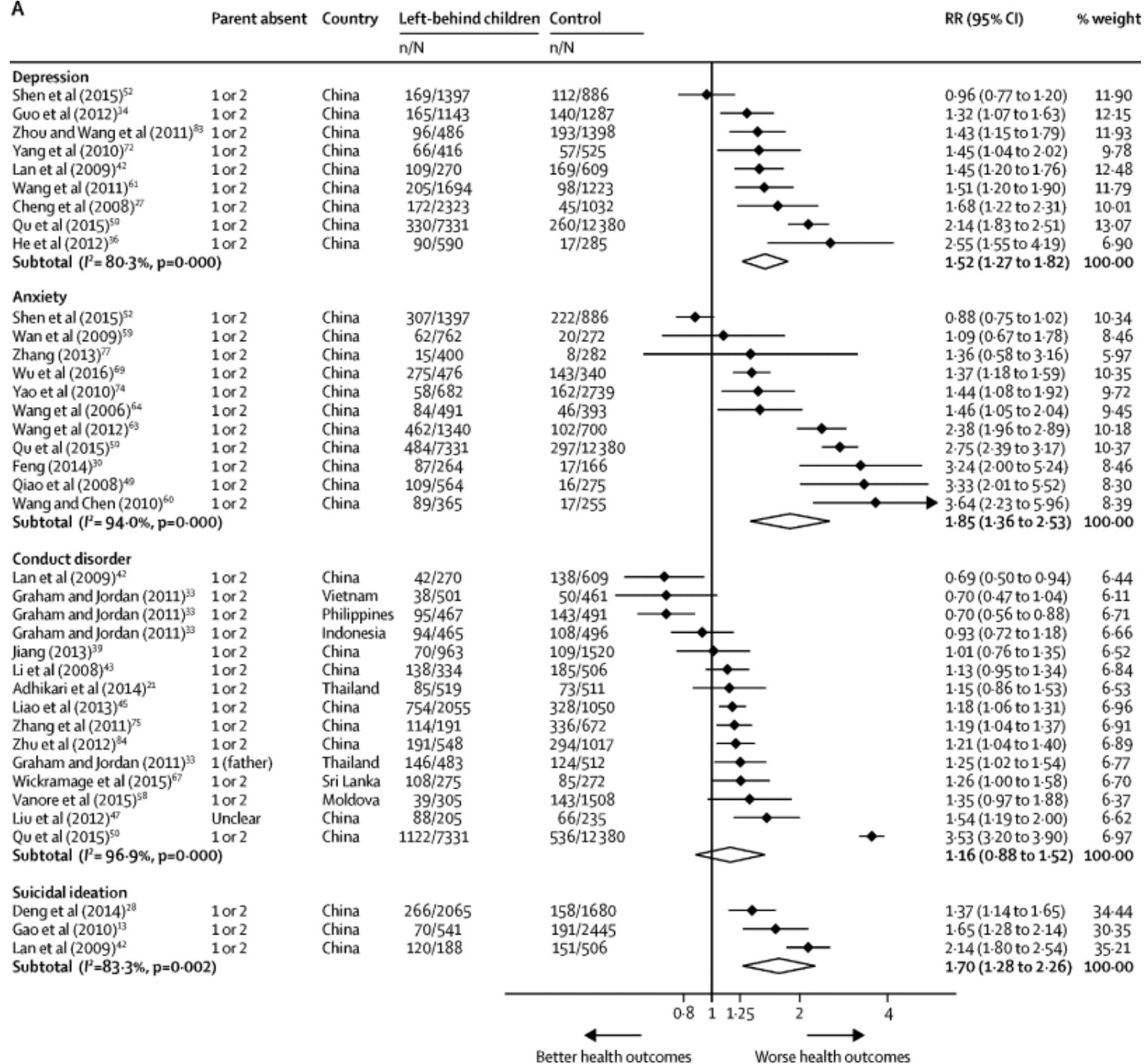
Globally, a growing number of children and adolescents are left behind when parents migrate. We investigated the effect of parental migration on the health of left behind-children and adolescents in low-income and middle-income countries (LMICs).

For this systematic review and meta-analysis we searched MEDLINE, Embase, CINAHL, the Cochrane Library, Web of Science, PsychINFO, Global Index Medicus, Scopus, and Popline from inception to April 27, 2017, without language restrictions, for observational studies investigating the effects of parental migration on nutrition, mental health, unintentional injuries, infectious disease, substance use, unprotected sex, early pregnancy, and abuse in left-behind children (aged 0–19 years) in LMICs. We excluded studies in which less than 50% of participants were aged 0–19 years, the mean or median age of participants was more than 19 years, fewer than 50% of parents had migrated for more than 6 months, or the mean or median duration of migration was less than 6 months. We screened studies using systematic review software and extracted summary estimates from published reports independently. The main outcomes were risk and prevalence of health outcomes, including nutrition (stunting, wasting, underweight, overweight and obesity, low birthweight, and anaemia), mental health (depressive disorder, anxiety disorder, conduct disorders, self-harm, and suicide), unintentional injuries, substance use, abuse, and infectious disease. We calculated pooled risk ratios (RRs) and standardised mean differences (SMDs) using random-effects models.





A



## **Evidence before this study**

Migration is increasing globally, which has resulted in a growing number of children and adolescents being left behind when their parents migrate. Before starting this study, we searched the scientific literature for articles on the effect of parental migration on child and adolescent health, and found two narrative reviews: one focused on left-behind children in the Philippines and the other on mental health outcomes in left-behind children in China. These reviews suggested that children benefited from the remittances their parents sent home in terms of improved education and reduced child labour, which could result in improved health, but reported that family separation might have long-term psychological and societal costs. We also identified more than 30 studies, mainly from China, investigating the effects of parental migration on a broad range of health outcomes across different countries. On Nov 26, 2018, we did an updated search of MEDLINE for systematic reviews with no date or language restrictions, using the broad search terms “(child\* OR adolescent) AND health AND (migration OR left-behind)”. Although we identified 99 systematic reviews, none reviewed the key areas of health of left-behind children and adolescents across all low-income and middle-income countries (LMICs).

## **Added value of this study**

This is the largest and most comprehensive study to date assessing the impact of parental migration on all key areas of child and adolescent health across all LMICs. Compared with children of non-migrants, left-behind children and adolescents had an increased risk of depression, suicidal ideation, and risk of anxiety. Left-behind children also had smaller increases in risk for wasting, stunting, and substance use. These results highlight a rarely discussed consequence of global migration with implications for global policy making and health-care provision in migrant-sending countries. Although a small number of individual studies found positive health effects of parental migration, overall we found no evidence of benefit across any of the health outcomes.

## **Implications of all the available evidence**

Our findings highlight the unmet health needs of left-behind children and adolescents. Research to date has focused primarily on China and longitudinal studies in a wider range of LMICs with high rates of emigration are needed to better understand risk and resilience factors within this population, and to inform policy and practice to address unmet health needs in left-behind children, adolescents, and their carers.



# Eicosapentaenoic acid and aspirin, alone and in combination, for the prevention of colorectal adenomas (seAFood Polyp Prevention trial): a multicentre, randomised, double-blind, placebo-controlled, 2 × 2 factorial trial

We aimed to test the efficacy of EPA and aspirin, alone and in combination and compared with a placebo, in individuals with sporadic colorectal neoplasia detected at colonoscopy. In a multicentre, randomised, double-blind, placebo-controlled, 2 × 2 factorial trial, patients aged 55–73 years who were identified during colonoscopy as being at high risk in the English Bowel Cancer Screening Programme (BCSP; ≥3 adenomas if at least one was ≥10 mm in diameter or ≥5 adenomas if these were <10 mm in diameter) were recruited from 53 BCSP endoscopy units in England, UK. Patients were randomly allocated (1:1:1:1) using a secure web-based server to receive 2 g EPA-free fatty acid (FFA) per day (either as the FFA or triglyceride), 300 mg aspirin per day, both treatments in combination, or placebo for 12 months using random permuted blocks of randomly varying size, and stratified by BCSP site. Research staff and participants were masked to group assignment.

The primary endpoint was the adenoma detection rate (ADR; the proportion of participants with any adenoma) at 1 year surveillance colonoscopy analysed in all participants with observable follow-up data using a so-called at-the-margins approach, adjusted for BCSP site and repeat endoscopy at baseline. The safety population included all participants who received at least one dose of study drug.

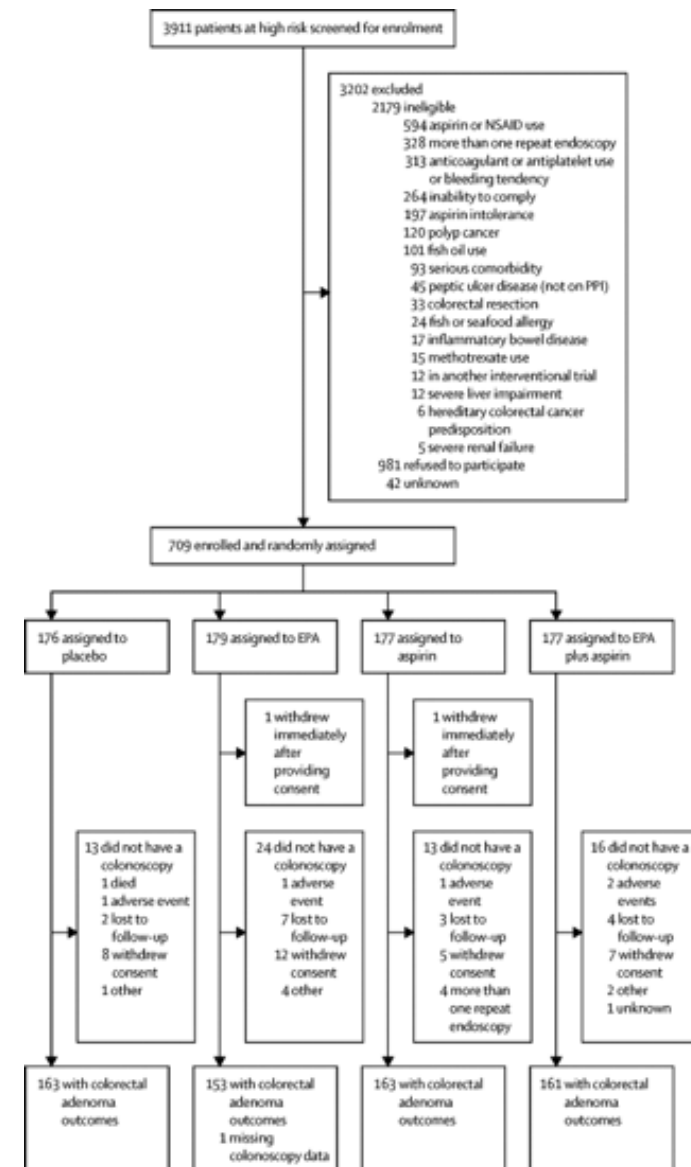


**Table 1 Baseline characteristics**

		(n=176)	(n=178)	(n=176)	(n=177)	(n=707)
Age (years)		65 (62–69)	65 (62–69)	65 (62–69)	66 (62–69)	65 (62–69)
Sex						
	Male	139 (79%)	138 (78%)	140 (80%)	146 (82%)	563 (80%)
	Female	37 (21%)	40 (22%)	36 (20%)	31 (18%)	144 (20%)
Excess bodyweight						
	Overweight (BMI 25–29.9)	76 (43%)	77 (43%)	81 (46%)	77 (44%)	311 (44%)
	Obese (BMI ≥30)	68 (39%)	70 (39%)	71 (40%)	61 (34%)	270 (38%)
	History of diabetes	24 (14%)	24 (13%)	18 (10%)	15 (8%)	81 (11%)
Cigarette smoking						
	Current smoker	34 (19%)	13 (7%)	27 (15%)	32 (18%)	106 (15%)

Boxes represent the median and IQR. Whiskers represent 1.5 times the IQR with outlier values (individual datapoints) above and below the IQR.

EPA=eicosapentaenoic acid.

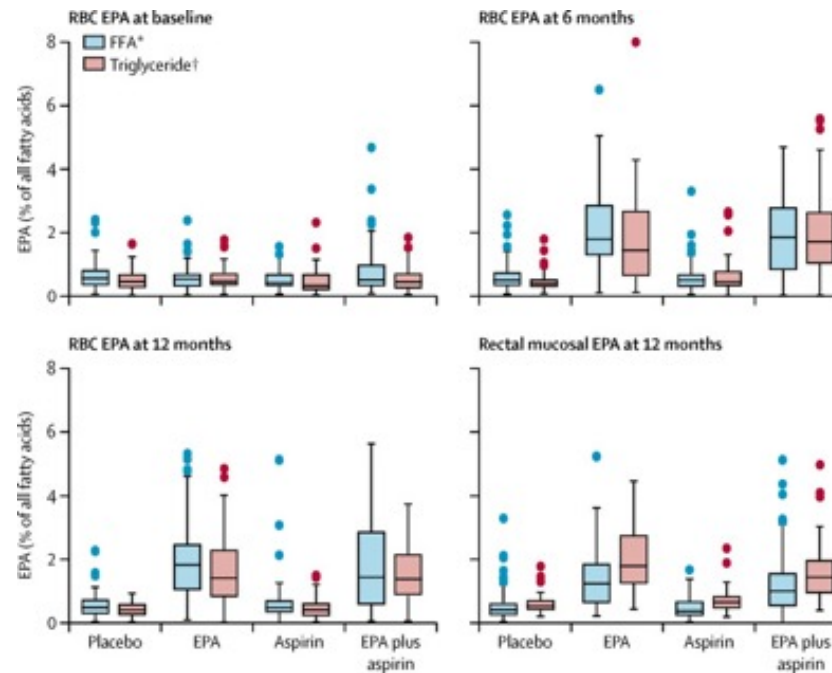
FFA=free-fatty acid.

RBC=red blood cell.

\*Individuals randomly assigned to EPA–FFA or its placebo.

†Individuals randomised to EPA–

triglyceride or its placebo.



## Research in context

### Evidence before this study

We searched PubMed for articles published in English between Jan 1, 1990, and Jan 1, 2011, using the terms “colorectal cancer”, “colorectal adenoma”, “chemoprevention”, “omega-3 polyunsaturated fatty acid”, “aspirin”, and “clinical trial”. We found one small randomised trial of eicosapentaenoic acid (EPA) for colorectal cancer chemoprevention in familial adenomatous polyposis and four randomised sporadic polyp prevention trials of aspirin, which used varying doses in different risk populations.

### Added value of this study

To our knowledge, this is the first randomised trial of EPA for sporadic colorectal cancer chemoprevention and the first evaluation of aspirin in a high-risk population within a high quality-assured national bowel cancer screening programme.

EPA and aspirin did not reduce the proportion of individuals with any colorectal adenoma (adenoma detection rate [ADR]), but they both decreased the recurrence of some subtypes of adenoma, measured by adenoma number, 1 year after clearance screening colonoscopy. There was evidence of selectivity for adenoma type and location.

### Implications of all the available evidence

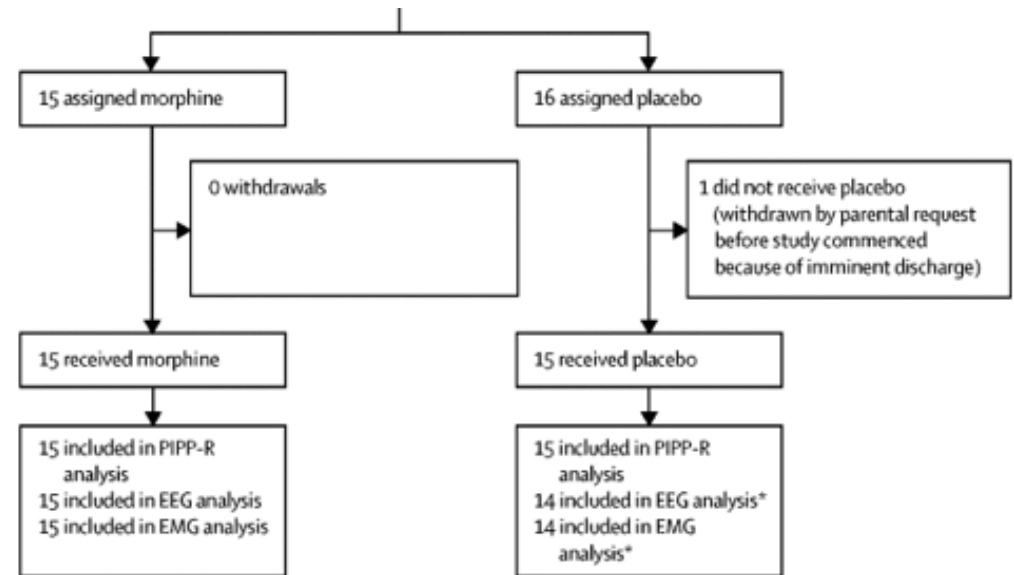
Although our trial found no effect on the primary outcome of the proportion of patients with at least one adenoma, both EPA and aspirin show some chemoprevention efficacy for colorectal cancer. The larger effect size of aspirin adds to the weight of evidence for its use in combination with endoscopic screening and surveillance, which provides suboptimal protection against right-sided colorectal cancer.

Our findings suggest that a precision medicine approach (for adenoma type and location) to colorectal cancer chemoprevention will be necessary, which mirrors best practice in colorectal cancer treatment based on molecular stratification.

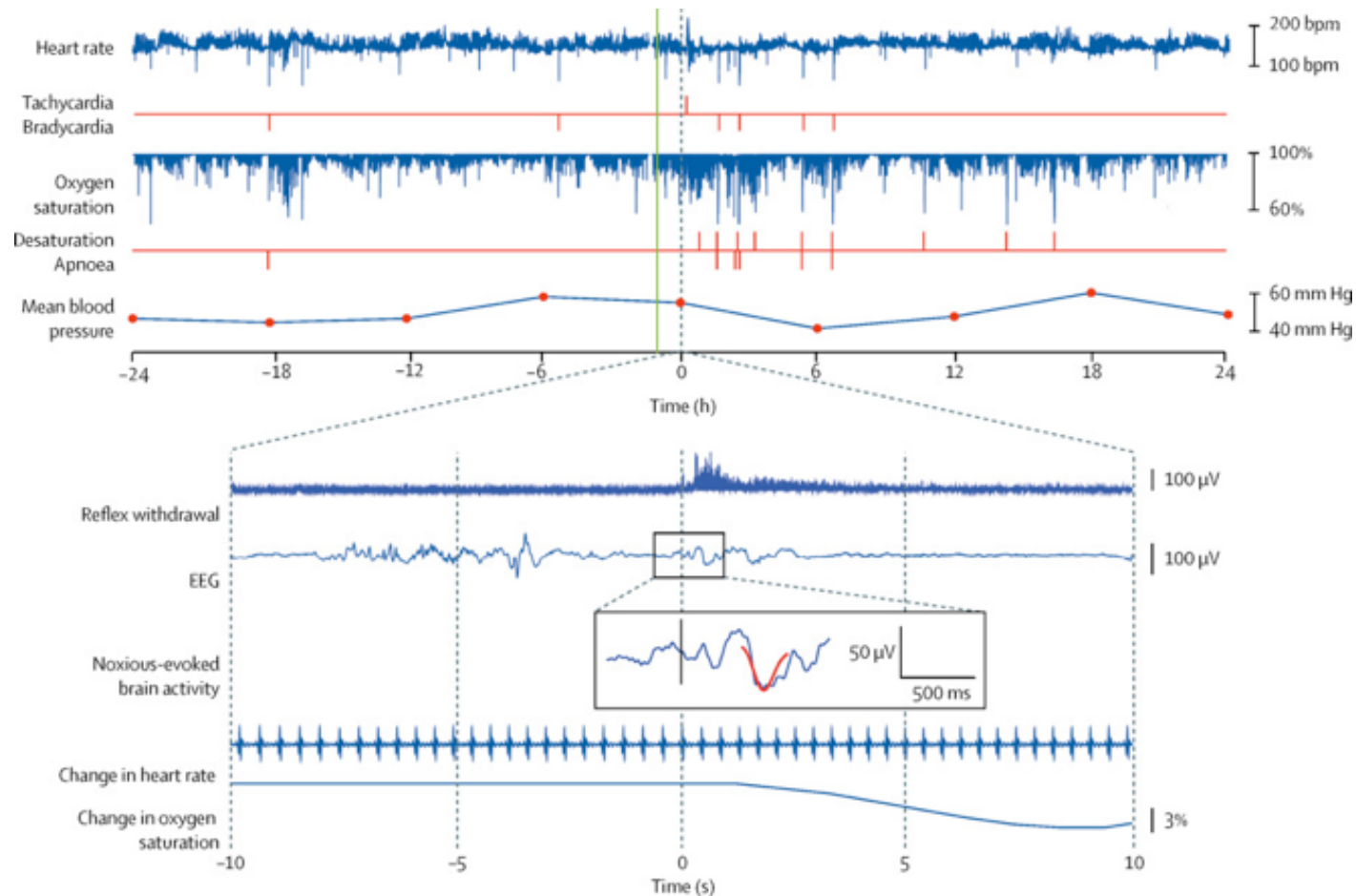
The trial raises the crucial question of whether ADR or adenoma number is the best measure of chemoprevention efficacy in polyp prevention trials that are based on quality-assured colonoscopy in individuals at high risk of colorectal cancer, in which the ADR is used as a performance indicator, and the adenoma recurrence rate is high.

# Analgesic efficacy and safety of morphine in the Procedural Pain in Premature Infants (Poppi) study

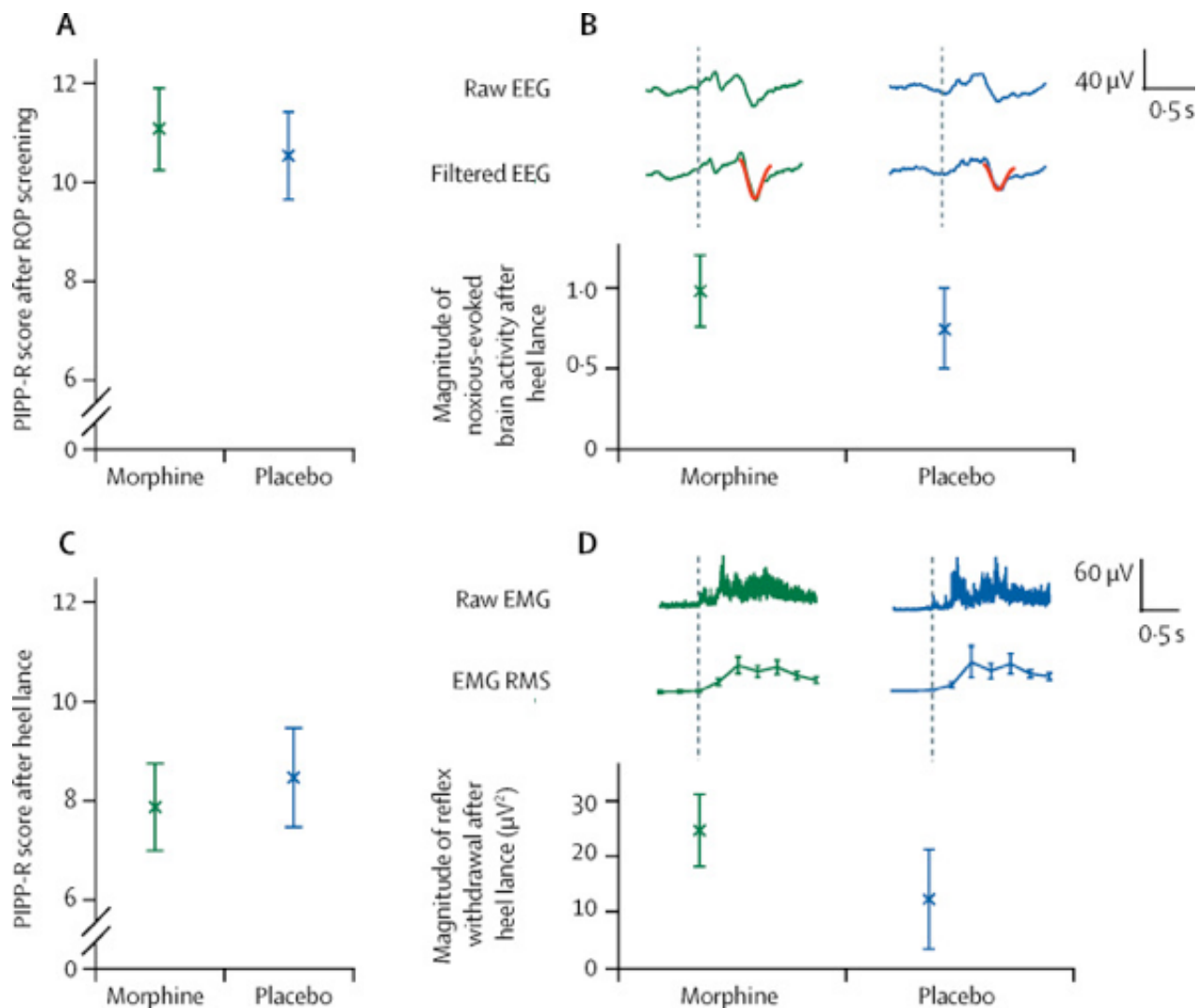
Infant pain has immediate and long-term effects but is undertreated because of a paucity of evidence-based analgesics. Although morphine is often used to sedate ventilated infants, its analgesic efficacy is unclear. We aimed to establish whether oral morphine could provide effective and safe analgesia in non-ventilated premature infants for acute procedural pain. In this single-centre masked trial, 31 infants at the John Radcliffe Hospital, Oxford, UK, were randomly allocated using a web-based facility with a minimisation algorithm to either 100 µg/kg oral morphine sulphate or placebo 1 h before a clinically required heel lance and retinopathy of prematurity screening examination, on the same occasion. Eligible infants were born prematurely at less than 32 weeks' gestation or with a birthweight lower than 1501 g and had a gestational age of 34–42 weeks at the time of the study. **The co-primary outcome measures were the Premature Infant Pain Profile–Revised (PIPP-R) score after retinopathy of prematurity screening and the magnitude of noxious-evoked brain activity after heel lancing.** Secondary outcome measures assessed physiological stability and safety. **Oral morphine (100 µg/kg) to non-ventilated premature infants has the potential for harm without analgesic efficacy. We do not recommend oral morphine for retinopathy of prematurity screening and strongly advise caution if considering this intervention for other purposes.**



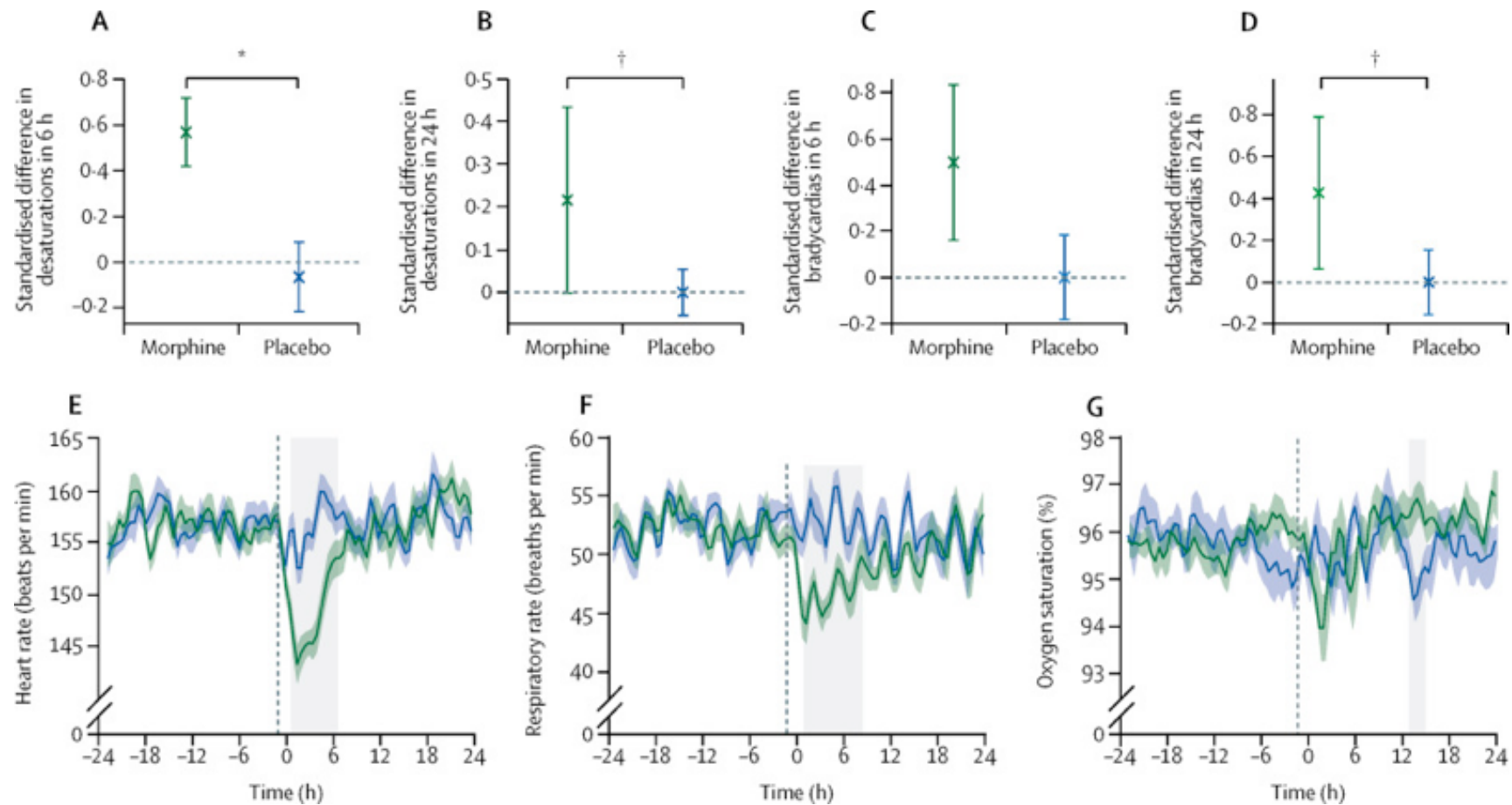
	Morphine (n=15)	Placebo (n=15)
<b>Characteristics at birth</b>		
Gestational age (weeks) <sup>†</sup>	28.1 (26.3–30.1)	28.6 (27.9–29.7)
Birthweight (g)	1107 (329)	1173 (350)
Birthweight Z-score	-0.4 (0.9)	-0.2 (1.0)
Intrauterine growth restriction <sup>*</sup>	2 (13%)	3 (20%)
Apgar score at 10 min <sup>‡</sup>	10.0 (9.0–10.0)	10.0 (8.0–10.0)



48 h records of heart rate, oxygen saturation, and mean blood pressure every 6 h are shown for the 24 h periods before and after the clinical procedure. Episodes of tachycardia, bradycardia, oxygen desaturation, and apnoea are identified (red vertical lines). The reflex withdrawal activity, EEG activity, and change in heart rate and oxygen saturation are shown in the 10 s before and after the heel lance. The noxious-evoked brain activity template is projected onto the EEG trace (overlaid in red). The time of drug administration is indicated by the green vertical line (approximately 1 h before the clinical procedure). This infant was chosen as a representative example because he had all clinical stability events (tachycardia, bradycardia, oxygen desaturation, and apnoea) and had clear changes in reflex withdrawal, brain activity, and physiology to the heel lance. Traces of noxious-evoked brain activity to the heel lance and 48 h physiological traces for all individual infants are in the appendix. bpm=beats per min. EEG=electroencephalogram.



Co-primary outcomes are shown in (A) and (B). (A) Mean (SE) PIPP-R scores after ROP screening. (B) Median (SE) magnitude of noxious-evoked brain activity after heel lance. The (Woody) filtered EEG is shown overlaid with the template of noxious-evoked brain activity (in red). Secondary outcomes are shown in (C) and (D). (C) Mean (SE) PIPP-R score after heel lance. (D) Median (SE) magnitude of reflex withdrawal activity after heel lance. Magnitude is quantified using RMS in 250 ms windows. EEG=electroencephalogram. EMG=electromyography. PIPP-R=Premature Infant Pain Profile-Revised. RMS=root-mean-square. ROP=retinopathy of prematurity.



(A) Median (SE) of the standardised difference in number of episodes of desaturation in the 6 h period after the clinical procedure compared with the 6 h period before. (B) Median (SE) of the standardised difference in number of episodes of desaturation in the 24 h period after the clinical procedure compared with the 24 h period before. (C) Median (SE) of the standardised difference in number of episodes of bradycardia in the 6 h period after the clinical procedure compared with the 6 h period before. (D) Median (SE) of the standardised difference in number of episodes of bradycardia in the 24 h period after the clinical procedure compared with the 24 h period before. (E) Mean (SE) heart rate during the 48 h monitoring period. (F) Mean (SE) respiratory rate during the 48 h monitoring period. (G) Mean (SE) oxygen saturation during the 48 h monitoring period. (E–G) Individual infant traces are baseline-corrected to the average baseline across all infants. Time zero is the point of the clinical procedure. Black vertical dashed line indicates the time of administration of morphine or placebo. Grey boxes indicate periods during which the treatment groups differed significantly. \* $p=0.0007$ . † $p=0.019$ .

### **Evidence before this study**

Morphine is one of the most frequently prescribed analgesics in neonatal practice. Although evidence suggests that intravenous morphine provides sedation in ventilated infants, and some research suggests it might provide effective analgesia for acute painful procedures (eg, chest drain insertion and central line placement), differences in study designs, dosing, heterogeneity of outcome measures, and administration of rescue boluses have made interpretation of the evidence challenging. A Cochrane review reported that evidence is insufficient to recommend routine clinical use of morphine for procedural pain relief in ventilated infants. Many neonatal formularies include oral morphine as a treatment for pain in neonates, and suggested doses are 50–200 µg/kg. A previous pilot study investigated the analgesic efficacy of oral morphine before retinopathy of prematurity screening, but findings were inconclusive because the study was stopped early owing to changes in Medicines and Healthcare products Regulatory Agency regulations.

### **Added value of this study**

In this study, 100 µg/kg oral morphine was administered to non-ventilated infants before retinopathy of prematurity screening and clinical heel lancing. Multiple modalities were used to quantify analgesic efficacy, which included changes in pain scores, noxious-evoked brain activity, and reflex withdrawal activity. A comprehensive approach was used to assess changes in oxygen saturation, respiratory rate, heart rate, and ventilation requirement in the 24 h period before and after the clinical procedures. In our study, administration of 100 µg/kg oral morphine in non-ventilated premature infants had profound respiratory adverse effects without suggestion of analgesic efficacy.

### **Implications of all the available evidence**

We do not recommend the use of oral morphine at a dose of 100 µg/kg in non-ventilated premature infants for retinopathy of prematurity screening. Morphine produces cardiorespiratory effects that last for an average of 6–8 h. If this dose or a greater dose of morphine were to be administered to infants for other clinical indications or in future clinical trials, the infant should be monitored continuously and clinicians should expect that these infants might require a substantial increase in respiratory support or resuscitation. Thus, morphine should not be administered unless resuscitative equipment is available immediately, staff are trained appropriately, and both the risks and potential benefits are considered carefully. Difficulties in measuring infant pain are widely recognised, and the methodology used in our trial to measure both analgesic efficacy and side-effects of a pharmacological intervention sets new standards for the conduct of clinical trials of analgesics in infants.

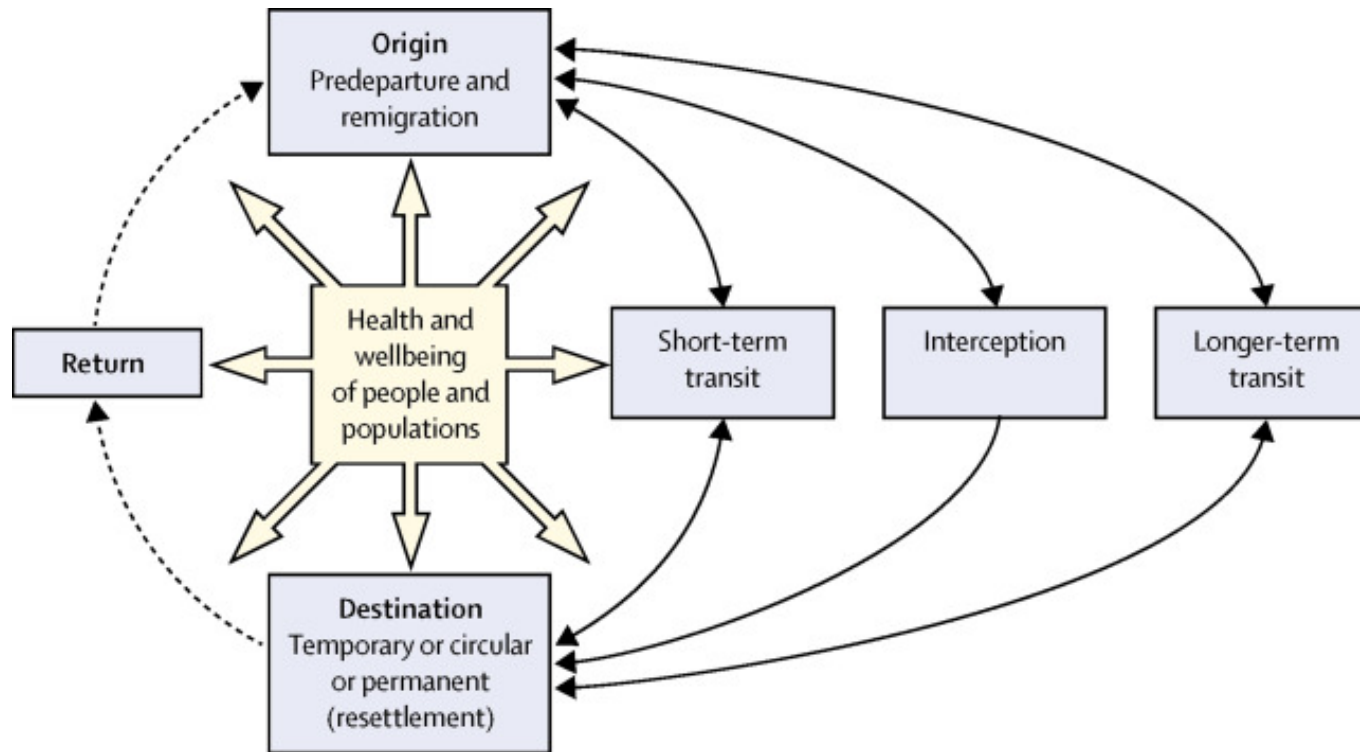


# The UCL–Lancet Commission on Migration and Health: the health of a world on the move

With one billion people on the move or having moved in 2018, migration is a global reality, which has also become a political lightning rod. Although estimates indicate that the majority of global migration occurs within low-income and middle-income countries (LMICs), the most prominent dialogue focuses almost exclusively on migration from LMICs to high-income countries (HICs). Nowadays, populist discourse demonises the very same individuals who uphold economies, bolster social services, and contribute to health services in both origin and destination locations. Those in positions of political and economic power continue to restrict or publicly condemn migration to promote their own interests. Meanwhile nationalist movements assert so-called cultural sovereignty by delineating an us versus them rhetoric, creating a moral emergency. In response to these issues, the UCL-*Lancet* Commission on Migration and Health was convened to articulate evidence-based approaches to inform public discourse and policy. The Commission undertook analyses and consulted widely, with diverse international evidence and expertise spanning sociology, politics, public health science, law, humanitarianism, and anthropology. The result of this work is a report that aims to be a call to action for civil society, health leaders, academics, and policy makers to maximise the benefits and reduce the costs of migration on health locally and globally. The outputs of our work relate to five overarching goals that we thread throughout the report.

## Key messages

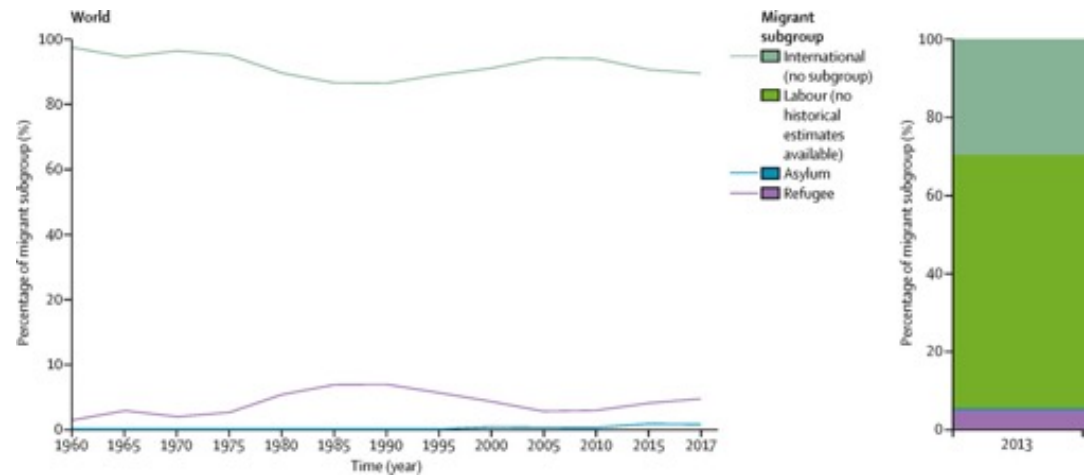
- We call on nation states, multilateral agencies, non-governmental organisations, and civil society to positively and effectively address the health of migrants by improving leadership and accountability. First, we urge the UN to appoint a Special Envoy on Migration and Health and national governments to have a country-level focal point for migration and health. This would enable much needed coordination and also ensure that migrants are included in all decisions about their health. Second, we propose that a Global Migration and Health Observatory is established to develop evidence-based migration and health indicators to ensure better reporting, monitoring, transparency, and accountability on the implementation of the Global Compact for Migration and the Global Compact on Refugees.
- International and regional bodies and states should re-balance policy making in migration to give greater prominence to health by inviting health representatives to high level policy making forums on migration. Health leaders and practitioners should fully engage in dialogues on the macroeconomic forces that affect population mobility and participate in multisector budgeting and programme planning for migrants.
- Racism and prejudice should be confronted with a zero tolerance approach. Public leaders and elected officials have a political, social, and legal responsibility to oppose xenophobia and racism that fuels prejudice and exclusion of migrant populations. Health professionals' and organisations' awareness of racism and prejudice should be strengthened through regulatory and training bodies including accreditation, educational courses, and continuous professional development. Civil society organisations should hold leaders to account to ensure the implementation of these obligations.
- Universal and equitable access to health services and to all determinants of the highest attainable standard of health within the scope of universal health coverage needs to be provided by governments to migrant populations, regardless of age, gender, or legal status. Solutions should include input from migrants and be specific to the diverse migrant populations. For those exposed to disaster or conflict, or both, mobility models and Disaster Risk Reduction systems should be integrated. Targeted interventions to improve the rights of migrant workers, their knowledge of workplace health and safety, and entitlement to health care are needed.



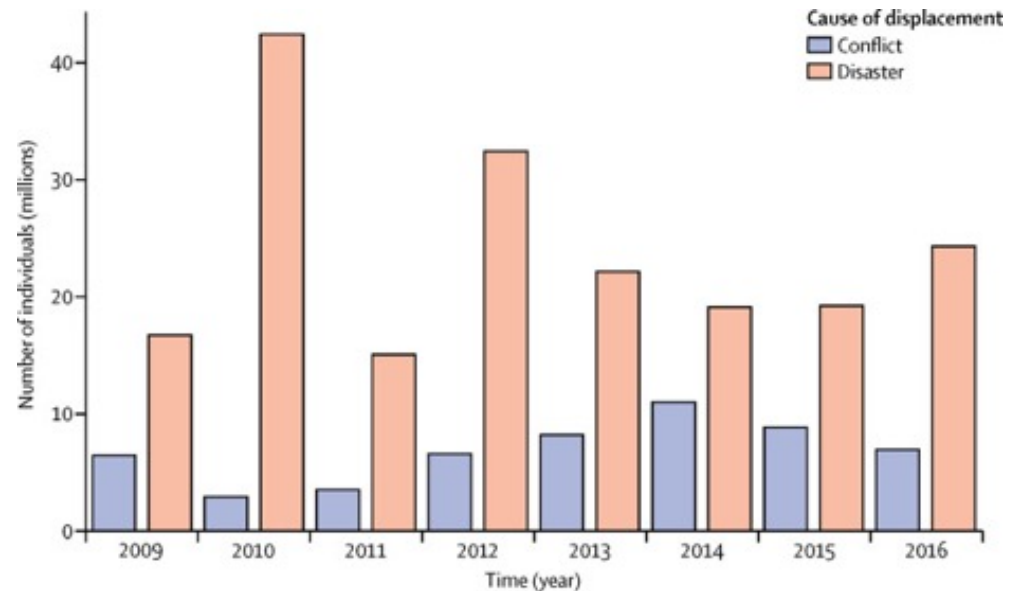
Migration trajectories involve various phases including, pre-departure circumstances at places of origin; short-term or long-term transit, which might involve interception by authorities, non-governmental groups, or criminal gangs; destination situations of long-term or short-term stay; and return to places of origin for resettlement or for temporary visits before remigration.

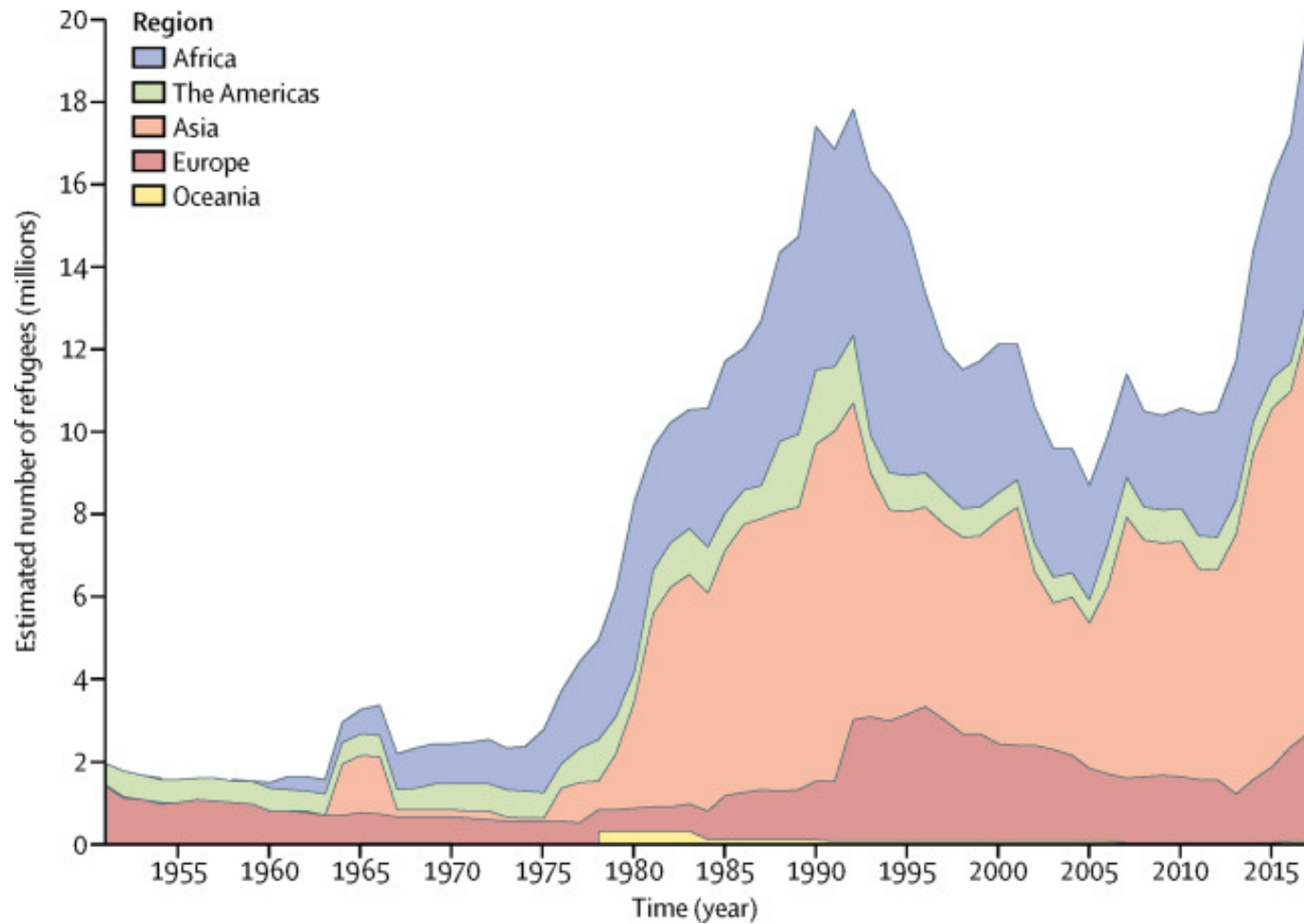
In each phase of a person's journey, potential health risks and possible health protective factors exist that can have a short-term or long-term effect on their wellbeing. As previously noted, the journeys are often diverse and rarely singular. It is common for labour migrants to undertake circular migration, transiting back and forth between their place of origin and destination, or remigrating to a new destination.

Percentage of all international migrants that were refugees, asylum seekers, and labour migrants, 1960–2017. Labour migration estimates only available for 2013. Refugee numbers are for those under the UN High Commissioner for Refugees' mandate and therefore do not include individuals under the UN Relief and Works Agency for Palestine Refugees in the Near East's mandate as data are not available back to 1960.

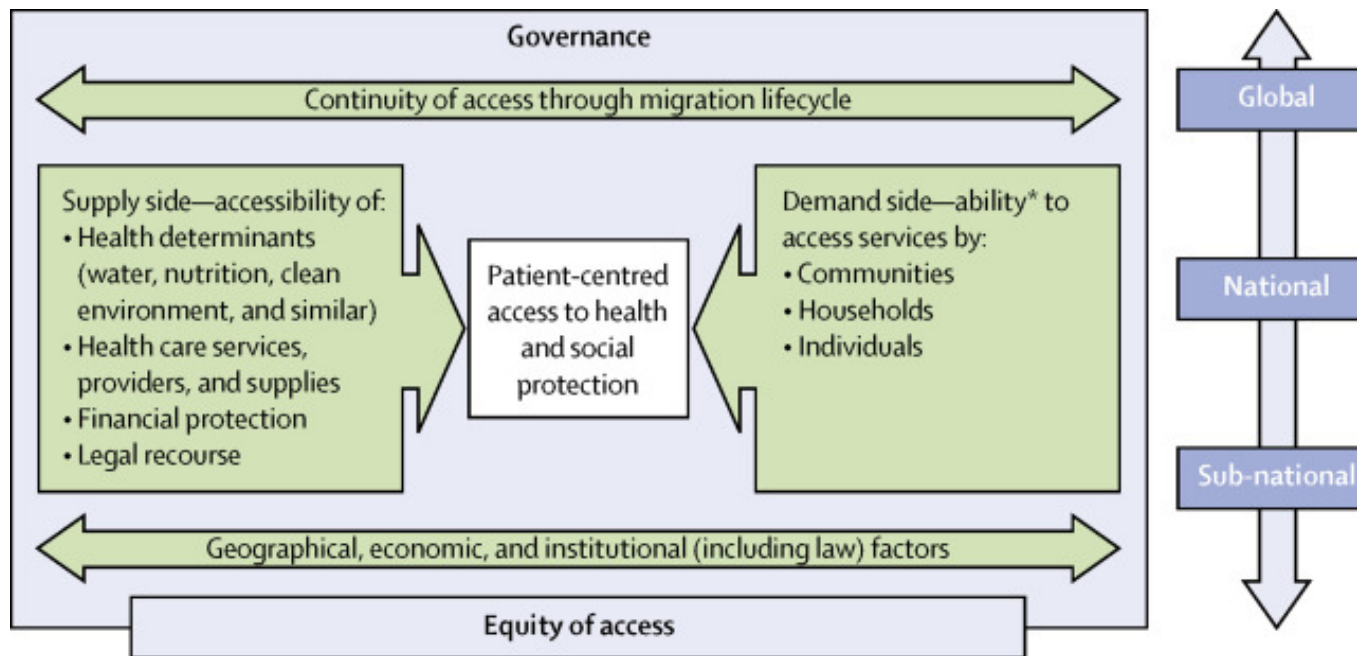


East Asia and Pacific was the region with the highest number of internally displaced people due to disasters and sub-Saharan Africa was the highest due to conflict and violence. Between 2008 and 2017, the number of individuals displaced because of conflict and violence was fewer than those resulting from disasters.





Historical data in this figure do not include 5.4 million Palestinian refugees under the UN Relief and Works Agency for Palestine Refugees in the Near East's mandate in 2017, as historical data for this group are not available. Interactive online version available.



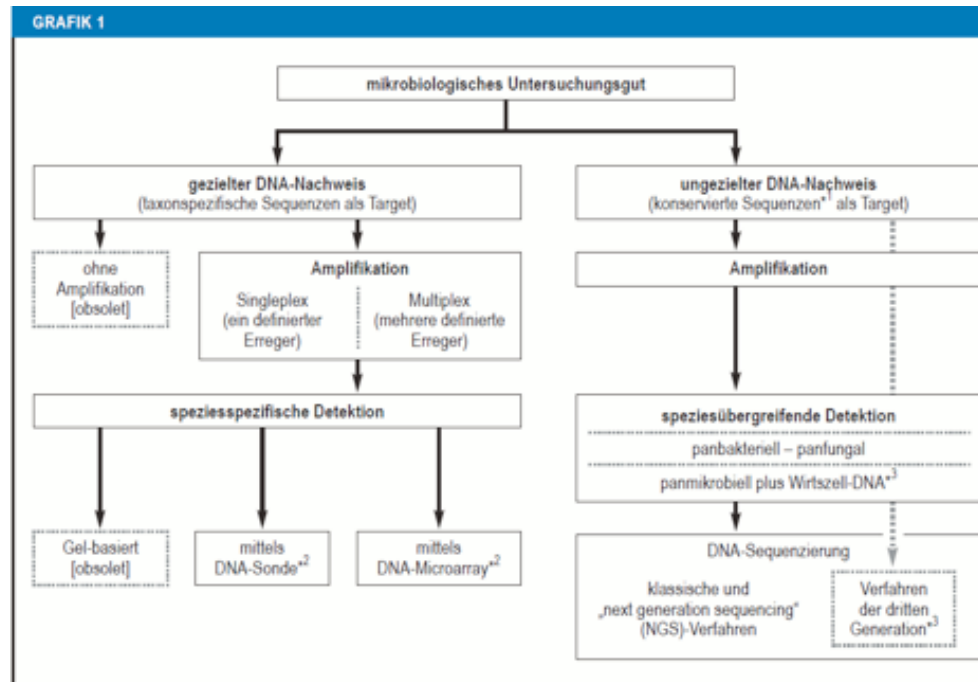
# Diagnostik von Blutstrominfektionen - Neue mikrobiologische Verfahren in der klinischen Praxis und Entwicklung

## New microbiological techniques in the diagnosis of bloodstream infections



Abbildung: Unterschiedlich lange bebrütete *Enterobacter-cloacae*-Kulturen auf einem Festnährmedium (Blutagarplatten) und ihr Einsatz in der Diagnostik

Die Geschwindigkeit der kulturellen Erregerdiagnostik ist durch die Mikroorganismen-Teilungsraten biologisch limitiert. Dies führte dazu, dass traditionell für jeden kulturbasierten Diagnostikschritt (primäre Anzucht, Isolierung von Mischkulturen, biochemische Identifizierung und Empfindlichkeitstestung) jeweils „Übernacht“-Kultivierungen stattfinden, die sich zu oft mehrtägigen ( $\geq 2-3$  Tage) Diagnostikzeiten aufaddierten. Somit kam es einer Revolution gleich, als mit der Polymerase-Kettenreaktion (PCR) die Nukleinsäureamplifikationstests (NAT) Einzug hielten, die den Erregernachweis beschleunigen und für schwierig oder nicht kultivierbare Erreger auch eine höhere Sensitivität und Spezifität erreichen konnten. Derzeit haben massenspektrometrische Verfahren die Erregerdiagnostik erneut revolutioniert und sind vielerorts bereits Teil der Routinediagnostik. Weitere Umwälzungen sind durch die routinemäßige Ganzgenom- beziehungsweise Mikrobiomsequenzierung sowie die Automatisierung kulturbasierter Prozeduren zu erwarten.



Gezielter und ungezielter Erregernachweis mittels DNA-basierter Methoden

<sup>1</sup> taxonspezifische Sequenzabschnitte umrahmend, <sup>2</sup> oder mittels alternativer DNA-basierter Methodik, <sup>3</sup> in Entwicklung

Die Vorteile der PCR und anderer NAT als kulturunabhängige Verfahren mit hohen Sensitivitäten und Spezifitäten führten nach ihrer Erstbeschreibung im Jahr 1985 zur schnellen Akzeptanz der Nukleinsäure-basierten Diagnostik. Typischerweise werden in diesem Verfahren analytische Sensitivitäten von 1 bis 100 Erregeräquivalenten an bakterieller oder fungaler DNA erreicht. Komplexe beziehungsweise Untersuchungsmaterialien mit inhomogener Erregerverteilung (zum Beispiel Gewebe, Blut, Stuhl) können zu drastischen Sensitivitäts- und Spezifitätsminderungen führen. Die NAT-Spezifität ist stark abhängig von der Auswahl der Zielstrukturen, der Primer- und Sondenkomposition und den PCR-/Microarray-Reaktionsbedingungen. Die offensichtlichen Vorteile der NAT führten oft zu einem unreflektierten und unzureichend validierten Einsatz. So wurden unter anderem der Einfluss präanalytischer Faktoren, die Bedeutung einer optimalen Nukleinsäure-Extraktion sowie Kontaminationsgefahren oft unterschätzt. Um ähnlichen „Fallstricken“ bei den derzeitigen technologischen Innovationen vorzubeugen, ist es essenziell, dass deren Testergebnisse in den Kontext mit anderen Befunden gestellt und kritisch bewertet werden.



Die offensichtlichen Vorteile der NAT führten oft zu einem unreflektierten und unzureichend validierten Einsatz (e13). So wurden unter anderem der Einfluss präanalytischer Faktoren, die Bedeutung einer optimalen Nukleinsäure-Extraktion sowie Kontaminationsgefahren oft unterschätzt. Um ähnlichen „Fallstricken“ bei den derzeitigen technologischen Innovationen vorzubeugen, ist es essenziell, dass deren Testergebnisse in den Kontext mit anderen Befunden gestellt und kritisch bewertet werden. Angesichts der Vielfalt der verschiedenen NAT-Systeme bezüglich des Detektionsumfanges, möglicher Einsatzbeschränkungen für die verschiedenen Untersuchungsmaterialien und der Unterschiede in den Gütekriterien (Sensitivität, Spezifität, prädikative Werte) empfiehlt sich eine enge Zusammenarbeit zwischen Klinik und mikrobiologischem Laboratorium, um eine optimierte Auswahl angepasst an die jeweiligen klinischen Erfordernisse treffen zu können. Das trifft besonders zu, wenn NAT-Verfahren zusätzlich zur konventionellen Diagnostik eingesetzt werden.

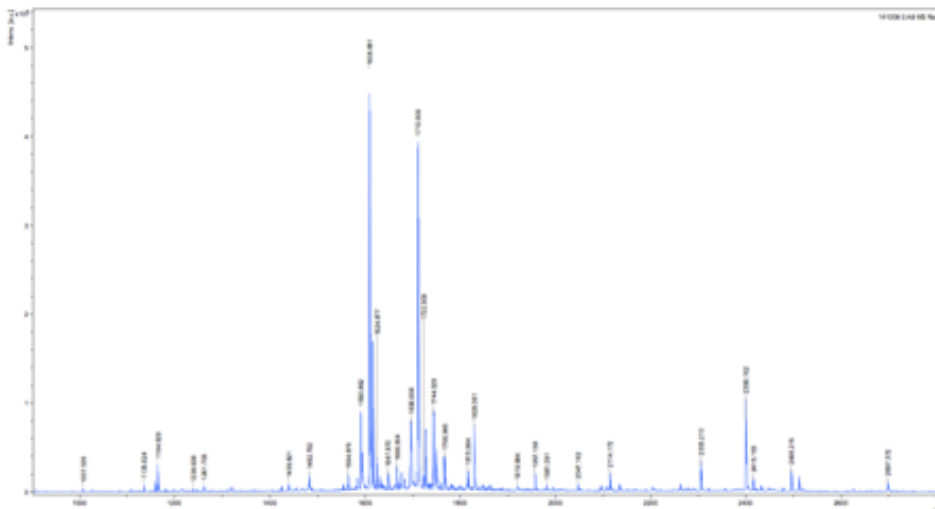
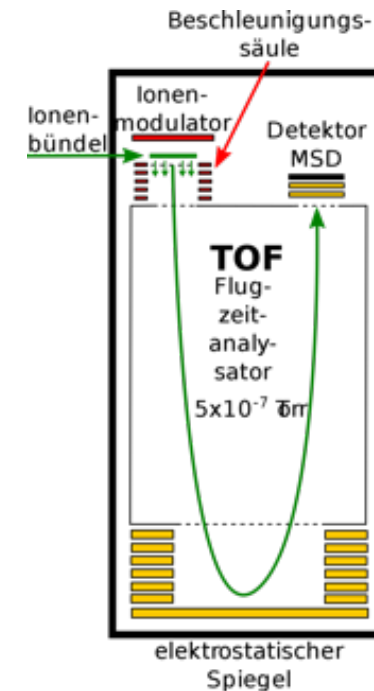
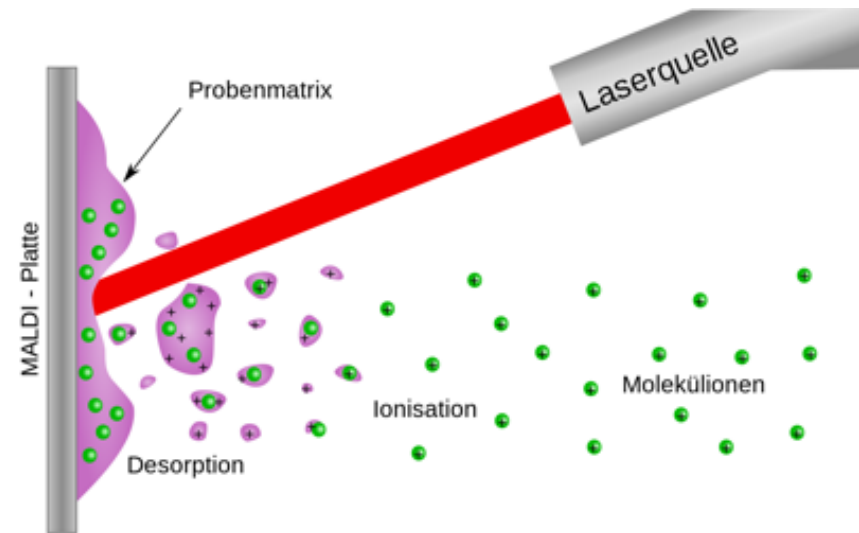
## KASTEN 1

### Fragen zur Bewertung von NAT-Befunden

- Kann ein positiver NAT-Befund per se die Ätiologie einer vermuteten Erkrankung erklären?
- Reflektiert ein positives NAT-Ergebnis tatsächlich den Erreger der vermuteten Infektionskrankheit oder handelt es sich um eine Kontamination des Untersuchungsmaterials, zum Beispiel durch Mikroorganismen, die die Haut besiedeln?
- Gibt es Widersprüche zu Ergebnissen der kulturbasierenden Diagnostik oder zu anderen Befunden?
- Kann eine unzulängliche Präanalytik (Probenentnahme und -transport) die Ursache für falsch-negative oder falsch-positive Ergebnisse darstellen?
- Sind Nachweise von Resistenzgenen bei der NAT-Untersuchung von Direktmaterial mit dem vermuteten Infektionserreger assoziiert oder stammen sie von anderen Mikroorganismen (zum Beispiel *mecA*-Gen-Nachweis von gleichfalls in dem Untersuchungsgut vorkommenden koagulasenegativen Staphylokokken)?

**MALDI-TOF** ist eine Methode der Massenanalyse von chemischen Verbindungen. Das Verfahren kombiniert die Matrix-Assistierte Laser-Desorption-Ionisierung (MALDI) mit der Flugzeitanalyse (time of flight) freigesetzter Ionen zur Massenspektrometrie.

Es erfolgt eine massenspektrometrische Auftrennung mikrobieller, vorrangig ribosomaler Proteine, wobei die gewonnenen Daten für die Identifikation von bakteriellen und fungalen Mikroorganismen verwendet werden. Ihre Hauptvorteile liegen in der extremen Schnelligkeit (Minuten) und Kostengünstigkeit einzelner Analysen bei hoher Spezifität. Obwohl es sich eigentlich um ein phänotypisches Verfahren handelt, beruht ihre einem NAT-Verfahren nahezu gleichkommende hohe Spezifität auf dem hohen Anteil ribosomaler Proteine im erzeugten Massenspektrum, die die ribosomalen Nukleinsäuresequenzen quasi widerspiegeln.



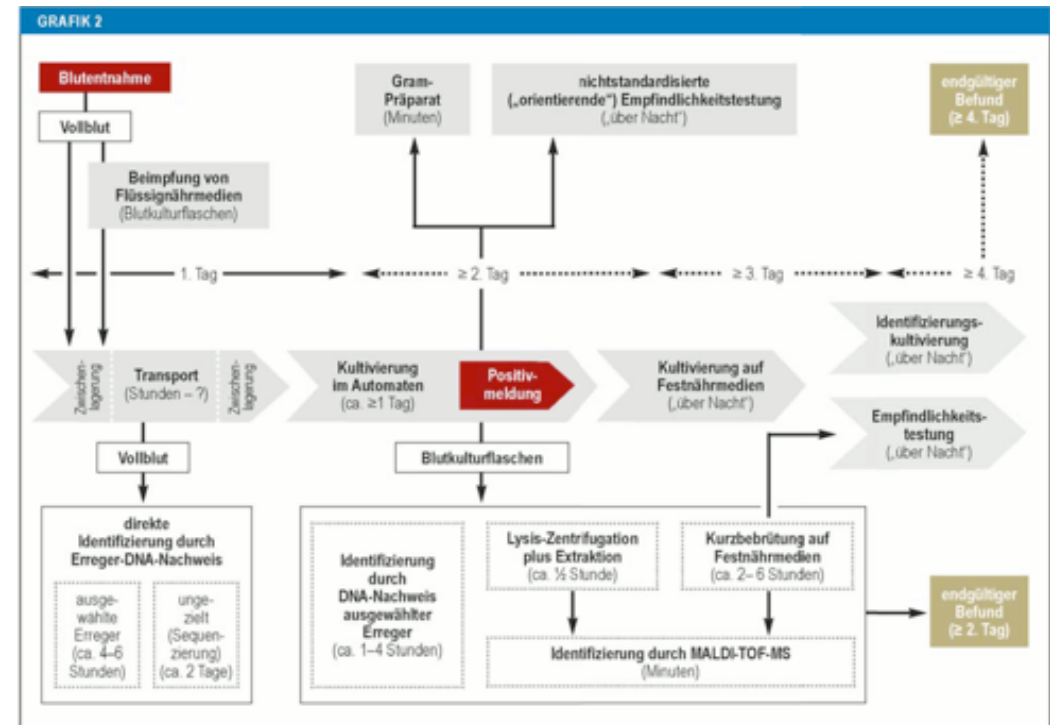
## Fortschritte bei der Diagnostik von Blutstrominfektionen

Die herkömmliche Diagnostik von Blutstrominfektionen besteht aus drei Schritten:

1. Inokulation des Patientenblutes in ein Flüssigmedium (Blutkulturflaschen) zur primären Erregeranzucht
2. nachfolgender Subkultivierung auf Festnährmedien Identifizierung und
3. Antibiotikaempfindlichkeitstestung.

Dieses Prozedere umfasst konventionell 3–4 Tage beziehungsweise bei beeinträchtigten (Antibiotikavorbehandelten) oder langsam wachsenden Erregern auch mehr und ist daher nicht schnell genug, um als Grundlage für frühe therapeutische Entscheidungen zu dienen.

Seit Jahrzehnten erfolgt die Bebrütung der Blutkulturflaschen mittels Blutkulturautomaten, die mikrobielles Wachstum registrieren und bei Erreichen eines Detektionsschwellenwertes ein Signal geben. Zur Speziesidentifizierung und Empfindlichkeitstestung wird üblicherweise ein Transfer vom Flüssignährmedium auf Festnährmedien mit nachfolgender Übernachtbebrütung zur Erzielung von Einzelkolonien vorgenommen. Parallel zur Anlage auf Festnährmedien wird ein Gram-Präparat angefertigt und mikroskopiert. Dessen Befund wird dem Kliniker im Idealfall 20–30 Minuten nach Positivmeldung der Blutkultur mitgeteilt und zur Anpassung der Antibiotikatherapie herangezogen.



Prozesse und Zeiten der klassischen Erregerdiagnostik von Blutstrominfektionen (grau hinterlegt) und moderne Möglichkeiten der Beschleunigung der Diagnostik (weiß hinterlegt)

## Massenspektrometrische Verfahren

Für eine direkte Erregeridentifikation aus positiv gemeldeten Blutkulturflaschen mittels MALDI-TOF-MS ist eine Probenaufbereitung durch vorgeschaltete Verfahren, wie das Lysis-Zentrifugation-Verfahren mit anschließender Äthanol-/Ameisensäure-Extraktion notwendig. Diese Schnellmethode – als „in house“-Adaptation oder als kommerzielles Verfahren verfügbar – zeigte Identifikationsraten von bis zu über 80 % innerhalb von circa 20–40 min beim Nachweis bakterieller Erreger. Bei Hefepilzen gelang eine direkte Identifikation in 62,5 % der Proben. Diese Vorgehensweise hat sich jedoch nicht allgemein durchgesetzt. Die Gründe hierfür liegen in einem relativ hohen zusätzlichen Aufwand, erhöhten Reagenzienkosten, mäßigen Identifizierungsraten sowie in der Einstufung als „add-on“-Diagnostik, da sie die Festnährmedien-Subkultivierung nicht ersetzt. Das führte dazu, dass die Proben aus organisatorischen Gründen nur schubweise (zum Beispiel zweimal täglich oder seltener) verarbeitet wurden und der antizipierte Schnelligkeitsvorteil sich deutlich relativierte.

## Direkte DNA-basierte Erregeridentifizierung aus Vollblut

Um die mikrobiologische Diagnostik von Blutstrominfektionen direkt aus Vollblutproben deutlich zu beschleunigen, wurden verschiedene experimentelle, später auch kommerziell verfügbare, speziesspezifische oder speziessübergreifende NAT eingeführt. Je nach Testsystem kann bei Multiplex-PCR-Systemen nach circa 3,5–8 Stunden ein Ergebnis vorliegen. Speziessübergreifende NAT-Testverfahren benötigen durch die erforderliche Sequenzierung des PCR-Amplifikats deutlich mehr Zeit (etwa plus einem Arbeitstag). NAT-Verfahren können im Gegensatz zu kulturbasierten Verfahren bereits bei zirkulierender mikrobieller DNA („DNAämie“) sowie bei avitalen Mikroorganismen beziehungsweise solchen im VBNC (viable-but-nonculturable)-Status positiv ausfallen. Während dies im Falle von Kontaminationen von Nachteil sein kann, könnte dieser Aspekt bei antibiotisch vorbehandelten Erregern zu verbesserter Sensitivität führen.

### KASTEN 2

#### Einschränkungen beim Einsatz von direkten Erregernachweisen aus Vollblut

- falsch-positive Ergebnisse durch
  - DNA-Nachweis von avitalen Erregern beziehungsweise von bereits suffizient therapierten Mikroorganismen
  - DNA-Nachweis von Kontaminanten (zum Beispiel von transienten Bakteriämien/Fungämien, vom ausgestanzten Hautzylinder bei der Probengewinnung)
- falsch-negative Ergebnisse durch
  - geringere Sensitivität im Vergleich zur Kultur (zum Beispiel durch artifizelle Adjustierung der Nachweisgrenzen)
  - Primer- und Sonden-Interferenz durch hohe Anteile nichtmikrobieller Wirts-DNA
  - Anwesenheit von Inhibitoren (zum Beispiel Heparin, Eisen und Immunglobuline)
- Diskrepanzen zum Ergebnis der konventionellen Blutkultur (fehlender oder abweichender Erregernachweis, gleichzeitiger Nachweis verschiedener Erreger)
- vergleichsweise hohe Kosten (Ausrüstung, Kits, Personalbindung)
- keine oder nur auf wenige (bekannte) Resistenzgene beschränkte Aussagen zur Antibiotikaempfindlichkeit
- keine Typisierungsmöglichkeit
- derzeit eingeschränkte Studienlage für die meisten Testsysteme

## **Antibiotika-Empfindlichkeitstestung und Resistenzgen-Nachweis**

Obwohl bereits die Spezies-Identifizierung hilfreiche Informationen für therapeutische Entscheidungen liefern kann, sind die Ergebnisse der antimikrobiellen Empfindlichkeitstestung ausschlaggebend für die endgültige Wahl der gezielten Therapie. Daher gilt es bei kritischen Infektionen auch möglichst zeitnah Ergebnisse der Empfindlichkeitstestung zu generieren.

Konventionell werden Einzelkolonien von Festnährmedien zur Empfindlichkeitstestung eingesetzt. Für die Diagnostik von Blutstrominfektionen bedeutet das eine erhebliche Zeitverzögerung durch notwendige Bebrütungszeiten nach dem Ausstreichen positiv gemeldeter Blutkulturflaschen.

## **Beschleunigung der Empfindlichkeitstestung durch Änderung der Kultivierungsmethodik**

Bei der direkten Inokulation von Testsystemen aus positiv gemeldeten Blutkulturflaschen wird nicht auf das Wachstum von subkultivierten Kolonien auf Festnährmedien gewartet. Durch Zentrifugation positiv gemeldeter Blutkulturflaschen gewonnene Zellpellets werden direkt für eine Inokulation in Empfindlichkeitstestungssysteme eingesetzt. Für Hefen wurde dadurch eine Ergebnisbeschleunigung von 15,1 Stunden erzielt

## **Einsatz der MALDI-TOF-MS zum beschleunigten Nachweis von Resistenzen und zur Empfindlichkeitstestung**

Die Vorteile der MALDI-TOF-MS hinsichtlich Zeitersparnis und einfacher Handhabung führten zu mehreren Ansätzen, diese Methodik auch für den Nachweis einzelner Resistenzmechanismen und aktuell auch als Alternative für die universelle Empfindlichkeitstestung zu adaptieren. So können antibiotikabedingte Veränderungen des Erregerproteoms zu Massenveränderungen führen, die dann mittels MALDI-TOF-MS nachweisbar werden. Eine neue Anwendung zum universellen Einsatz der MALDI-TOF-MS zur schnellen Empfindlichkeitstestung beruht auf der wachstumsbasierten Differenzierung in „empfindlich“ und „resistent“ – ähnlich wie in der konventionellen Empfindlichkeitstestung. Unter Einsatz von Breakpoint-Konzentrationen zugesetzter Antibiotika wird mittels MALDI-TOF-MS gemessen, ob mikrobielles Wachstum zu testender Isolate stattfindet (= resistent) oder nicht (= empfindlich).

## **Direkte DNA-basierte Detektion von Resistenzgenen in Vollblutproben**

Idealerweise könnte bei Monoinfektionen die direkt aus Vollblutproben isolierte mikrobielle DNA nicht nur zur Erregeridentifizierung, sondern parallel auch zum Nachweis von den die Antibiotikaresistenz determinierenden Genen beziehungsweise – wenn mutationsbedingt – entsprechenden DNA-Abschnitten eingesetzt werden.

## Resümee

Die moderne mikrobiologische Diagnostik von Blutstrominfektionen ist auf dem Weg, sich dem Zeitpunkt der klinischen Verdachtsdiagnose einer Blutstrominfektion zu nähern, ist aber immer noch davon entfernt, unmittelbaren Einfluss auf die antibiotische Initialtherapie zu haben. Die MALDI-TOF-MS kombiniert mit dem Einsatz kurzbebrüteter Festnährmedien, hat zu einer enormen Beschleunigung der Identifizierung und der Empfindlichkeitstestung beigetragen. PCR-basierte Schnellteste können bei erfolgloser Kultivierung von Erregern von Blutstrominfektionen hilfreich sein, die Kultur aber nicht ersetzen. Die Vorteile der neuen Technologien können nur wirksam werden, wenn die Präanalytik, Arbeitsabläufe und -zeiten und das Qualitätsmanagement optimal angepasst werden sowie wesentliche Indikationen und Limitationen der einzelnen diagnostischen Verfahren dem anfordernden Arzt auch bekannt sind.

### **Erregerdiagnostik**

Die Relevanz einer schnellen Erregerdiagnostik ergibt sich aus der Erregervirulenz und der Existenz resistenter Erreger-Phänotypen und wirtsseitig aus der zunehmend infektionsgefährdeteren Patientenstruktur mit immer mehr älteren, multimorbiden, immunkompromittierten und/oder mit Fremdkörpern versehenen Patienten.

### **Polymerase-Kettenreaktion**

Mit Entwicklung der Polymerase-Kettenreaktion (PCR) konnte der Erregernachweis beschleunigt und für schwierig oder nicht kultivierbare Erreger auch eine höhere Sensitivität und Spezifität erreicht werden.

### **PCR und Kulturverfahren**

Je nach Indikation können beide diagnostischen Strategien in synergistischer Weise zu einer validen Erregeridentifizierung und Empfindlichkeitsbestimmung sowie zur weiteren Erregercharakterisierung beitragen.

### **MALDI-TOF-MS-Systeme**

MALDI-TOF-MS-Systeme haben im Verlauf nur weniger Jahre in vielen Laboratorien die konventionelle Erregeridentifizierung mittels biochemischer Verfahren fast vollständig abgelöst und sind auf dem Weg, auch zur Antibiotikaempfindlichkeitstestung eingesetzt zu werden.

### **Spezifität der Nukleinsäureamplifikationstests (NAT)**

Die NAT-Spezifität ist stark abhängig von der Auswahl der Zielstrukturen, der Primer- und Sondenkomposition und den PCR-/Microarray-Reaktionsbedingungen.

RESEARCH ARTICLE

Cardiovascular and skeletal muscle health with lifelong exercise

Kevin J. Gries, Ulrika Raue, Ryan K. Perkins, Kaleen M. Lavin, Brittany S. Overstreet,  
Leonardo J. D'Acquisto, Bruce Graham, W. Holmes Finch, Leonard A. Kaminsky, Todd A. Trappe,  
and Scott Trappe

*Human Performance Laboratory, Ball State University, Muncie, Indiana*

Submitted 21 February 2018; accepted in final form 22 August 2018

YE = young exercisers, LLE = Life-long exercisers, OH = old healthy

Table 1. *Subject characteristics*

	Women			Men				
				LLE				
	YE, <i>n</i> = 10	LLE, <i>n</i> = 7	OH, <i>n</i> = 10	YE, <i>n</i> = 10	All, <i>n</i> = 21	Performance, <i>n</i> = 14	Fitness, <i>n</i> = 7	OH, <i>n</i> = 10
Age, yr	25 ± 1	72 ± 2	75 ± 1	25 ± 1	74 ± 1	74 ± 1	75 ± 2	75 ± 1
Height, cm	167 ± 2	164 ± 2	157 ± 2	181 ± 2	180 ± 2	179 ± 2	182 ± 3	177 ± 2
Weight, kg	60 ± 2	61 ± 4	65 ± 1	75 ± 3	79 ± 2	77 ± 2	83 ± 5	88 ± 3
BMI, kg/m <sup>2</sup>	21 ± 1	23 ± 1	27 ± 1	23 ± 1	24 ± 1	24 ± 1	25 ± 1	28 ± 1
Body fat, %	23 ± 1*	30 ± 2†	41 ± 2	18 ± 2*	24 ± 1†	22 ± 1‡	27 ± 1	32 ± 1
Steps per day	11,518 ± 1,404*	7,463 ± 683	6,801 ± 823	9,404 ± 635	9,560 ± 619	9,369 ± 725	10,006 ± 1,265	5,813 ± 488*

Values are means ± SE. BMI, body mass index; LLE, lifelong exercisers; OH, old healthy; YE, young exercisers. \**P* < 0.05 vs. other groups; †*P* < 0.05 vs. OH; ‡*P* < 0.05 vs. LLE Fitness.

Table 2. Prescribed medications and blood markers for general health

	Women			Men				
				LLE				
	YE, n = 10	LLE, n = 7	OH, n = 10	YE, n = 10	All, n = 21	Performance, n = 14	Fitness, n = 7	OH, n = 10
Medications, % of group								
Beta Blockers	—	—	10	—	10	—	29	30
Blood Pressure§	—	29	20	—	43	36	57	70
Thyroid	10	43	40	—	14	7	29	20
Cholesterol	—	14	30	—	52	57	43	70
TG, mg/dl	79 ± 13	105 ± 16	123 ± 14	86 ± 6	78 ± 5†	73 ± 5	88 ± 10	112 ± 15
HDL, mg/dl	79 ± 7	83 ± 7	62 ± 5	56 ± 5	65 ± 3†	66 ± 3	63 ± 4	51 ± 2
Glucose, mg/dl	91 ± 3	101 ± 5	100 ± 4	90 ± 2	95 ± 2	93 ± 1‡	100 ± 3	105 ± 4
Hemoglobin, g/dl	12.4 ± 0.3	12.7 ± 0.2	13.1 ± 0.3	14.8 ± 0.2	14.5 ± 0.2	14.7 ± 0.2	13.9 ± 0.4	14.4 ± 0.6
Hematocrit, %	38 ± 1	38 ± 1	40 ± 1	44 ± 1	43 ± 1	43 ± 1‡	41 ± 1	42 ± 2
Total testosterone, ng/dl	38 ± 9*	14 ± 3	14 ± 3	580 ± 41	554 ± 52	591 ± 73	479 ± 50	418 ± 85
Estrogen, pg/ml	178 ± 30*	83 ± 16	105 ± 10	—	—	—	—	—

Values are means ± SE. HDL, high-density lipoprotein; LLE, lifelong exercisers; OH, old healthy; TG, triglycerides; YE, young exercisers. \**P* < 0.05 vs. other groups. †*P* < 0.05 vs. OH; ‡*P* < 0.05 vs. LLE Fitness; §not including β blockers.

Table 3. Exercise history of lifelong exercising cohorts

Age, yr	Mode	Women			Men						
					Performance			Fitness			
		day/wk	h/wk	Intensity§	Mode	day/wk	h/wk	Intensity§	day/wk	h/wk	Intensity§
20–29	Team sports, run, cycle, swim, ski, dance	3.5 ± 0.9	4.4 ± 1.8	1.6 ± 0.4	Team sports, run, cycle	4.1 ± 0.7	6.9 ± 2.8	2.0 ± 0.3	3.6 ± 1.0	5.4 ± 4.2	1.6 ± 0.4
30–39	Run, cycle, swim, ski, dance, yoga	4.2 ± 0.8	5.4 ± 1.4	1.6 ± 0.4	Team sports, run, cycle	4.4 ± 0.5	7.7 ± 2.1	2.3 ± 0.1*	3.6 ± 1.1	6.2 ± 3.2	1.4 ± 0.4
40–49	Run, cycle, swim, ski, dance, yoga	5.1 ± 0.5	8.3 ± 1.1	1.9 ± 0.2	Run, cycle, swim	4.4 ± 0.5	7.1 ± 0.9	2.1 ± 0.2	4.9 ± 0.5	7.5 ± 2.9	2.2 ± 0.2
50–59	Run, cycle, swim, ski, dance, yoga	4.9 ± 0.5	7.6 ± 1.3	1.9 ± 0.2	Run, cycle, swim	4.4 ± 0.3	7.2 ± 0.9	2.2 ± 0.1	5.4 ± 0.4	7.1 ± 1.5	2.0 ± 0.0
60–69	Run, cycle, swim, ski, dance, yoga	4.9 ± 0.6	7.6 ± 1.3	2.3 ± 0.1	Run, cycle, swim	4.5 ± 0.3	8.3 ± 1.2	2.2 ± 0.1	4.9 ± 0.6	5.8 ± 1.3	2.0 ± 0.0
Current	Run, cycle, swim, ski, dance, yoga	4.7 ± 0.4	6.8 ± 1.0	2.1 ± 0.2	Run, cycle, swim	4.5 ± 0.3	8.5 ± 1.4	2.2 ± 0.1*	4.9 ± 0.7	7.4 ± 1.9	1.5 ± 0.2
	Lifelong average	4.6 ± 0.3	6.6 ± 0.6	1.9 ± 0.1	Lifelong average	4.4 ± 0.2	7.6 ± 0.7	2.1 ± 0.1*	4.6 ± 0.3	6.6 ± 0.9	1.8 ± 0.1

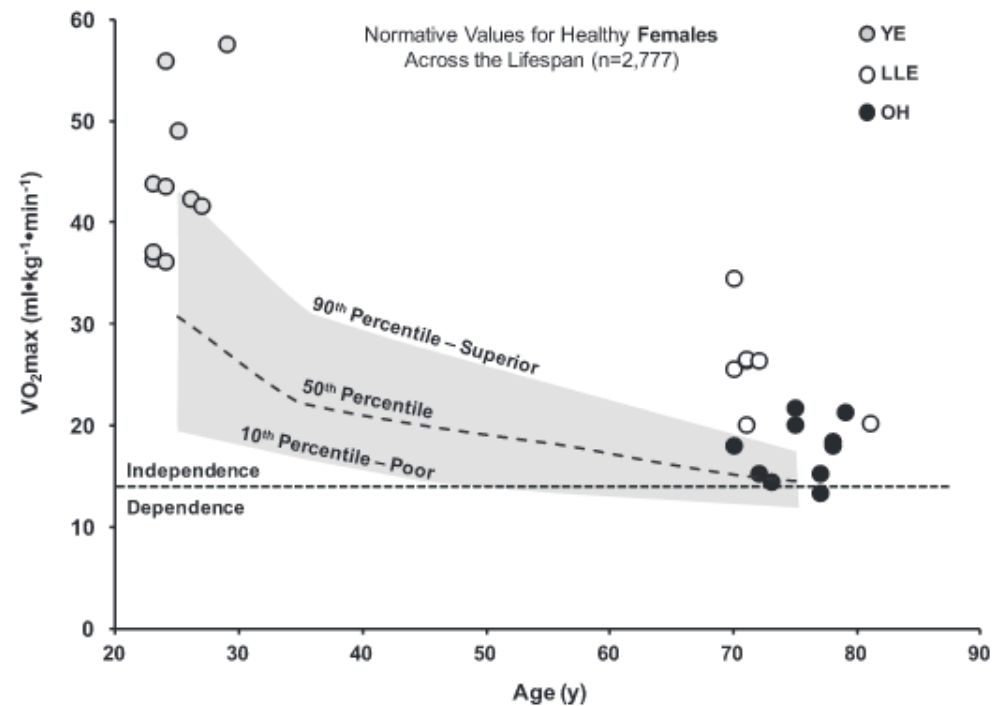
Values are means ± SE. Data were gathered from a self-reported exercise history questionnaire. In the case that a subject reported more than one training intensity, the values were weighted to calculate an intensity mean (e.g., 80% of training at a 2 and 20% of training at a 3 resulted in an overall training intensity of 2.2). LLE, lifelong exerciser. \**P* < 0.05 vs. LLE fitness; §levels of self-reported intensity were 1 (light), 2 (moderate), and 3 (hard).



Table 4. Maximal exercise data

	Women			Men				
	YE, <i>n</i> = 10	LLE, <i>n</i> = 7	OH, <i>n</i> = 10	LLE				
				YE, <i>n</i> = 10	All, <i>n</i> = 21	Performance, <i>n</i> = 14	Fitness, <i>n</i> = 7	OH, <i>n</i> = 10
$\dot{V}O_{2max}$ , l/min	2.66 ± 0.14*	1.58 ± 0.15†	1.15 ± 0.05	3.92 ± 0.17*	2.67 ± 0.10†	2.89 ± 0.10‡	2.24 ± 0.12	1.95 ± 0.16
$\dot{V}O_{2max}$ , ml·kg <sup>-1</sup> ·min <sup>-1</sup>	44 ± 2*	26 ± 2†	18 ± 1	53 ± 3*	34 ± 1†	38 ± 1‡	27 ± 2	22 ± 1
$\dot{V}O_{2max}$ , ml·kg LBM <sup>-1</sup> ·min <sup>-1</sup>	61 ± 3*	39 ± 2	32 ± 1	67 ± 2*	47 ± 2†	51 ± 1‡	40 ± 2	34 ± 1
Ventilation, l/min	101 ± 5*	61 ± 5†	42 ± 2	139 ± 6*	100 ± 4†	108 ± 4‡	84 ± 4	71 ± 6
Heart rate, beats/min	188 ± 2*	164 ± 2†	152 ± 5	193 ± 3*	157 ± 5	167 ± 4‡	138 ± 10	144 ± 6
O <sub>2</sub> pulse, ml O <sub>2</sub> /beat	14.2 ± 0.8*	9.6 ± 0.9	7.6 ± 0.4	20.4 ± 0.9*	17.2 ± 0.6†	17.4 ± 0.5	16.7 ± 1.4	13.7 ± 1.2
RER	1.21 ± 0.02	1.27 ± 0.05	1.24 ± 0.03	1.25 ± 0.02	1.20 ± 0.01	1.21 ± 0.01	1.18 ± 0.03	1.24 ± 0.02
Peak power, W	231 ± 10*	138 ± 11†	91 ± 5	332 ± 11*	222 ± 9†	240 ± 9‡	185 ± 8	151 ± 8

Values are means ± SE. LBM, lean body mass; LLE, lifelong exercisers; OH, old healthy; RER, respiratory exchange ratio;  $\dot{V}O_{2max}$ , maximal oxygen consumption; YE, young exercisers. \**P* < 0.05 vs. other groups; †*P* < 0.05 vs. OH; ‡*P* < 0.05 vs. LLE fitness.



LLEP = Life-long exercise „performance“  
 LLEF = Life-long exercise „fitness“

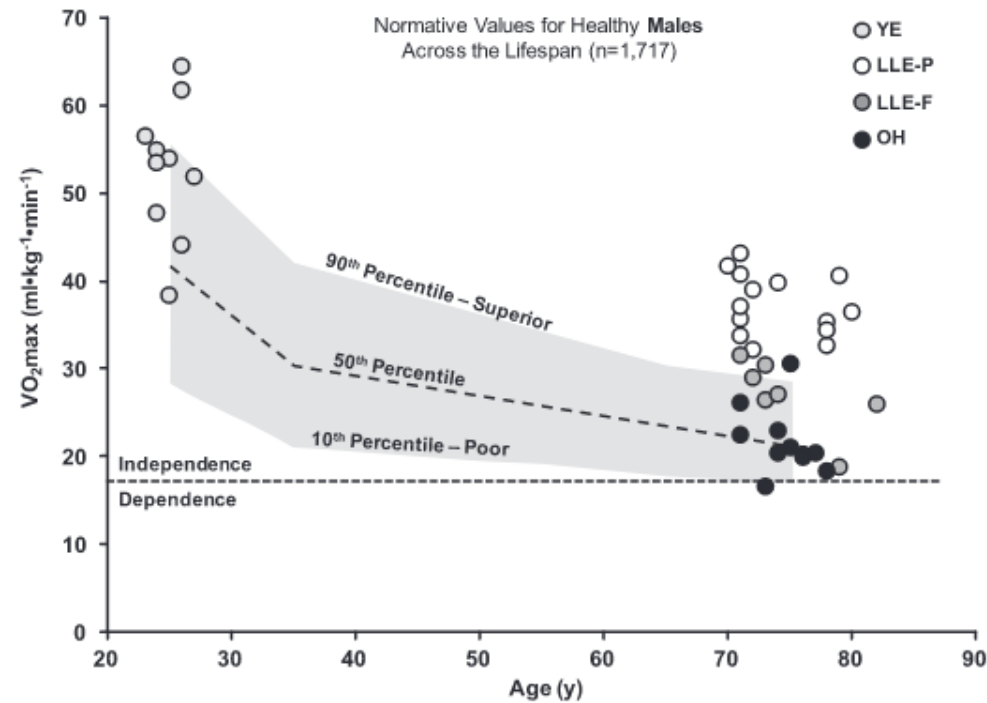
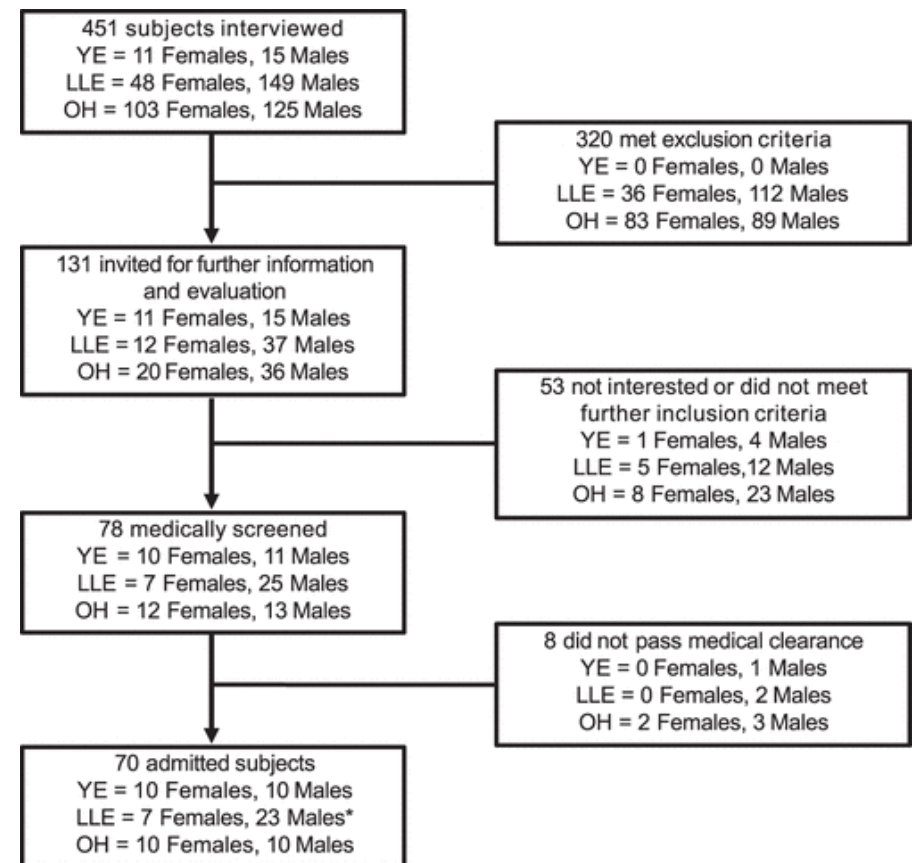


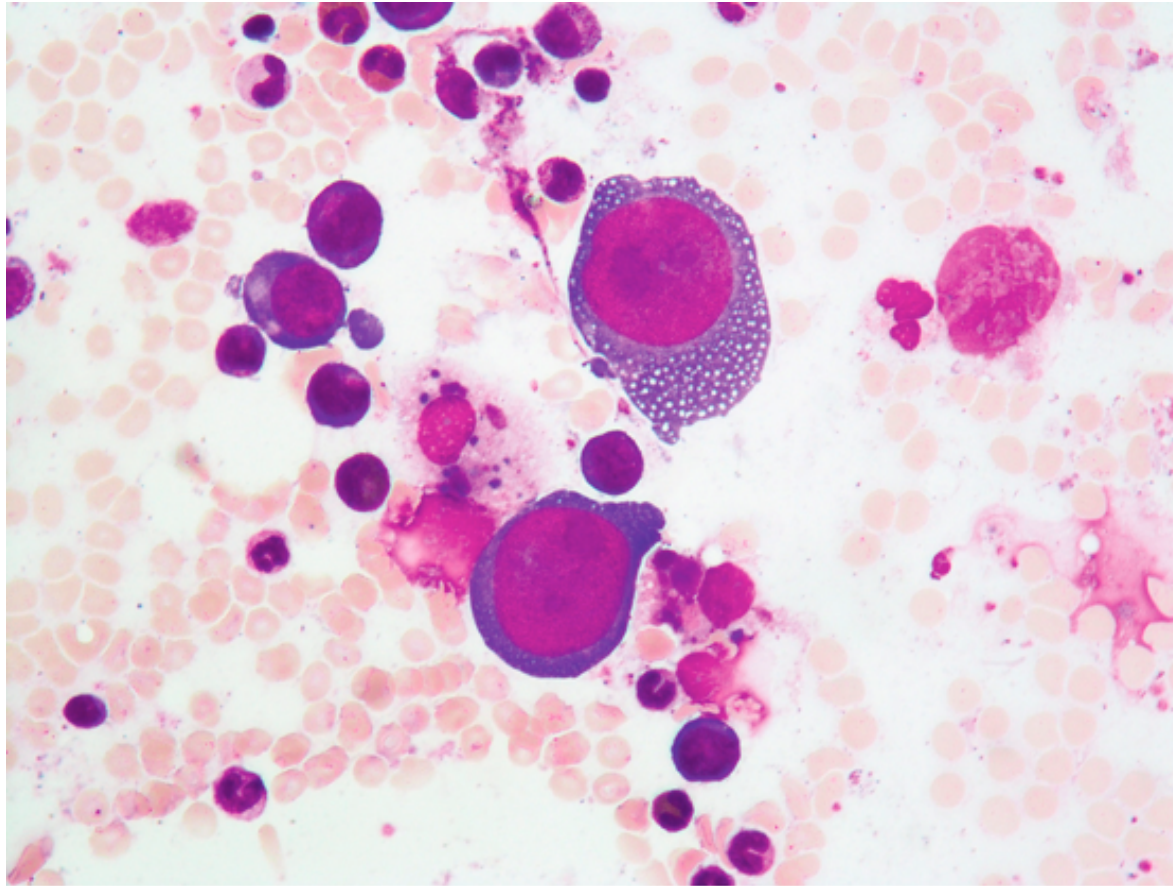
Table 6. *Skeletal muscle (vastus lateralis) capillarization profile*

	Women			Men				
	YE, n = 10	LLE, n = 7	OH, n = 10	YE, n = 10	All, n = 21	Performance, n = 14	Fitness, n = 7	OH, n = 10
Capillaries/mm <sup>2</sup>	377 ± 27	338 ± 22	281 ± 12*	363 ± 19	347 ± 14	372 ± 13‡	298 ± 22	248 ± 15*
Capillaries/fiber	1.7 ± 0.2	1.6 ± 0.2	1.1 ± 0.1*	2.3 ± 0.2	2.4 ± 0.1	2.4 ± 0.1	2.2 ± 0.1	1.5 ± 0.1*
CCEF	4.3 ± 0.4	3.8 ± 0.4	2.8 ± 0.2*	5.4 ± 0.3	5.3 ± 0.2	5.4 ± 0.3	4.9 ± 0.3	3.5 ± 0.3*

Values are means ± SE. CCEF, capillaries in contact with each fiber; LLE, lifelong exercisers; OH, old healthy; YE, young exercisers. \*P < 0.05 vs. other groups; ‡P < 0.05 vs. LLE fitness.

In summary, lifelong aerobic exercise provided substantial benefits for  $\text{Vo}_{2\text{max}}$  and skeletal muscle metabolic fitness among women and men in their eighth decade of life. The greater  $\text{Vo}_{2\text{max}}$  in the LLE cohort compared with OH remarkably decreases the relative risk of mortality and provides for a large physiological reserve above the frailty threshold, with further benefit from vigorous lifelong training. For skeletal muscle, 50+ years of lifelong aerobic exercise fully preserve skeletal muscle capillarization and aerobic enzymes, regardless of intensity. These data support the idea that skeletal muscle metabolic fitness may be easier to maintain with lifelong aerobic exercise than more central aspects of the cardiovascular system. The conservation of the skeletal muscle presented here may translate to other biological signatures of skeletal muscle health and warrants further investigation.





A 67-year-old woman presented to the emergency department with a 6-week history of progressive exertional dyspnea. Her medical history was notable for lung transplantation that had been performed 8 years earlier. Immunosuppressive medications included mycophenolate mofetil and tacrolimus. Laboratory studies showed normocytic anemia, with a hemoglobin level of 6.9 g per deciliter (reference range, 11.9 to 17.2). The hemoglobin level had been 12.7 g per deciliter 6 weeks earlier. White-cell and platelet counts were normal. The reticulocyte index was 0%, which aroused concern for red-cell aplasia or aplastic anemia. Bone marrow aspiration was performed and showed normal granulopoiesis and megakaryopoiesis, but reduced erythropoiesis. Giant proerythroblasts with basophilic and vacuolated cytoplasm, uncondensed chromatin, and large, intranuclear, purple-colored viral inclusions were present on the aspirate. These findings supported a diagnosis of parvovirus B19 infection, which was confirmed by polymerase-chain-reaction testing. The patient was treated with red-cell transfusions and intravenous immune globulin. By the time of hospital discharge, the hemoglobin level had increased, and at a 6-month follow-up, the anemia had completely resolved.